

85-33  
GC  
1211  
.N48  
S86  
1985

NOAA Grant Report

---

SYNOPTIC INVESTIGATION OF NUTRIENT CYCLING IN THE COASTAL  
PLUME OF THE HUDSON AND RARITAN RIVERS: PLANKTON DYNAMICS

Thomas C. Malone  
Mira B. Chervin-Ledman  
Jeanne C. Stepien  
Christopher Garside  
Carol D. Litchfield  
James P. Thomas

Rockville, Maryland  
April 1985

**noaa**

NATIONAL OCEANIC AND ATMOSPHERIC ADMINISTRATION

---

National Ocean Service

SYNOPTIC INVESTIGATION OF NUTRIENT CYCLING IN THE COASTAL  
PLUME OF THE HUDSON AND RARITAN RIVERS: PLANKTON DYNAMICS

Thomas C. Malone<sup>1</sup>  
Mira B. Chervin-Ledman<sup>2</sup>  
Jeanne C. Stepien  
Lamont-Doherty Geological Observatory  
Palisades, New York 10964

Christopher Garside  
Bigelow Laboratory for Ocean Sciences  
McKown Point  
West Boothbay Harbor, Maine 04575

Carol D. Litchfield<sup>3</sup>  
Center for Coastal and Environmental Studies  
Rutgers - The State University  
New Brunswick, New Jersey 08903

James P. Thomas  
National Marine Fisheries Service  
Sandy Hook, New Jersey 07732

LIBRARY

NOV 28 2005

National Oceanic &  
Atmospheric Administration  
U.S. Dept. of Commerce

<sup>1</sup>Current address: Horn Point Environmental Laboratory,  
University of Maryland/C.E.E.S., Cambridge, Maryland 21613

<sup>2</sup>Current address: New York City Department of Environmental  
Protection, Municipal Building, New York, New York 10007

<sup>3</sup>Current address: E.I. Du Pont de Nemours and Co., Haskell  
Laboratory, Newark, Delaware 19711

GC  
1211  
.N48  
S86  
1985

Atlantic Office, Stony Brook, New York

Coastal and Estuarine Assessment Branch  
Ocean Assessments Division  
Office of Oceanography and Marine Assessment  
National Ocean Service  
National Oceanic and Atmospheric Administration  
U.S. Department of Commerce

Report under Grant NA82RBA6047 to  
Atlantic Office, Ocean Assessemnts Divison

#### NOTICE

This report has been reviewed by the National Ocean Service of the National Oceanic and Atmospheric Administration (NOAA) and approved for publication. Such approval does not signify that the contents of this report necessarily represent the official position of NOAA or of the Government of the United States, nor does mention of trade names or commercial products constitute endorsement or recommendation for their use.

CONTENTS

SUMMARY 1

1.0 INTRODUCTION . . . . . 4

    1.01 Background . . . . . 4

    1.02 Objectives . . . . . 9

2.0 METHODS . . . . . 10

    2.01 Sampling . . . . . 10

    2.02 Hydrographic Properties . . . . . 14

    2.03 Dissolved Organic Matter . . . . . 15

    2.04 Suspended Organic Matter . . . . . 15

    2.05 Phytoplankton Photosynthesis . . . . . 16

    2.06 Nitrogen Uptake by Phytoplankton . . . . . 16

    2.07 Microbial Respiration . . . . . 17

    2.08 Macrozooplankton . . . . . 17

    2.09 Bacterial Biomass and Heterotrophic Potential . . . . . 18

3.0 WATER COLUMN PROCESSES . . . . . 19

    3.01 Seasonal Variation . . . . . 19

    3.02 Drogue Tracks . . . . . 33

    3.03 Hydrography . . . . . 35

    3.04 Phytoplankton Biomass . . . . . 44

    3.05 Suspended and Dissolved Organic Matter . . . . . 51

    3.06 Photosynthetic Production of Organic Matter . . . . . 64

    3.07 Light-Saturated Photosynthesis . . . . . 72

    3.08 Uptake of Nitrate and Ammonium by Phytoplankton . . . . . 74

    3.09 Biomass and Abundance of Copepods . . . . . 79

    3.10 Plankton Respiration . . . . . 81

    3.11 Assimilation of Particulate Organic Matter  
        by Copepods . . . . . 83

4.0 BENTHIC AND PLANKTONIC BACTERIA . . . . . 90

    4.01 Abundance . . . . . 90

    4.02 Heterotrophic Potential . . . . . 95

5.0 CONCLUSIONS AND IMPLICATIONS . . . . . 100

    5.01 Assimilation Capacity: Inorganic Nitrogen  
        Inputs . . . . . 100

    5.02 Assimilation Capacity: Organic Inputs . . . . . 105

6.0 ACKNOWLEDGMENTS . . . . . 111

7.0 REFERENCES . . . . . 113

## SUMMARY

Runoff from the Hudson and Raritan Rivers is a major source of new nutrients and organic matter in the apex of the New York Bight, particularly off the coast of New Jersey. This report describes the results of a research program designed to determine the importance of these anthropogenic nutrients relative to other sources and to document their effects on biological activity and related water quality parameters. Our emphasis on interactions involving phytoplankton and zooplankton populations reflects the following considerations:

- (1) planktonic organisms are the first to be exposed to anthropogenic materials which are transported into the coastal zone via estuarine runoff and atmospheric fallout;
- (2) the production and consumption of organic matter by primary and secondary producers account for most material fluxes in marine ecosystems; and
- (3) the ability of coastal ecosystems to assimilate anthropogenic nutrient inputs depends on how phytoplankton and zooplankton populations respond to such inputs.

Phytoplankton productivity, based on a decade of measurements, averages  $590 \text{ g C m}^{-2} \text{ y}^{-1}$  over the  $1250 \text{ km}^2$  area of the apex. This is more than three times the anthropogenic input of particulate organic carbon (POC). Seasonally, phytoplankton productivity exceeds anthropogenic inputs except during late fall-early winter when productivity is low due to low incident radiation and temperature. Phytoplankton growth is generally high and temperature limited but can experience transient nutrient limitation on a time scale of hours-days. Under most conditions, phytoplankton productivity is governed by mean light intensity of the euphotic zone, temperature, the dilution rate of the plume, and grazing rate.

Concentrations of particulate organic carbon (POC) and dissolved organic carbon (DOC) are high in the apex relative to other coastal regions, POC due to high phytoplankton productivity and DOC due to export from the estuary. Exceptions occur when productivity is low (late fall-early winter), and POC supplied by runoff and resuspension predominate, and when productivity is exceptionally high

(4 to 6 g C m<sup>-2</sup> d<sup>-1</sup>), and DOC release is high enough to cause an increase in DOC above the background input from runoff.

The impact of phytoplankton production on dissolved oxygen concentrations in bottom water is minimal as a consequence of biomass exports and copepod grazing. Most biomass produced prior to the development of the seasonal thermocline appears to be exported from the apex. During summer, most phytoplankton biomass is metabolized in the surface layer and affects dissolved oxygen in bottom water indirectly via fecal pellet production by organisms grazing on phytoplankton. The input of POC to bottom water by copepods alone potentially accounts for 30 to 40 percent of the oxygen demand below the pycnocline during July.

Phytoplankton production is essential for copepod growth. Although organic detritus accounts for an average of 70 percent of the POC assimilated by copepods, detritus appears to be used primarily for maintenance between encounters with high phytoplankton crops. Accumulations of phytoplankton biomass and organic detritus are mainly limited by physical processes except during summer when copepod grazing is a major governing factor. Thus, the development and dissipation of phytoplankton blooms are physically forced during most of the year, except during summer, when phytoplankton distributions are largely governed by grazing.

High grazing rates by copepods also appear to limit accumulations of bacteria in the surface layer and to promote bacterial growth in the bottom layer during July. Bacterial abundance is generally higher in the plume than in other coastal regions and tends to be high when phytoplankton biomass is high. Thus, variations in abundance and growth potential of bacteria appears to be intimately related to phytoplankton production and copepod grazing.

These patterns of biological activity and environmental regulation are reflected in the relationship between new nitrogen inputs, nitrogen cycling, and biomass exports from the euphotic zone. Nitrogen regeneration in the plume accounts for more than 60 percent of nitrogen assimilated by phytoplankton during May and July and less than 40 percent during March and November. High regeneration rates during summer

are also implied by variations in the proportion of dissolved inorganic nitrogen accounted for by  $\text{NH}_4$  in the surface layer, in the concentration of  $\text{NH}_4$  in the bottom layer, in the potential turnover rate of urea in bottom water, in copepod respiration, and in microbial respiration. Anthropogenic nitrogen inputs potentially account for 24, 65, 26, and 113 percent of new nitrogen assimilated by phytoplankton during March, May, July, and November, respectively. Thus, anthropogenic nitrogen accounts for a large fraction of the input of new (allochthonous) nitrogen to the apex and is assimilated within the apex, except during November-January when productivity is low. However, given the importance of inputs of new nitrogen from adjacent coastal water and the importance of light as a factor limiting phytoplankton growth, increased nitrogen loading is unlikely to directly influence phytoplankton productivity in the apex but will influence the area over which productivity is high.

Phytoplankton production exceeds respiration by a factor of 3.5 during March, and it is likely that most production is exported from the apex. During July, production and respiration are in balance and most production is grazed while in the surface layer of the apex. Under these conditions, the organic input to bottom water and benthos (in the form of fecal pellets) due to copepod grazing alone is on the order of  $0.8 \times 10^6 \text{ kg C d}^{-1}$ . This is higher than inputs due to ocean dumping of sludge and dredge spoils combined ( $0.6 \times 10^6 \text{ kg C d}^{-1}$ ) and accounts for 37 percent of respiration below the pycnocline.

Evaluation of the fate of phytoplankton production and anthropogenic organic inputs suggest that anthropogenic inputs are less efficiently metabolized within the apex and contribute more to oxygen demand below the pycnocline. Thus, a major goal of waste management programs for coastal environments should be to limit or reduce the input of anthropogenic organic matter.

## 1.0 INTRODUCTION

### 1.01 Background

Anthropogenic inputs of nutrients to the coastal zone have increased rapidly over the last three decades as a consequence of increases in the rates of sewage production, agricultural fertilization, and urbanization (e.g., Milliman 1981; van Bennekom and Salomons 1981). For example, Walsh et al. (1981) estimate that the input of anthropogenic nitrogen has increased by an order of magnitude. Increases in the supply of nutrients such as nitrogen are likely to have significant effects on water quality, food chain dynamics, and fish yields, depending on how plankton populations respond in time and space.

The production and consumption of organic matter by primary and secondary producers less than 1 mm in size account for most material fluxes in marine ecosystem. Phytoplankton, because of their role as primary producers and their high cell surface area-to-volume ratios, play a central role in the flux of nutrients, organic matter, and associated pollutants. This is especially true in well-fertilized plume ecosystems, such as the apex of the New York Bight (Fig. 1) which receives the nutrient-rich discharge of the Hudson and Raritan Rivers. Phytoplankton production in this region (area = 1250 km<sup>2</sup>) is among the highest in the world's oceans, averaging 590 g C m<sup>-2</sup> yr<sup>-1</sup> (Malone et al. in press a) or 85 percent of particulate organic carbon inputs to the apex (Segar and Berberian 1976; Garside and Malone 1978). Productivity fluctuates between 0.1 and 10 g C m<sup>-2</sup> d<sup>-1</sup> depending on time of year and location within the apex (Malone 1976; Malone and Chervin 1979). Given the influence of such high and variable levels of phytoplankton productivity on water quality (dissolved oxygen concentration, turbidity, and distributions of biologically active pollutants) and fisheries, it is clear that the environmental regulation of phytoplankton productivity and the fate of the biomass produced must be understood for the development of a rational waste management program for the coastal zone.

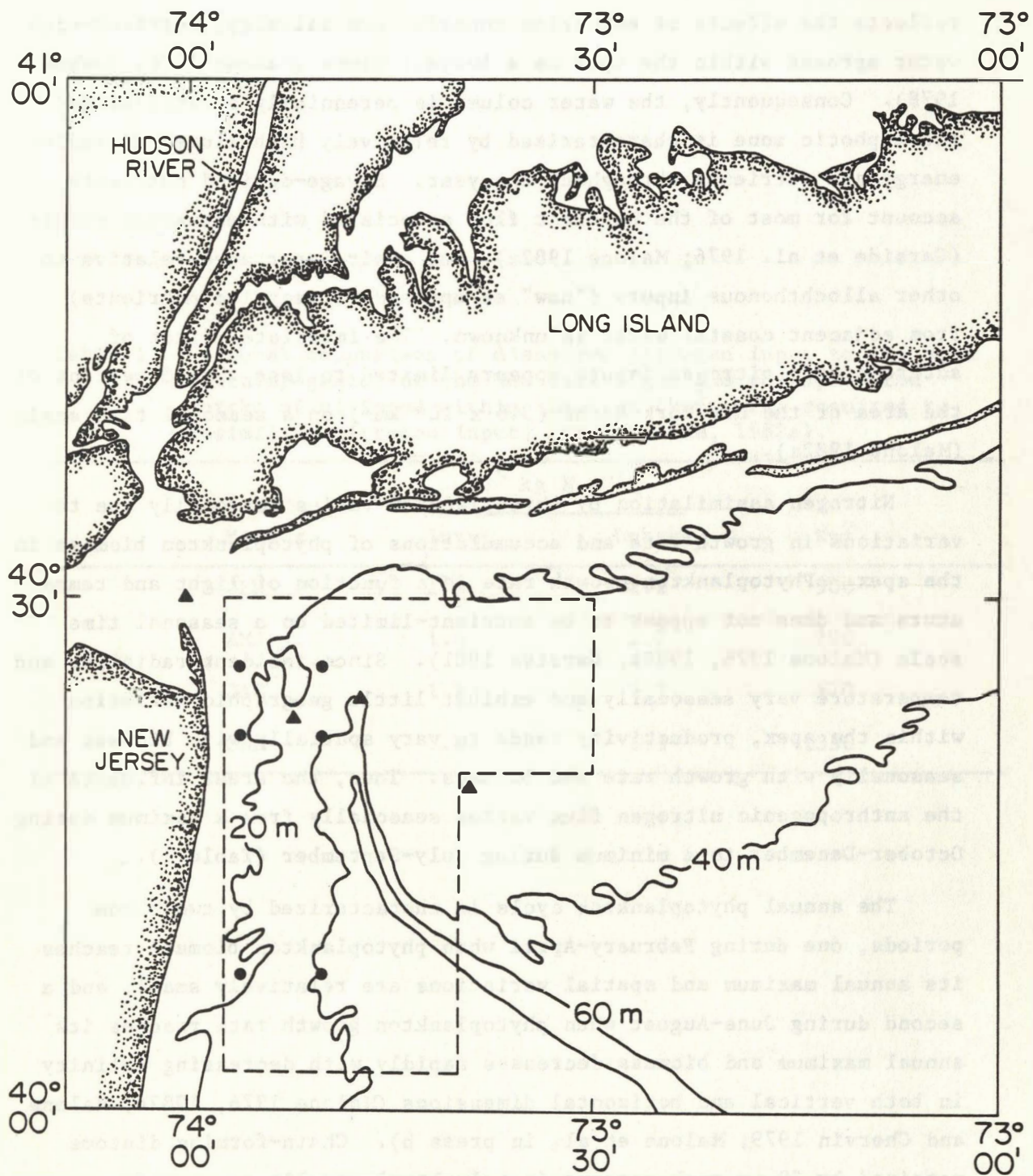


Figure 1. Reference stations (●, water column; ▲, benthic) and area within which drogues drifted (Bounded by dashed line). The apex is bounded to the south by 40°10'N and to the east by 73°30'W.

Phytoplankton production (biomass yield) in coastal environments is most often nitrogen-limited (Ryther and Dunstan 1971). High phytoplankton productivity in the apex relative to other coastal regions reflects the effects of estuarine runoff. Low salinity, nutrient-rich water spreads within the apex as a buoyant plume (Malone 1976; Bowman 1978). Consequently, the water column is perennially stratified and the euphotic zone is characterized by relatively high fluxes of radiant energy and nutrients throughout the year. Sewage-derived nutrients account for most of the nutrient flux associated with estuarine runoff (Garside et al. 1976; Malone 1982a), but their importance relative to other allochthonous inputs ("new" as opposed to recycled nutrients) from adjacent coastal water is unknown. The immediate effect of anthropogenic nitrogen inputs appears limited to less than 5 percent of the area of the New York Bight ( $3.6 \times 10^4 \text{ km}^2$ ) on a seasonal time scale (Malone 1982a).

Nitrogen assimilation by phytoplankton varies seasonally due to variations in growth rate and accumulations of phytoplankton biomass in the apex. Phytoplankton growth rate is a function of light and temperature and does not appear to be nutrient-limited on a seasonal time scale (Malone 1976, 1982b; Garside 1981). Since incident radiation and temperature vary seasonally and exhibit little geographic variation within the apex, productivity tends to vary spatially with biomass and seasonally with growth rate and biomass. Thus, the areal influence of the anthropogenic nitrogen flux varies seasonally from a maximum during October-December to a minimum during July-September (Table 1).

The annual phytoplankton cycle is characterized by two bloom periods, one during February-April when phytoplankton biomass reaches its annual maximum and spatial variations are relatively small, and a second during June-August when phytoplankton growth rate reaches its annual maximum and biomass decreases rapidly with decreasing salinity in both vertical and horizontal dimensions (Malone 1976, 1982b; Malone and Chervin 1979; Malone et al. in press b). Chain-forming diatoms retained by 20- $\mu\text{m}$  mesh screens (netplankton) usually account for most productivity during February-April, while small, solitary chlorophytes and microflagellates which are passed by 20- $\mu\text{m}$  mesh screens

Table 1. Seasonal comparison of dissolved nitrogen input to the apex (anthropogenic) of the New York Bight and phytoplankton uptake of nitrogen within the apex (km<sup>2</sup>, area required to assimilate nitrogen input) (from Malone, 1982a).

Months	10 <sup>5</sup> kg N d <sup>-1</sup>		Km <sup>2</sup>
	Input	Uptake	
JFM	1.6	2.2	900
AMJ	1.6	2.7	700
JAS	1.2	2.1	670
OND	1.6	1.5	1350

(nanoplankton) account for most productivity during June-August (Malone 1976; Malone and Chervin 1979). Variations in biomass are mainly related to growth rate and circulation patterns during the diatom bloom period and to growth rate and grazing patterns during the nanoplankton bloom period (Malone and Chervin 1979; Malone et al. in press b).

The "fate" of phytoplankton biomass produced in the apex and, therefore, its impact on water quality and fisheries, depends to a great extent on copepod grazing. That is, as the proportion of phytoplankton production grazed by copepods decreases, the proportion available for export and metabolism by microheterotrophs increases. This results in greater oxygen demand per unit input of organic matter and a smaller flux of organic matter (food) into food chains leading to commercial fisheries. Copepods account for more than 70 percent of the macrozooplankton in the apex (Malone 1976; Chervin 1978) and are a major link between primary producers and higher trophic levels. The seasonal cycle of copepod biomass is characterized by a winter minimum and a summer maximum, with peaks during spring and summer related to breeding and growth within the estuarine-apex system and peaks during fall due to onshore transport of larger, offshore populations (Chervin 1978). Rates of organic matter assimilation and respiration by copepods follow a similar annual cycle. Copepods assimilate up to 60 percent of phytoplankton production during summer, compared to less than 5 percent during winter.

Monthly oxygen and carbon budgets are strongly influenced by seasonal variations in phytoplankton productivity and zooplankton grazing, as well as by ocean dumping and episodes of high estuarine runoff. Garside and Malone (1978) calculated spatially averaged rates of water column and benthic respiration. Benthic oxygen demand in carbon equivalents ranged from 0.34 to 0.98 g C m<sup>-2</sup> d<sup>-1</sup> (annual mean = 0.70 g C m<sup>-2</sup> d<sup>-1</sup>), compared to measured rates of 0.36 to 0.63 g C m<sup>-2</sup> d<sup>-1</sup> (annual mean 0.50 g C m<sup>-2</sup> d<sup>-1</sup>) reported by Thomas et al. (1976). In both cases, benthic oxygen demand was lowest during February-April and highest during August-September, i.e., oxygen demand was correlated with temperature with a Q<sub>10</sub> of 1.3 to 2.4. High rates of benthic

oxygen demand also were associated with sewage sludge and dredge spoil dump sites (Thomas et al. 1976) and with periods of high estuarine runoff (Garside and Malone 1978). No relationship between benthic oxygen demand and phytoplankton productivity was found in either study. In contrast, water column respiration was unrelated to ocean dumping and estuarine runoff but was correlated with phytoplankton productivity, increasing from a winter minimum of  $0.22 \text{ g C m}^{-2} \text{ d}^{-1}$  to a summer maximum of  $2.28 \text{ g C m}^{-2} \text{ d}^{-1}$  (Garside and Malone 1978). Thus, particulate organic carbon inputs associated with ocean dumping and estuarine runoff appear to be metabolized mainly by benthic organisms while most phytoplankton production appears to be metabolized by zooplankton or exported from the apex.

#### 1.02 Objectives

The flux of sewage-derived nutrients from the New York metropolitan area represents a major and continuous input of new nutrients to the apex. The high level of phytoplankton productivity supported by this and other inputs of new nutrients is expressed in terms of oxygen demand, water clarity, food-chain dynamics, fish yields, and pollutant transport, depending on how the phytoplankton biomass produced is distributed in time and space and on the response of heterotrophic consumers to this production.

Previous studies have been concerned with variations in biological activity on a seasonal time scale (e.g., Malone 1976; Thomas et al. 1976). The information on annual cycles of biological activity and associated environmental parameters which resulted from these studies provided the framework required to perform the Synoptic Investigation of Nutrient Cycling (SINC) described herein. The general purpose of this field study was to determine the pathways and rates by which organic matter is produced and processed by organisms on time scales at which interactions between organisms and their environments actually occur. The extent to which variations in these pathways and rates were expressed in terms of the nutrient assimilation capacity of the plume is discussed. More specifically, major objectives were:

- (1) to identify sources and sinks of inorganic nutrients and organic matter,

(2) to determine how these sources and sinks vary on ecologically meaningful time and space scales, and

(3) to evaluate the influences of biological processes on the fluxes and distributions of inorganic nutrients, dissolved oxygen, and organic matter.

This report describes time- and space-dependent variations in biological processes that play a major role in the flux of carbon, nitrogen, and oxygen in the apex. These processes include phytoplankton productivity and nitrogen uptake, release of dissolved organic carbon (DOC) by phytoplankton, plankton respiration, and the assimilation and respiration of particulate organic matter by copepod populations. The emphasis on copepods reflects not only their importance as a major link between primary producers and higher trophic levels, but also their role in regulating the amount of organic matter available for export from the water column and for heterotrophic metabolism by microorganisms. In this context, the heterotrophic potential of bacterial populations was studied in both benthic and water column environments. Distributions of these processes and related environmental properties were determined during periods of environmental extremes with respect to incident radiation, temperature, vertical mixing, and estuarine runoff in order to evaluate the effects of these factors on the relationship between anthropogenic nutrient inputs and the production and fate of phytoplankton biomass.

A complete listing of data summarized in this report is available from the National Oceanographic Data Center.

## 2.0 METHODS

### 2.01 Sampling

The time and space scales on which measurements were made were established on the basis of the potential response times of key groups of organisms and the dominant scales of environmental variability to which these organisms are likely to respond. Since the residence time of water in the apex is on the order of five to ten days (Ketchum et al. 1951; Han and Niedrauer 1981); storm events occur every five to ten days on average (Walsh et al. 1978); and phytoplankton generation times

range between one and ten days on average (Malone and Chervin 1979), field studies of at least two weeks involving hourly and daily sampling were deemed necessary.

Cruises were conducted on the following dates: May 9-20, 1977 (SINC I); July 18-29, 1977 (SINC II); November 9-21, 1977 (SINC III); and March 5-16, 1978 (SINC IV). Cruises were timed to coincide with periods of high estuarine runoff (SINC I), high surface temperature and incident radiation (SINC II), low incident radiation (SINC III), and low temperature (SINC IV). In general, each cruise was just long enough to document the development or dissipation of biological responses to environmental perturbations but not the complete evolution of the response. We recommend that future studies of nutrient and plankton dynamics be conducted for at least three weeks to increase the probability of observing the complete evolution of phytoplankton blooms and associated plankton processes.

Eulerian and Lagrangian methods of sampling were used. Vertical distributions of properties were determined at fixed locations at the beginning and end of each cruise (Fig. 1). Horizontal distributions of chlorophyll a (an index of phytoplankton biomass) were determined from continuous, underway measurements of in vivo fluorescence at least once and usually two or three times during the course of each cruise. These measurements were used to define the structure of the plume before and after sequential measurements in time while following a drogue. The latter was done to establish biological time-series that could be used to study interactions between planktonic organisms and their environment on time scales at which cause-effect interactions are likely to occur. Given the importance of estuarine runoff as a nutrient source, we attempted to tag parcels of estuarine water as they moved into the apex and mixed with coastal water. Drogues were deployed with their sail set at five meters so that their movement would reflect the drift of surface water in the plume. Once deployed, measurements were made at three- to six-hour intervals within one hundred meters of the drogue until the time series was terminated.

The following properties were measured at reference stations: temperature and salinity (continuous CTD profiles), dissolved oxygen

and inorganic nutrients (discrete samples with Niskin bottles), chlorophyll a and particulate organic carbon and nitrogen (Niskin bottles), dissolved organic carbon (Niskin bottles), and the biomass and taxonomic composition of macrozooplankton (202- $\mu$ m mesh nets on paired half-meter frames). Once a drogue was launched, a 24-hour sampling cycle was initiated and continued throughout the period of each drogue study. Sampling routines were started at about sunrise (SR), mid-morning (MM), noon (N), sunset (SS), and midnight (MN) as follows:

SR	CTD Submersible pump Hydrocast 2
MM	CTD Submersible pump Submarine quantum meter Hydrocast 2
N	Hydrocast 1 Zooplankton tow 1 Zooplankton tow 2 CTD Submersible pump Hydrocast 2 Hydrocast 3
SS	CTD Submersible pump Hydrocast 2
MN	Zooplankton tow 1 CTD Submersible pump Hydrocast 2

A submersible pump was used to obtain continuous vertical profiles of in vivo chlorophyll fluorescence. Fluorescence, CTD, and quantum meter profiles were used to select the depths sampled on hydrocast 2. Three to six depths were sampled to collect water for most of the properties and rates measured (Table 2). Surface water for copepod grazing and respiration experiments was collected on hydrocast 1. Hydrocast 3 used sterile Niskin "butterfly" samplers to collect samples for measurements of heterotrophic potential, bacterial abundance, glycolate

Table 2. Measurements made on samples collected on Hydrocast 2 at three to six depths from near-surface to near-bottom (SR - sunrise, MM - midmorning, N - noon, SS - sunset, MN - midnight).

Measurements	Time of Day				
	SR	MM	N	SS	MN
<b>Rate Processes</b>					
Microbial respiration			X		X
Photosynthetic capacity	X		X		X
Primary productivity		X			
Inorganic nitrogen uptake		X			
<b>Properties</b>					
Temperature, salinity	X	X	X	X	X
Dissolved oxygen	X	X	X	X	X
Inorganic nutrients	X	X	X	X	X
Dissolved organic carbon	X	X	X	X	X
Particulate organic C,N	X	X	X	X	X
Chlorophyll <u>a</u>			X		X
Phytoplankton taxonomy		X			
Size frequency distributions			X		

concentration, and urea concentration. Zooplankton tow 1 was performed to collect samples for biomass and taxonomy; zooplankton tow 2 provided live copepods for grazing and respiration experiments.

Benthic samples for bacteriological analysis and measurements of sediment properties were collected at fixed stations (Fig. 1) and at stations occupied at noon along each drogue track. Samples were collected with either a Smith-McIntyre or Shipek grab. Subsamples for physical-chemical measurements (temperature, Eh, water content, dry weight, urea, glycolate, and ATP) and microbiological studies (bacterial abundance and heterotrophic potential) were collected immediately. The upper 1 to 5 cm of undisturbed sediment was subsampled with sterile 50 ml centrifuge tubes. Between 50 ml 450 g (wet weight) of sediment was suspended in sterile artificial sea water for subsequent microbial analyses (section 2.09).

## 2.02 Hydrographic Properties

Vertical profiles of temperature and conductivity were obtained with an InterOcean model 660 CSTD on SINC I and II and with a Plessey model 9040 CTD on SINC III and IV. Data were recorded by hand from a digital display on SINC I. A depth-driven, dual pen, strip-chart recorder was used to obtain continuous profiles on the remaining SINC cruises.

Samples for nutrient analysis were filtered through a Whatman GFC filter (after rinsing with sample water) directly into 128-ml wide-mouth Nalgene bottles. Two filtrates were collected for each depth sampled. One (80 ml) was frozen to  $-20^{\circ}\text{C}$ , transported on dry ice to the Bigelow Laboratory of Ocean Science, thawed, and analyzed for dissolved organic nitrogen, nitrate and nitrite, phosphate, and silicate. The samples were analyzed using a Technicon autoanalyzer system (Garside et al. 1976). The second filtrate (100 ml) was analyzed for ammonia within 1 hour of collection as described by Garside et al. (1978). Precision was  $\pm 0.10 \mu\text{g-at l}^{-1}$  or better for all measurements.

Dissolved oxygen was measured using the azide modification of the iodometric method except that 0.0375 N phenylarsine oxide was used in place of sodium thiosulfate (Kroner et al. 1964; U.S. Environmental

Protection Agency, 1974) All samples were collected in duplicate. Total alkalinity was measured as described by Strickland and Parsons (1972). A Corning model 130 pH meter calibrated against pH 4 and 7 buffers was used to measure pH.

Photosynthetically active radiation (PAR, 400-700 nm) was measured with a Lambda quantum sensor (Li-190S) and recorded with a digital integrator (Li-500). Downwelling PAR was measured with a submersible quantum sensor (Li-192S) and a Lambda Li-185 photometer equipped with a strip-chart recorder. Secchi disc measurements were made in conjunction with downwelling PAR profiles.

### 2.03 Dissolved Organic Matter

Samples for dissolved organic carbon (DOC) analysis were collected in 250 ml polyethylene bottles and filtered through combusted Whatman GF/C glass fiber filters. About 80 ml of filtrate was frozen to  $-20^{\circ}\text{C}$  in acid-washed and well rinsed (with filtrate) 100-ml narrow-mouth, glass bottles. DOC analyses were conducted by Dr. J. Sharp (University of Delaware). After thawing the samples to room temperature, 0.1 ml of phosphoric acid was added to each sample which was then bubbled with oxygen for 10 minutes. Three 5 ml aliquots were taken from each sample and placed into 10 ml combusted ampules containing 200 mg of potassium persulfate. After bubbling with oxygen for 10 seconds, the ampules were sealed and autoclaved at  $130^{\circ}\text{C}$  for 45 minutes, cooled, and analyzed with a Beckman model 865 infrared analyzer (precision  $\pm 0.05 \text{ mg l}^{-1}$ ). Standards were run every five to seven samples, and DOC concentrations were calculated from integrated areas.

Urea was measured (precision  $\pm 6 \text{ nM}$ ) following reaction with diacetylmonoxime thiosemicarbazide as described by Nakas and Litchfield (1976). The method of Shah and Wright (1974) was used to measure glycolic acid (precision  $\pm 10 \text{ nM}$ ).

### 2.04 Suspended Organic Matter

Surface and vertical (submersible pump) distribution of in vivo chlorophyll were determined by continuous fluorometry. Calibration samples were collected every 30 minutes during surface mapping and at the surface and bottom of each vertical profile. Chlorophyll a was

then measured in vitro as described below. All particulate measurements on discrete samples were made after filtration onto Gelman Type A-E glass fiber filters. Many samples were fractionated by pre-filtration through 20- $\mu\text{m}$  mesh screens so that quantitative estimates of the net- and nano-fractions could be made.

Extracted (90% acetone) chlorophyll a (precision  $\pm 0.1 \mu\text{g l}^{-1}$ ) was measured by fluorometry (Strickland and Parsons 1972). Particulate organic carbon ( $\pm 0.04 \text{ mg l}^{-1}$ ) and nitrogen ( $\pm 0.006 \text{ mg l}^{-1}$ ) were determined with a HP-185 CHN analyzer (Strickland and Parsons 1972). The frequency distribution of particle size between 2  $\mu\text{m}$  and 100  $\mu\text{m}$  was determined using a model TA Coulter counter equipped with 140- $\mu\text{m}$  and 280- $\mu\text{m}$  aperture tubes (Strickland and Parsons 1972). Phytoplankton samples were preserved with basic Lugol's solution and enumerated by the inverted microscope technique.

#### 2.05 Phytoplankton Photosynthesis

Nanoplankton ( $< 20 \mu\text{m}$ ) and netplankton ( $> 20 \mu\text{m}$ ) primary productivity were measured in duplicate using the fractionation and scintillation counting procedures described by Malone (1976). The photosynthetic production of particulate organic carbon was measured by the  $^{14}\text{C}$  technique (precision  $\pm 15 \mu\text{g C l}^{-1} \text{ d}^{-1}$ ). In situ primary productivity was estimated from 24-hour on deck incubations in sunlight using neutral density filters to simulate the range of light intensities to which phytoplankton were exposed in the euphotic zone. Photosynthetic capacity was determined on surface samples incubated for two hours at surface water temperature under light intensities of 4-420  $\mu\text{E m}^{-2} \text{ s}^{-1}$  (cool-white fluorescent). Estimates of DOC release by phytoplankton were made on filtrates from samples used to estimate particulate carbon production. Measurement of  $^{14}\text{C}$ -labelled DOC were made as described by Schindler et al. (1972) and modified by O'Reilly et al. (1976).

#### 2.06 Nitrogen Uptake by Phytoplankton

Uptake rates of nitrate and ammonia were estimated by the  $^{15}\text{N}$  technique (Barsdate and Dugdale 1965; Pavlou et al. 1974). Surface samples were transferred to 2-liter bottles equipped with silicone rubber stoppers. Duplicate bottles were inoculated with  $^{15}\text{NH}_3$  or  $^{15}\text{NO}_3$

resulting in an increase in concentration of 10  $\mu\text{M}$ . Samples were incubated for four to eight hours around local apparent noon, at sea surface temperature, under four to six levels of incident sunlight. Following incubation, samples were filtered through combusted type AE Gelman glass fiber filters and stored in an evacuated dessicator for analysis with an AEI-MS10 mass spectrometer.

#### 2.07 Microbial Respiration

Ten acid-washed and baked (232°C for one hour) 300-ml BOD bottles were filled with water from each depth sampled. Half were fixed immediately and dissolved oxygen measured as described in section 2.02. The remaining five bottles for a given depth were incubated in the dark at  $\pm 1^\circ\text{C}$  of in situ temperature for 12 (July) or 24 hours (March, May, November). The rate of oxygen consumption was calculated as the difference between the concentration of dissolved oxygen before and after the incubation period. Rates of respiration (precision  $\pm 1.3 \mu\text{g C l}^{-1} \text{ hr}^{-1}$ ) were calculated from the disappearance of oxygen and were converted to carbon assuming a respiratory quotient of 1.

#### 2.08 Macrozooplankton

Replicate zooplankton samples were obtained with paired half-meter, 202- $\mu\text{m}$  nets equipped with inner and outer TSK flowmeters. Nets were towed obliquely over the entire water column for five to thirty minutes, depending on the density of organisms. Half of each catch was preserved in 4 percent buffered formalin for enumeration and identification. The remaining half was briefly rinsed with distilled water and frozen for dry weight analysis. In the laboratory, copepods from the preserved samples were identified to species; all other organisms were identified to order or class. Samples for dry weight analysis were thawed, dried to constant weight at 60°C and weighed on a semi-micro balance after cooling in a desiccator.

Shipboard feeding experiments were conducted by incubating copepods for 24 hours (noon to noon) in 2.5 liter bottles strapped to a rotating wheel (3-5 rpm) and immersed in flowing seawater (Martin 1968). Water for incubations was collected from a depth of 2-3 m and passed through a 202- $\mu\text{m}$  mesh to remove macrozooplankton. Twenty to 100

copepods, obtained from a short tow in the upper 10 m, were added to each experimental bottle. Biomass-specific rates have been found to be unaffected by the concentration of organisms between 5 and 50 individuals liter<sup>-1</sup> (Chervin 1978). Assimilation per copepod was calculated from the difference between particulates (chlorophyll a, POC) in control bottles (no copepods added) and experimental bottles. The product of assimilation per copepod ( $\mu\text{g C copepod}^{-1} \text{d}^{-1}$ ) and copepod abundance in the water column (number m<sup>-3</sup>) yielded total rates of water column assimilation ( $\text{mg C m}^{-3} \text{d}^{-1}$ ).

Respiration per copepod was calculated from the change in oxygen over the incubation period. Oxygen concentrations were measured using a YSI oxygen probe. Rates of respiration were calculated from the disappearance of oxygen and converted to carbon assuming a respiratory quotient of 1. Rates of respiration per copepod ( $\mu\text{g C copepod}^{-1} \text{d}^{-1}$ ) were multiplied by copepod abundance to yield rates of water column respiration ( $\text{mg C m}^{-3} \text{d}^{-1}$ ).

## 2.09 Bacterial Biomass and Heterotrophic Potential

The abundance of heterotrophic bacteria was estimated from total colony-forming units (CFU) and by acridine orange direct counts ( $\pm 0.8 \log_{10}$  units) using the epifluorescence technique described by Hobbie et al. (1977). A low, nutrient-enriched seawater agar (ESWA) was the basic medium used to isolate bacteria (Litchfield et al. 1975). Selective media for organisms capable of growing on urea and glycolic acid were also used (Litchfield et al. 1976). Five replicates were run per treatment and incubated at 12-15°C. After 14 days, CFUs were enumerated weekly for up to 6 weeks or until the numbers stabilized (precision  $\pm 0.5 \log_{10}$  units).

The procedure of Wright and Hobbie (1966) as modified by Hobbie and Crawford (1969) was used to determine rates of heterotrophic uptake and decomposition of <sup>14</sup>C-labelled urea and glycolic acid ( $\pm 10$  percent). Glycolic acid was used because it apparently is released by phytoplankton and assimilated by bacteria (Fogg and Watt 1965; Wright and Shah 1975). Urea is distributed widely in coastal environments and is often an excretory product of higher animals (Remsen et al. 1974; Nakas and Litchfield 1976).

All samples were incubated in sealed 60-ml serum bottles at in situ temperatures  $\pm 2^{\circ}\text{C}$ . Three to four concentrations of each substrate were run in triplicate for three incubation periods. The  $^{14}\text{CO}_2$  given off during the course of incubations was absorbed by phenethylamine in filter paper suspended over the sample. Experiments were terminated by adding 1 ml of 2N  $\text{H}_2\text{SO}_4$ . Net uptake and respired  $^{14}\text{CO}_2$  were measured by the channels ratio method with a liquid scintillation counter. Samples for net uptake were filtered through 0.2- $\mu\text{m}$  Gelman Filters, washed with 2 ml of artificial seawater, and counted. Kinetic parameters were calculated from a linear transformation of the Michaelis-Menton equation when saturation kinetics were followed (Wright and Hobbie 1966). Controls for abiological decomposition included the addition of 1.0 ml 37 percent formaldehyde to serum bottles prior to adding the sample.

Since protein synthesis and turnover in eucaryotic organisms are inhibited by exposure to cycloheximide (Davis et al. 1972), experiments were run to evaluate the assumption that glycolate and urea were metabolized by procaryotic organisms (bacteria). Procaryotes accounted for more than 85 percent of the activity in all cases.

Sediment pH, Eh, percent moisture, and dry weight were determined as described by Litchfield et al. (1975). Following immediate extraction with 3N  $\text{H}_2\text{SO}_4$  and freezing, ATP was measured as described by Karl and LaRock (1975). Urea ( $\pm 6$  nM) was analyzed by the diacetylmonoxime thiosemicarbazide procedure (Nakas and Litchfield 1976) and glycolate ( $\pm 10$  nM) by the method of Shah and Wright (1974), except that  $^{14}\text{C}$ -glycolate was added as a tracer and sediments were extracted directly with  $\text{H}_2\text{SO}_4$ .

### 3.0 WATER COLUMN PROCESSES

#### 3.01 Seasonal Variation

The annual cycle of freshwater flow is characterized by a spring maximum and a summer minimum (Table 3). Monthly mean volume transport of freshwater in the Hudson River during 1977-1978 was similar to the long-term mean for 1947-1977. Volume flow of the Raritan River is less than 10 percent of the flow of the Hudson River (Duedall et al. 1979).

Table 3. Volume transport of freshwater  $\bar{Q}_f$  = 31-year mean flow of the Hudson River at Green Island;  $Q_f$  = mean flow at Green Island from January-March 1978 and from April-December 1977;  $(Q_f)_t$  = mean flow into the apex at the beginning of each cruise;  $(Q_f)_{t+1}$  = mean flow into the apex at the end of each cruise (flows into the apex were calculated as described by Hammond [1975] using a 14-day mean and assuming a 14-day lag [Stewart 1958]).

Month	$10^6 \text{ m}^3 \text{ d}^{-1}$			
	$\bar{Q}_f$	$Q_f$	$(Q_f)_t$	$(Q_f)_{t+1}$
Jan	47	64		
Feb	52	35		
Mar	81	54	90	80
Apr	104	100		
May	62	39	99	129
Jun	34	18		
Jul	22	14	24	21
Aug	18	13		
Sep	19	31		
Oct	25	74		
Nov	39	57	123	67
Dec	48	65		
Mean	46	47		

Volume transport of freshwater into the apex varied during and between cruises from a maximum of  $129 \times 10^6 \text{ m}^3 \text{ d}^{-1}$  toward the end of the May cruise, to a minimum of  $21 \times 10^6 \text{ m}^3 \text{ d}^{-1}$ , toward the end of the July cruise. Such fluctuations influence vertical and horizontal salinity and density gradients in the apex but do not affect the fluxes of dissolved inorganic nitrogen and phosphorus from the estuary (Garside et al. 1976; Simpson et al. 1977; Malone 1982a), i.e., since sewage wastes are the major source of nitrogen and phosphorus and phytoplankton uptake within the estuary is generally low, fluxes out of the estuary show little variation due to the compensating effect of flow and concentration.

Vertical and horizontal salinity gradients were present during all cruises. Surface water was generally 1-3 ‰ fresher than bottom water (Table 4), and horizontal gradients within the apex were characterized by differences of 1-8 ‰ (Fig. 2). Gradients in both dimensions were greatest when the volume transport of freshwater into the apex was high during May and November. These changes reflected variations in the minimum salinity near the mouth of the estuary rather than the maximum salinity along the seaward boundary of the study area.

While horizontal salinity gradients were well developed, temperature showed little horizontal variation compared to seasonal variations between cruises (Table 4). Surface temperatures increased from 0.9-2.78°C during March to 19.01-22.56°C during July. Bottom temperature varied over a smaller range, increasing from a minimum of 3.01°C during March to a maximum of 13.8°C during November. The seasonal thermocline was beginning to form during May and was breaking down during November. Thus, vertical density gradients were weakest during March due to wind mixing and the compensating effect of vertical temperature and salinity gradients on density. Vertical density gradients were strongest during May and July due to less frequent wind events and the additive effect of vertical temperature and salinity gradients on density.

Such variations in vertical stratification are important because they influence the average amount of light available for photosynthesis and the effect of plankton metabolism on the distribution of nutrients,

Table 4. Mean temperature (T, °C) and salinity (S, ‰) of the surface and bottom layers at reference stations (n = 6) at the beginning and end of each cruise (C = coefficient of variation).

Date	Surface layer				Bottom layer			
	T	C	S	C	T	C	S	C
6 Mar	0.90	64%	30.53	4%	3.01	62%	32.35	2%
15 Mar	2.78	10%	31.12	2%	3.08	15%	32.31	1%
9 May	9.05	1%	30.87	3%	6.71	22%	32.80	2%
19 May	13.22	6%	29.81	6%	6.09	15%	32.85	1%
19 July	22.56	4%	30.30	2%	11.88	9%	32.45	1%
28 July	19.01	10%	30.91	3%	11.05	11%	32.52	1%
9 Nov	13.79	1%	29.64	8%	13.80	1%	31.65	2%
20 Nov	11.56	2%	30.75	6%	7.45	87%	33.56	4%

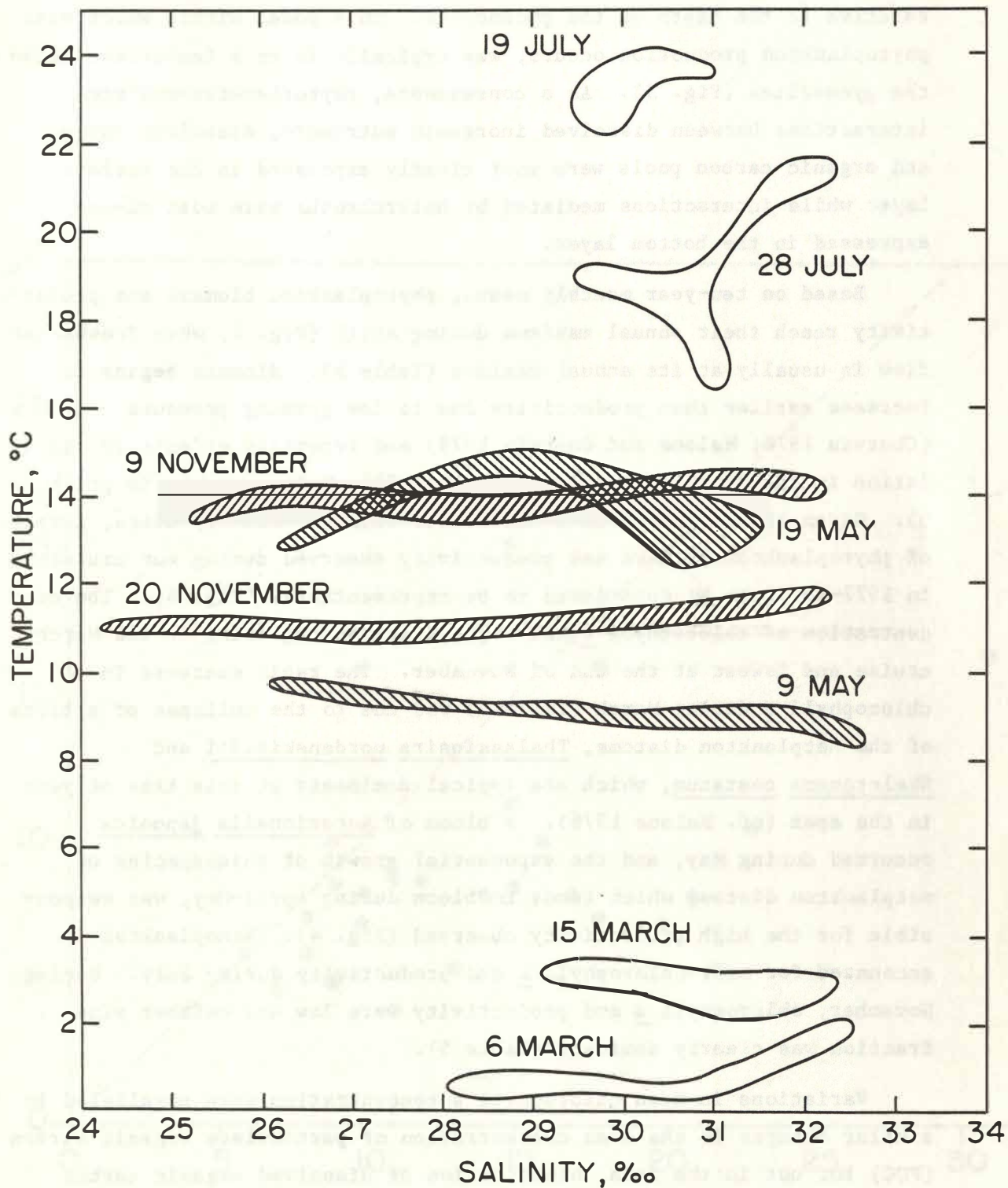


Figure 2. Temperature-salinity envelopes for surface water at reference stations sampled at the beginning and end of each cruise.

oxygen, and organic matter. Of particular importance in this regard is the depth of the euphotic zone (surface to the one percent light depth) relative to the depth of the pycnocline. This zone, within which most phytoplankton production occurs, was typically in or a few meters above the pycnocline (Fig. 3). As a consequence, phytoplankton-mediated interactions between dissolved inorganic nutrients, dissolved oxygen, and organic carbon pools were most clearly expressed in the surface layer while interactions mediated by heterotrophs were most clearly expressed in the bottom layer.

Based on ten-year monthly means, phytoplankton biomass and productivity reach their annual maximum during April (Fig. 4) when freshwater flow is usually at its annual maximum (Table 3). Biomass begins to increase earlier than productivity due to low grazing pressure (Chervin 1978; Malone and Chervin 1979) and retention effects of circulation in the apex (Charnell and Hansen 1974; Malone et al. in press b). Given the large variance associated with the monthly means, levels of phytoplankton biomass and productivity observed during our cruises in 1977-1978 can be considered to be representative (Fig. 4). The concentration of chlorophyll a was highest at the beginning of the March cruise and lowest at the end of November. The rapid decrease in chlorophyll a during March (Table 5) was due to the collapse of a bloom of the netplankton diatoms, Thalassiosira nordenskioldii and Skeletonema costatum, which are typical dominants at this time of year in the apex (cf. Malone 1976). A bloom of Asterionella japonica occurred during May, and the exponential growth of this species of netplankton diatom, which tends to bloom during April-May, was responsible for the high productivity observed (Fig. 4). Nanoplankton accounted for most chlorophyll a and productivity during July. During November, chlorophyll a and productivity were low and neither size fraction was clearly dominant (Table 5).

Variations in mean chlorophyll a concentration were paralleled by similar changes in the mean concentration of particulate organic carbon (POC) but not in the mean concentration of dissolved organic carbon (DOC). Thus, variations in mean POC were related to variations in chlorophyll a in both surface and bottom layers, except during November when POC was generally higher than expected based on chlorophyll a,

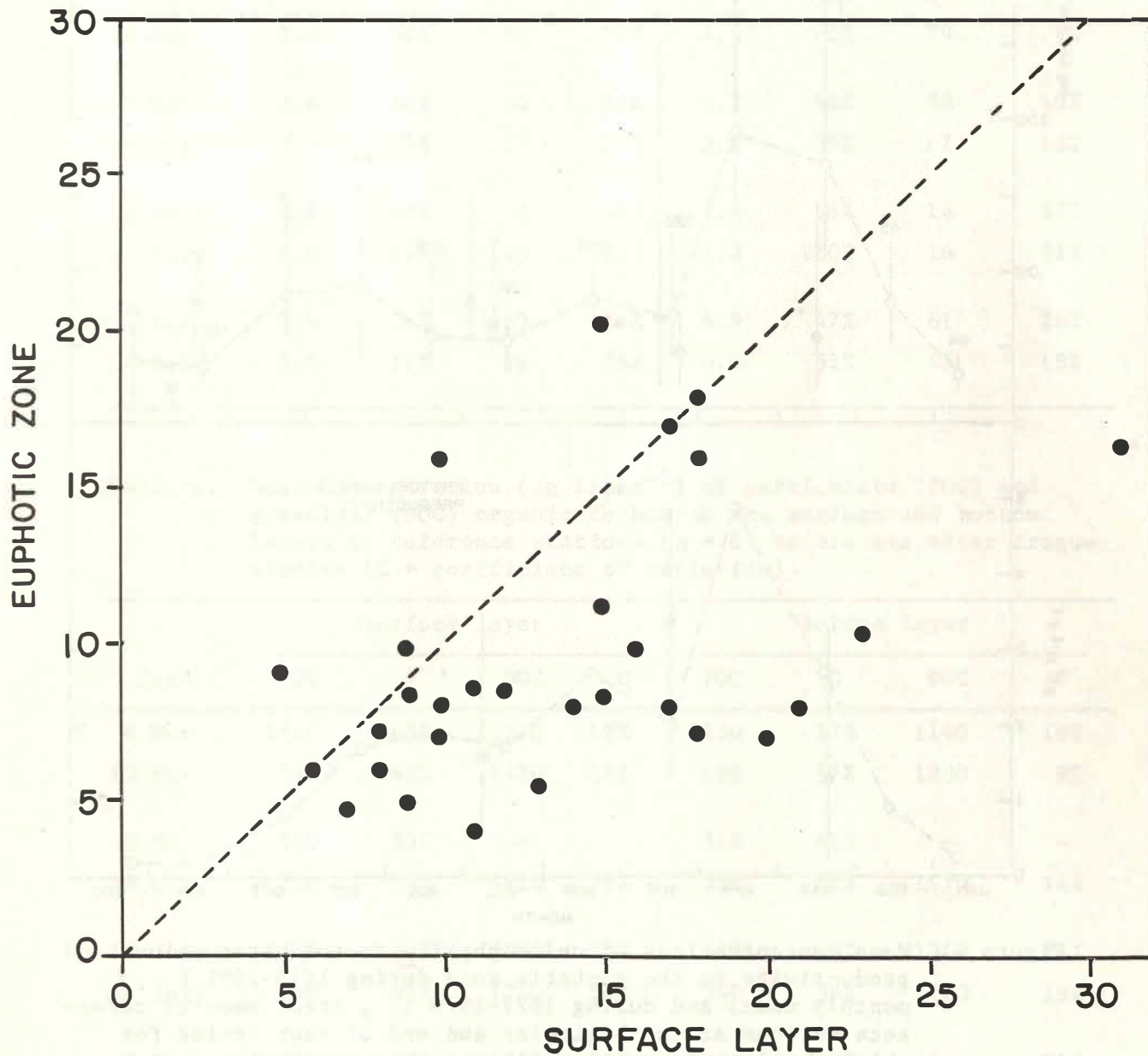


Figure 3. Relationship between depth (meters) of the euphotic zone (one percent light depth) and depth of the surface layer (depth of maximum gradient in the pycnocline).

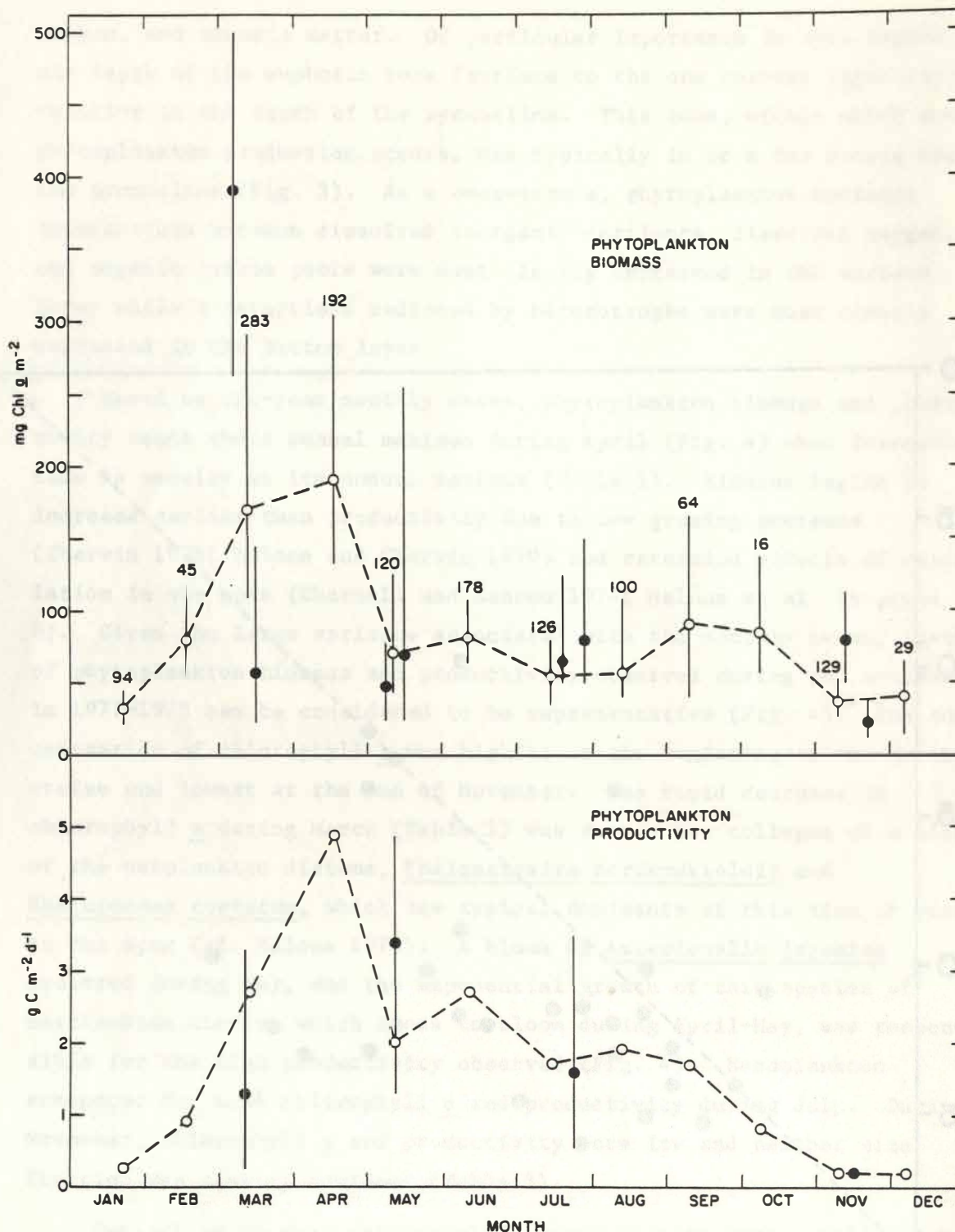


Figure 4. Mean concentrations of chlorophyll a in the water column and productivity in the euphotic zone during 1973-1981 (○, monthly mean) and during 1977-1978 (●, areal mean of reference stations at the beginning and end of each cruise for chlorophyll a and mean of all measurements during each cruise for productivity) (geometric mean  $\pm$  95% confidence limits; numbers above confidence bars indicate the number of samples used to calculate means).

Table 5. Mean concentration ( $\mu\text{g liter}^{-1}$ ) of chlorophyll a and the proportion of chlorophyll a accounted for by netplankton in the surface and bottom layers at reference stations (n = 6) at the beginning and end of each cruise (C = coefficient of variation).

Date	Surface layer				Bottom layer			
	Chl	C	Percent net	C	Chl	C	Percent net	C
6 Mar	18.0	55%	90	5%	19.2	43%	89	4%
15 Mar	3.2	97%	64	36%	4.8	80%	79	5%
9 May	3.6	62%	50	23%	2.2	96%	38	40%
19 May	5.5	177%	59	37%	2.2	95%	67	18%
19 July	6.1	68%	3	41%	1.0	56%	14	37%
28 July	8.0	67%	10	187%	1.2	130%	16	92%
9 Nov	3.4	26%	59	12%	4.9	47%	61	28%
20 Nov	1.2	37%	28	55%	0.9	52%	45	18%

Table 6. Mean concentration ( $\mu\text{g liter}^{-1}$ ) of particulate (POC) and dissolved (DOC) organic carbon in the surface and bottom layers at reference stations (n = 6) before and after drogue studies (C = coefficient of variation).

Date	Surface layer				Bottom layer			
	POC	C	DOC	C	POC	C	DOC	C
6 Mar	1510	48%	1270	19%	1250	37%	1140	18%
15 Mar	550	45%	1420	16%	490	57%	1230	9%
9 May	540	33%	-	-	560	41%	-	-
19 May	770	74%	1850	21%	390	41%	1470	14%
19 July	1050	39%	2060	23%	420	45%	1350	24%
28 July	940	45%	1750	14%	340	59%	1160	13%
9 Nov	940	43%	1350	33%	1950	78%	1580	21%
20 Nov	520	40%	1490	21%	470	28%	1200	14%

especially in the bottom layer. POC and DOC concentrations varied over comparable ranges, POC from 0.1 to 4.4 mg liter<sup>-1</sup> and DOC from 0.4 to 3.2 mg liter<sup>-1</sup>, although POC was more variable than DOC during any given cruise (Table 6). POC concentrations were highest in the surface layer during March and July and in the bottom layer during March and November. DOC concentrations were highest in the surface layer during July and in the bottom layer during November. These concentrations are high compared to other continental shelf environments where POC and DOC are typically less than 2.0 mg liter<sup>-1</sup> and 2.5 mg liter<sup>-1</sup>, respectively (Menzel and Ryther 1970; Riley 1970; Fredericks and Sackett 1970; Haines and Dunstan 1975).

Similarly, the concentration of dissolved inorganic nutrients was influenced by phytoplankton uptake and heterotrophic regeneration. Mean concentrations of ammonium and phosphate were lowest in the surface layer at the beginning of the March cruise and highest in the bottom layer during July (Table 7). Mean silicate concentration was also highest in the bottom layer during July and was lowest in the surface layer at the end of the May cruise. Silicate was also near depletion during March. Mean nitrate concentration was low in the surface layer at the beginning of the July cruise and high in the surface layer during November. Low concentrations of phosphate (March), silicate (May), and nitrate (July) in the surface layer coincided with high phytoplankton biomass and reflect high rates of phytoplankton uptake within the plume relative to inputs to the plume (sections 3.03 and 3.04). High concentrations of ammonium, phosphate, and silicate in the bottom layer during July were probably the result of high rates of regeneration relative to uptake.

Nutrient ratios based on ambient concentrations give a further indication of patterns of nutrient depletion and regeneration (Table 8). Nutrient ratios in the surface layer indicate which nutrient element is most likely to limit phytoplankton production in the event of a bloom (cf. Ryther and Dunstan 1971). Biomass ratios of N:P are usually 10:1 to 15:1 for nutrient-saturated phytoplankton. Ratios of Si:N are usually 1:1 to 2:1 in nutrient-saturated diatom populations. Thus, phosphorus and silicon were potentially limiting during March;

Table 7. Mean concentration ( $\mu\text{g-at liter}^{-1}$ ) of inorganic nutrients in surface (S) and bottom (B) layers at reference stations (n = 6) before and after drogue studies.

Date	Layer	NO <sub>3</sub>	C	NH <sub>4</sub>	C	PO <sub>4</sub>	C	SiO <sub>4</sub>	C
6 Mar	S	2.44	76%	1.00	11%	0.03	139%	1.22	19%
	B	4.16	54%	1.62	40%	0.67	82%	2.65	57%
15 Mar	S	2.94	41%	1.79	14%	0.17	70%	0.90	21%
	B	3.00	33%	2.03	22%	0.72	70%	1.55	41%
9 May	S	1.52	151%	2.04	67%	1.86	25%	1.86	67%
	B	0.65	56%	3.00	63%	2.56	19%	5.84	10%
19 May	S	1.15	213%	1.72	32%	1.18	24%	0.15	188%
	B	1.75	60%	4.85	26%	3.35	23%	7.23	20%
19 July	S	0.16	171%	1.49	39%	1.64	33%	2.79	59%
	B	2.04	23%	7.10	36%	3.52	16%	15.22	12%
28 July	S	2.98	81%	4.31	67%	4.24	57%	9.25	38%
	B	3.06	19%	7.68	16%	5.21	22%	19.08	16%
9 Nov	S	6.02	84%	7.10	85%	2.31	25%	8.08	53%
	B	2.00	40%	2.88	41%	2.06	25%	4.62	13%
20 Nov	S	7.45	87%	7.33	65%	2.96	23%	9.17	56%
	B	3.81	16%	3.30	58%	1.03	25%	6.26	6%

Table 8. Mean proportion of ammonium in the dissolved inorganic nitrogen pool (% NH<sub>4</sub>) and atomic ratios of dissolved inorganic nitrogen to phosphate-phosphorus (N:P) and silicate-silicon to dissolved inorganic nitrogen (Si:N) in the surface and bottom layers at reference stations (n = 6) at the beginning and end of each cruise.

Date	Surface layer			Bottom layer		
	% NH <sub>4</sub>	N:P	Si:N	% NH <sub>4</sub>	N:P	Si:N
6 Mar	29	115	0.3	28	9	0.5
15 Mar	38	28	0.2	40	7	0.3
9 May	57	2	0.5	82	1	1.6
19 May	60	2	0.1	73	2	1.1
19 July	90	1	1.8	78	3	1.7
28 July	59	2	1.3	72	2	1.8
9 Nov	54	6	0.6	59	2	1.0
20 Nov	50	5	0.6	46	4	0.9

Table 9. Percent oxygen saturation (C = coefficient of variation) in the surface and bottom layers at reference stations (n = 6) at the beginning and end of each cruise.

Date	Surface layer		Bottom layer	
	Mean	C	Mean	C
6 Mar	108	3%	104	4%
15 Mar	106	3%	98	3%
9 May	102	2%	85	5%
19 May	123	11%	82	8%
19 July	119	12%	56	14%
28 July	93	20%	58	13%
9 Nov	96	5%	91	3%
20 Nov	96	4%	92	2%

silicon was potentially limiting during May; and nitrogen was potentially limiting during July.

The proportion of dissolved inorganic nitrogen accounted for by ammonium gives an indication of nitrogen regeneration in situ. Ammonium in the surface layer increased from 29 percent in March to 90 percent in July (Table 8). Variations between cruises were correlated with temperature ( $r^2 = 0.82$ ), suggesting that regeneration rates were temperature-dependent as has been reported for the apex based on monthly observations (Malone 1976). In the bottom layer, where phytoplankton uptake is negligible, temperature also accounted for 90 percent of the variation in ammonium concentration ( $Q_{10} = 2.02$ ) and 78 percent of the variation in phosphate concentration ( $Q_{10} = 2.04$ ), excluding November when estuarine export and mixing predominated over biological processes (sections 3.03 and 3.04). Such temperature-dependent annual cycles of regeneration are consistent with the development of large accumulations of phytoplankton biomass over the continental shelf during winter and early spring (Malone and Chervin 1979; Malone et al. in press a,b), with the annual cycle of benthic oxygen demand (Garside and Malone 1978), and with the annual cycle of grazing and respiration by copepods (Chervin 1978; Malone and Chervin 1979; Chervin et al. 1981).

Patterns of nutrient depletion and regeneration were also reflected in distributions of dissolved oxygen as deviations from 100 percent saturation (Table 9). Surface water was supersaturated on average during March, May, and July when nutrients were low and phytoplankton biomass was high. Under these conditions, percent saturation was negatively correlated with nutrient concentration (Table 10). Silicate, the nutrient most likely to be limiting during March and May, decreased in concentration as percent saturation increased above 100 percent. Likewise, percent saturation increased as ammonium was depleted during July (beginning of cruise). When nutrient concentrations were high during July (end of cruise) and November, oxygen concentration was at or below saturation and correlations between percent saturation and nutrient concentration were not found.

Table 10. Correlation and linear regression analyses of percent oxygen saturation on nutrient concentration ( $\mu\text{g-at liter}^{-1}$ ) in surface and bottom layers at reference stations ( $n = 12$ ,  $r^2 =$  coefficient of determination,  $a =$  intercept,  $b =$  slope). Of the major nutrients, only these were significantly correlated with percent saturation.

Date	Nutrient	$r^2$	a	b
6 Mar	silicate	0.85	114	-5.9
15 Mar	silicate	0.81	114	-12.2
9 May	silicate	0.69	114	-7.2
19 May	silicate	0.88	125	-6.7
19 July	ammonium	0.82	108	-6.5
28 July	ammonium	0.85	115	-8.2

Dissolved oxygen in bottom water decreased from near saturation during March to less than 60 percent saturation during July. This decline occurred as the seasonal thermocline began to form, was inversely correlated with temperature ( $r^2 = 0.98$ ,  $Q_{10} = 2.34$ ), and coincided with increases in bottom concentrations of ammonium and phosphate. Thus, low saturation levels of dissolved oxygen were not only a consequence of increased vertical stratification (isolation from atmospheric oxygen) but were also due to an increase in the rate of respiratory oxygen consumption below the pycnocline (benthic and water column).

Given this overview of seasonal variation, the remainder of this report is concerned primarily with variations on a time scale of hours to days during environmental extremes with respect to incident radiation (November - May, July), temperature (March - July), freshwater flow (May, November - July), and vertical mixing (March, November - May, July).

### 3.02 Drogue Tracks

Drogues were deployed near the mouth of the Hudson-Raritan estuary in the general vicinity of the northernmost reference stations (Fig. 1). A total of eighteen drogue studies lasting from 10 to 69 hours were completed (Table 11). Of these, nine were recovered because they drifted out of the study area (usually into the surf zone), four because of ship traffic and other logistic reasons, one because of heavy seas, and four because the ship had to return to port. Net speed of drift ranged from 0.7 to 30.3 km d<sup>-1</sup>, compared to 2 to 4 km d<sup>-1</sup> estimated from salt balance calculations (Ketchum et al. 1951). A wider range of drift speeds from short-term drogue studies was expected since salt balance calculations integrate over the water column and tend to minimize local effects of tides and episodic wind events. Drift was generally to the southwest at intermediate speeds (1 to 15 km d<sup>-1</sup>) during March and July, to the north at slower speeds (1 to 10 km d<sup>-1</sup>) during May, and to the east at high speeds (23 to 30 km d<sup>-1</sup>) during November.

Table 11. Drogue studies (Time = length of study, hours; Speed = net speed, km d<sup>-1</sup>; Head = compass heading for the direction of net drift).

Study	Date	Launched		Recovered		Time	Speed	Head
		Latitude	Longitude	Latitude	Longitude			
1	6 Mar	40°21.8'	73°50.9'	40°00.1'	73°50.6'	69.0	14.3	180°
2	9	40°22.0'	73°51.0'	40°23.0'	73°55.4'	47.0	3.3	290°
3	12	40°25.0'	73°51.9'	40°21.4'	73°57.8'	21.0	10.1	240°
4	13	40°21.9'	73°50.7'	40°23.8'	73°57.0'	15.0	14.9	290°
1	10 May	40°24.9'	73°55.0'	40°20.2'	73°56.2'	32.5	6.8	200°
2	12	40°25.0'	73°52.2'	40°24.8'	73°49.5'	10.2	8.7	70°
3	13	40°25.0'	73°52.7'	40°27.5'	73°51.7'	21.3	5.6	20°
4	14	40°19.8'	73°54.9'	40°20.5'	73°54.8'	52.2	0.7	05°
5	16	40°21.4'	73°52.5'	40°25.6'	73°51.2'	17.5	9.6	15°
6	17	40°20.0'	73°52.7'	40°23.5'	73°54.3'	51.2	3.2	340°
1	19 Jul	40°22.1'	73°52.7'	40°19.4'	73°58.3'	17.5	12.7	240°
2	20	40°22.0'	73°50.1'	40°15.5'	73°58.8'	33.0	12.8	230°
3	22	40°22.0'	73°45.0'	40°21.1'	73°45.6'	54.8	1.2	240°
4	26	40°22.0'	73°50.0'	40°16.9'	73°54.5'	40.0	7.2	220°
1	10 Nov	40°24.0'	73°52.8'	40°23.7'	73°28.2'	28.0	29.4	90°
2	16	40°24.0'	73°52.8'	40°30.6'	73°31.2'	34.0	22.9	65°
3	17	40°24.0'	73°52.7'	40°22.4'	73°33.0'	22.0	30.3	95°
4	18	40°24.0'	73°52.6'	40°20.7'	73°36.4'	18.5	30.1	95°

While circulation in the apex is complex and poorly understood, net drogue velocities illustrate some of the general features. Drift to the southwest during March and July reflected the prevailing drift of low salinity water along the coast of New Jersey (Bowman and Wunderlich 1976). Drift to the north during May was probably due to the effect of the anticyclonic (clockwise) gyre present in the apex (Charnell and Hansen 1974), i.e., drogues were influenced by the western limb of the gyre. Rapid easterly drift of the drogues during November was observed during a period of persistent westerly wind (10 to 15 m s<sup>-1</sup>) following two days of gale force northeasterly wind during November 7-8. Westerly wind favors offshore (easterly) transport of surface water (Hopkins and Dieterle in press), which is consistent with the drogue velocities observed during this period.

### 3.03 Hydrography

March 1978: Surface water in the study area became saltier and warmer during the period of observation (Fig. 2). Although freshwater transport into the apex decreased somewhat during the study period (Table 3), this trend was largely a consequence of the northerly wind that prevailed (5 to 10 m s<sup>-1</sup>) throughout most of the cruise. Northerly wind favors southward flow and onshore Ekman transport of surface water (Beardsley et al. 1976; Hopkins and Dieterle in press) which would have the effect of transporting warmer, more saline water into the region.

The first time series was continued for three days as the drogue drifted south down the axis of the plume. The second time series lasted for two days as the drogue drifted onshore normal to the axis of the plume. During the first time series, surface water salinity decreased by 1.3 ‰, from less than 31.0 ‰ near the mouth of the estuary to greater than 32.0 ‰ downstream (Fig. 5). As surface salinity increased, vertical salinity (Fig. 5) and density (Fig. 6) gradients decreased until the water column was vertically homogeneous. The reverse occurred during the second time series. Vertical gradients became more pronounced as salinity decreased and the drogue drifted onshore across the axis of the plume.

Of the major nutrients, nitrate and ammonium were present in excess relative to phosphate and silicate. For the most part, silicate

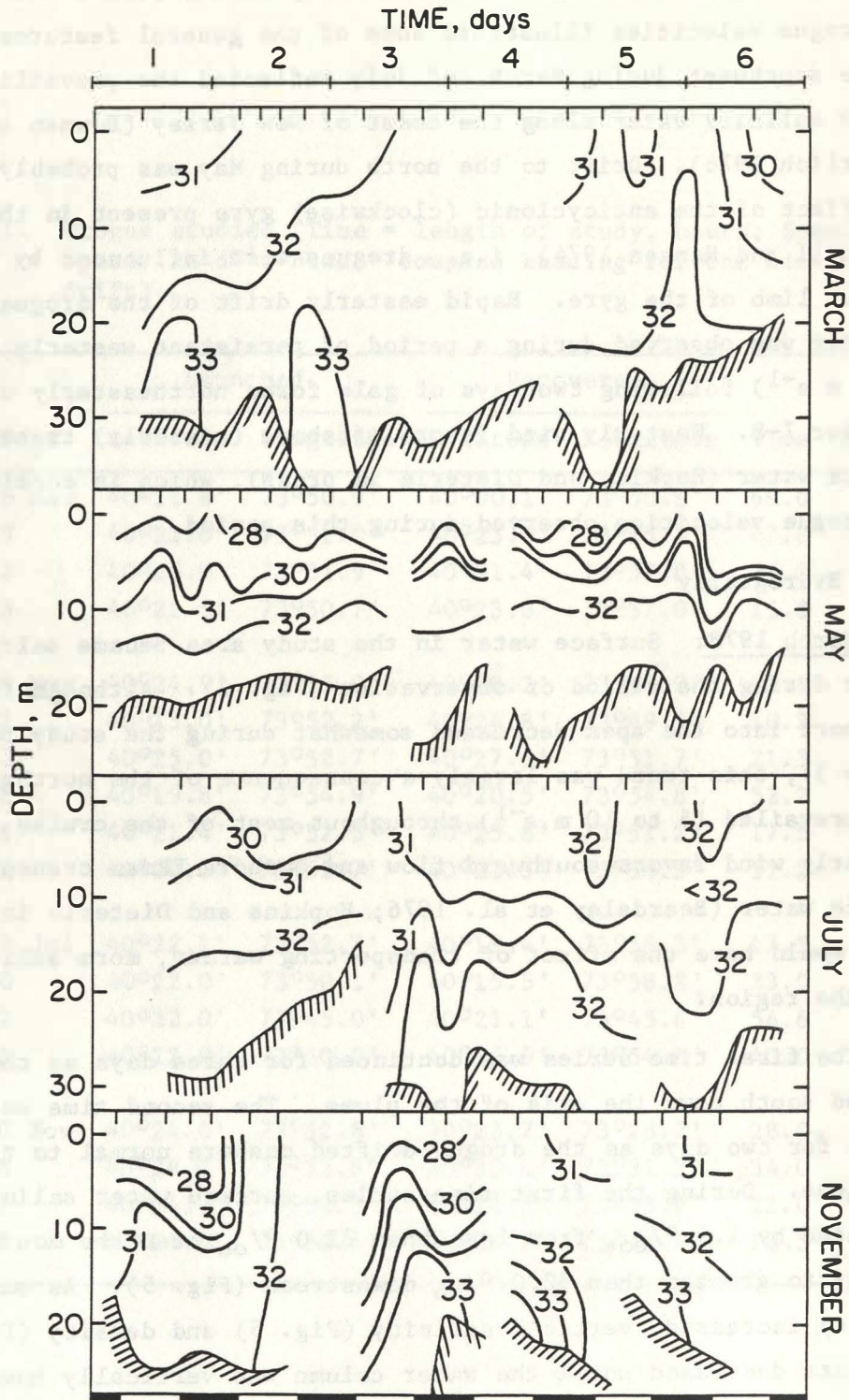


Figure 5. Vertical distribution of salinity ( $^{\circ}/_{\infty}$ ) during March (drogues 1 and 2), May (drogues 4, 5, and 6), July (drogues 2, 3, and 4), and November (drogues 1, 2, 3, and 4); see Table 11 for dates and positions.

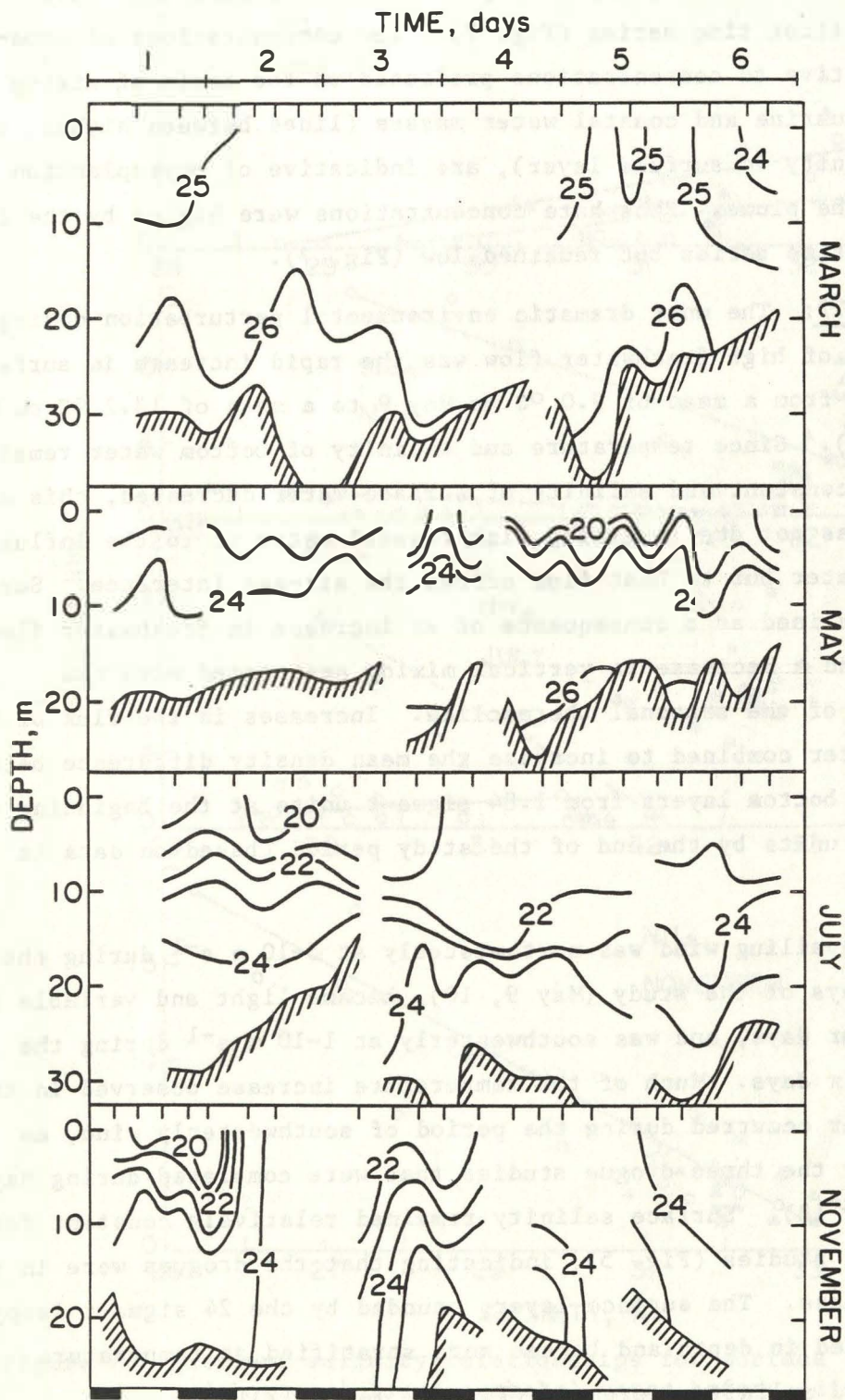


Figure 6. Vertical distribution of sigma-t as in Fig. 5.

concentrations were 1-2  $\mu\text{g-at liter}^{-1}$  when salinity was less than 32 ‰ and 1-5  $\mu\text{g-at liter}^{-1}$  at higher salinities. Phosphate was frequently undetectable, especially at salinities less than 31.5 ‰ during the first time series (Fig. 7). Low concentrations of phosphate, relative to concentrations predicted on the basis of mixing between estuarine and coastal water masses (lines between highest and lowest salinity in surface layer), are indicative of phytoplankton uptake in the plume. Phosphate concentrations were higher by the third and fourth time series but remained low (Fig. 7).

May 1977: The most dramatic environmental perturbation during this period of high freshwater flow was the rapid increase in surface temperature from a mean of 9.0 °C on May 9 to a mean of 13.2 °C on May 19 (Table 4). Since temperature and salinity of bottom water remained relatively constant and salinity of surface water decreased, this warming trend was not due to mixing with coastal water or to the influx of estuarine water but to heat flux across the air-sea interface. Surface salinity declined as a consequence of an increase in freshwater flow (Table 3) and a decrease in vertical mixing associated with the development of the seasonal thermocline. Increases in the flux of heat and freshwater combined to increase the mean density difference between surface and bottom layers from 1.84 sigma-t units at the beginning to 3.5 sigma-t units by the end of the study period (based on data in Table 4).

The prevailing wind was northwesterly at 5-10  $\text{m s}^{-1}$  during the first two days of the study (May 9, 10), became light and variable for the next four days, and was southwesterly at 1-10  $\text{m s}^{-1}$  during the remaining six days. Much of the temperature increase observed in the surface layer occurred during the period of southwesterly wind, as indicated by the three drogoue studies that were completed during May 14 to 19 (Table 12). Surface salinity remained relatively constant during these drogoue studies (Fig. 5), indicating that the drogues were in the same water mass. The surface layer, bounded by the 24 sigma-t isopycnal, decreased in depth and became more stratified as temperature increased and salinity decreased (Fig. 6, Table 12).

Nutrient concentrations in the surface layer were high and variable until May 14-15 when ammonium and silicate began to decline (Table

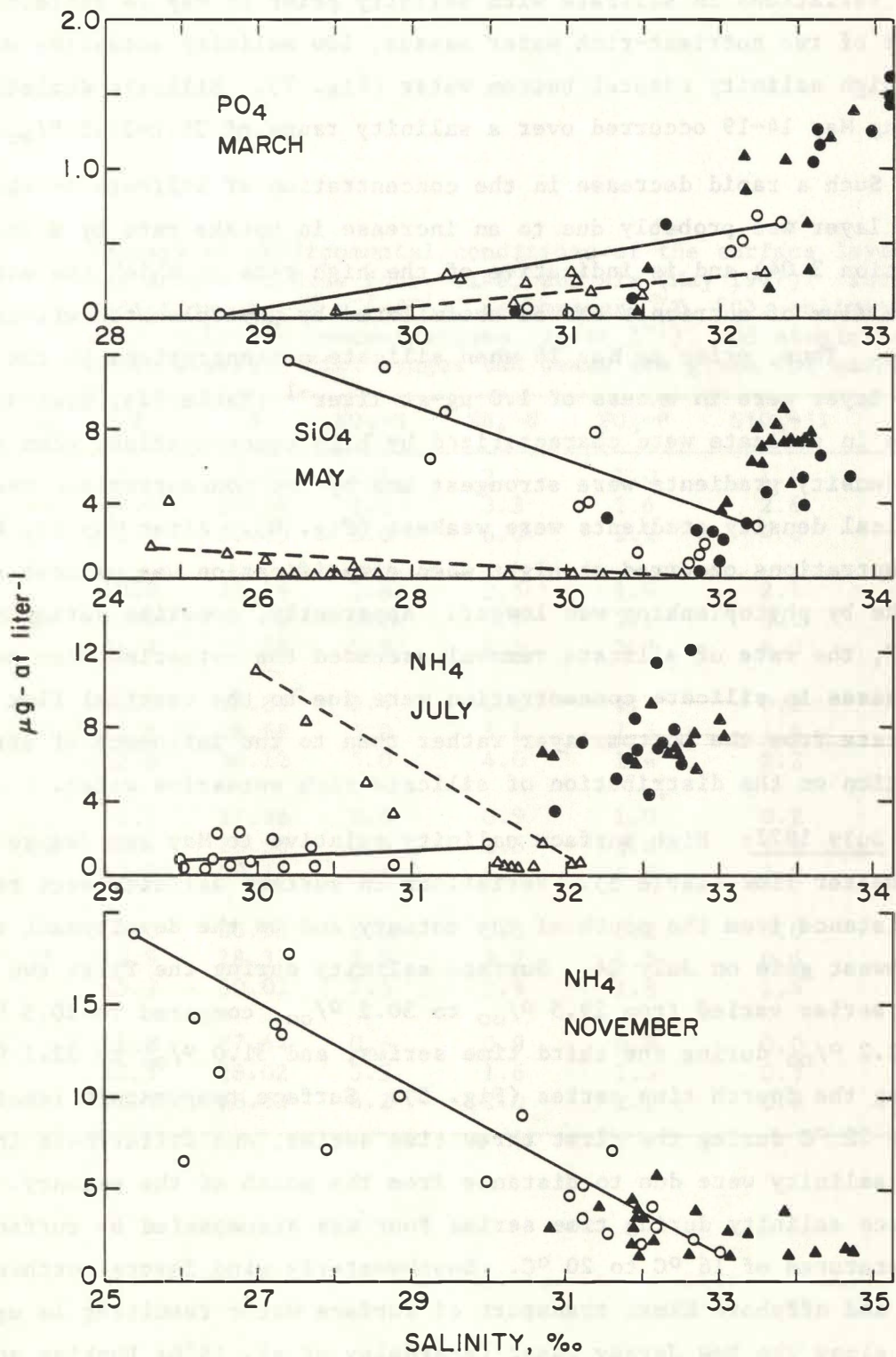


Figure 7. Nutrient-salinity relationships for surface (open symbols) and bottom (closed symbols) water before (circles) and after (triangles) drogue studies; lines indicate predicted conservative distributions.

12). Silicate decreased most rapidly and was nearly depleted by May 18. Variations in silicate with salinity prior to May 14 reflected the input of two nutrient-rich water masses, low salinity estuarine water and high salinity coastal bottom water (Fig. 7). Silicate depletion during May 14-19 occurred over a salinity range of 26.1-31.5 ‰.

Such a rapid decrease in the concentration of silicate in the surface layer was probably due to an increase in uptake rate by diatoms (section 3.04) and is indicative of the high rate at which the estuarine flux of nutrients can be assimilated by phytoplankton within the plume. Thus, prior to May 16 when silicate concentrations in the surface layer were in excess of  $1.0 \mu\text{g-at liter}^{-1}$  (Table 12), diel variations in silicate were characterized by high concentrations when vertical density gradients were strongest and by low concentrations when vertical density gradients were weakest (Fig. 8). After May 16, high concentrations occurred at night when stratification was weakest and uptake by phytoplankton was lowest. Apparently, sometime during May 16-17, the rate of silicate removal exceeded the estuarine flux so that increases in silicate concentration were due to the vertical flux of silicate from the bottom layer rather than to the influence of stratification on the distribution of silicate-rich estuarine water.

July 1977: High surface salinity relative to May was due to low freshwater flow (Table 3). Variations in surface salinity were related to distance from the mouth of the estuary and to the development of a southwest gale on July 24. Surface salinity during the first two time series varied from 29.5 ‰ to 30.2 ‰, compared to 30.5 ‰ to 32.2 ‰ during the third time series, and 31.0 ‰ to 32.2 ‰ during the fourth time series (Fig. 5). Surface temperature remained above 22 °C during the first three time series, and differences in surface salinity were due to distance from the mouth of the estuary. High surface salinity during time series four was accompanied by surface temperatures of 16 °C to 20 °C. Southwesterly wind favors northward flow and offshore Ekman transport of surface water resulting in upwelling along the New Jersey coast (Beardsley et al. 1976; Hopkins and Dieterle in press). Thus, the decrease in temperature and increase in salinity of the surface layer between the third and fourth time series were due to the development of an upwelling circulation.

Table 12. Summary of environmental conditions of the surface layer during drogue studies four, five, and six (May 1977): incident radiation ( $I_0$ ,  $E m^{-2} d^{-1}$ ), temperature (T,  $^{\circ}C$ ), salinity (S, ppt), nutrient concentrations ( $\mu g-at l^{-1}$ ), and atomic ratios; depth averaged diel ranges and means are given for each day.

Day	$I_0$	T	S	$NO_3-N$	$NH_4-N$	$PO_4-P$	$SiO_4-Si$	Si:N
14	48	10.0	28.43	1.1	2.1	1.0	1.4	0.44
		10.9	29.34	2.6	3.3	1.6	2.6	
		11.9	30.15	5.0	6.0	2.2	4.0	
15	49	10.8	28.36	3.8	2.5	1.8	2.1	0.35
		11.0	28.68	5.2	3.7	2.1	3.1	
		11.2	29.32	5.9	4.6	2.3	4.0	
16	40	10.5	26.89	0.4	2.6	1.3	0.2	0.23
		11.4	28.58	3.0	3.1	1.5	1.4	
		12.8	30.12	5.0	4.0	1.6	2.2	
17	38	11.2	27.86	0.6	0.9	1.0	0.2	0.22
		12.4	28.50	2.5	2.6	1.4	1.1	
		13.7	29.11	4.7	6.5	1.9	2.2	
18	35	11.0	26.93	1.0	1.5	1.2	0.0	0.11
		12.9	28.37	3.3	2.2	1.5	0.6	
		15.2	30.03	7.5	2.9	1.8	1.4	
19		11.8	27.44	0.6	0.9	0.8	0.0	0.06
		12.5	28.02	3.5	1.6	1.3	0.3	
		12.8	28.53	6.2	2.0	2.1	0.8	

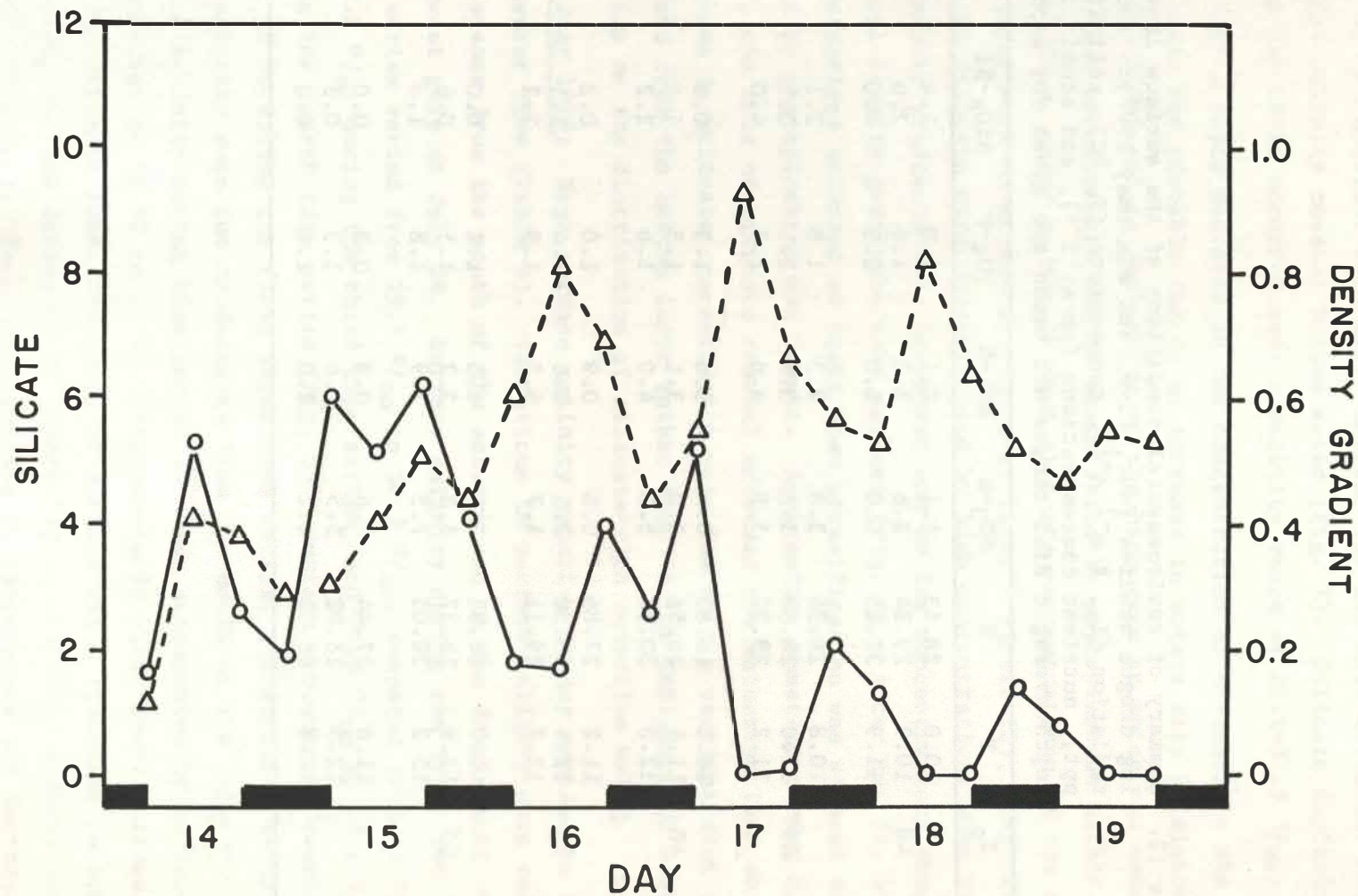


Figure 8. Variations in the maximum concentrations of silicate (O,  $\mu\text{g-at liter}^{-1}$ ) in the surface layer and the density gradient ( $\Delta$ ,  $\sigma\text{-t m}^{-1}$ ) across the surface layer during May 14-19.

The southwest wind event had a marked effect on water column stratification (Fig. 6). Vertical density gradients decreased from time series two to time series three due to an increase in surface salinity with distance from the estuary. Between time series three and four, increased mixing associated with upwelling resulted in less vertical stratification during time series four (Fig. 6).

Upwelling also influenced nutrient distributions. Prior to the wind event, nutrient concentrations were low and showed little variability with salinity in the apex (e.g., Fig. 7). Nitrate was near depletion and ammonium accounted for a mean of 90 percent of dissolved inorganic nitrogen. This is typical of the well-stratified summer regime and implies that phytoplankton uptake and nutrient flux from the estuary and from regeneration were in approximate steady-state and that ammonium regeneration rate was high (Malone 1976). Following the wind event, nutrient concentrations were higher and tended to decrease with increasing salinity in the surface layer (Table 7, Fig. 7). This suggests that the increase in nutrient concentration of the surface layer was caused by two processes: (1) upwelling of nutrient-rich bottom water and (2) disruption of the balance between the estuarine nutrient flux and phytoplankton uptake. The former would give rise to a general increase in nutrient concentration while the latter would restore the inverse relationship between nutrient concentration and salinity which characterizes the plume when phytoplankton productivity is low as in November.

November 1977: Water column stability decreased during the study period and with distance from the estuary (Fig. 6) as salinity increased and temperature decreased in the surface layer (Figs. 2 and 5). These trends coincided with a decrease in freshwater flow (Table 3) and a persistent westerly wind with speeds of 5 to 20 m s<sup>-1</sup>. Thus, the decrease in temperature and increase in salinity were probably due to upwelling and lower freshwater transport, both of which would have the effect of reducing water column stability.

With the exception of phosphate, which varied between 1.5 and 3.5  $\mu\text{g-at liter}^{-1}$  independent of salinity, nutrient concentrations were inversely related to salinity throughout the cruise. For example,

ammonium in the surface layer declined in concentration from 18.8  $\mu\text{g-at liter}^{-1}$  at 25.4 ‰ to 1.5  $\mu\text{g-at liter}^{-1}$  at 33.0 ‰. This behavior indicates that phytoplankton uptake was low and that nutrient concentrations were mainly a function of mixing between nutrient-rich estuarine water and nutrient-poor coastal water.

#### 3.04 Phytoplankton Biomass

March 1978: Chlorophyll a concentrations were high at the beginning of the cruise, surface concentrations decreasing from greater than 25  $\mu\text{g liter}^{-1}$  near the mouth of the estuary to less than 10  $\mu\text{g liter}^{-1}$  along the southern boundary of the plume (Fig. 9). Concentrations were also high in the bottom layer and tended to increase with distance from the mouth of the estuary (Fig. 10). The relationship between chlorophyll a and salinity during this period (March 5-8) indicates that phytoplankton biomass in the surface layer was equal to or greater than expected on the basis of mixing between low and high salinity water masses (Fig. 11), a pattern which is indicative of past growth within the plume. High concentrations of chlorophyll a in the bottom layer suggest that much of the biomass produced during this bloom had also begun to sink from the euphotic zone, a phenomenon which occurs frequently during the diatom bloom period (Malone and Chervin 1979; Malone et al. in press a,b).

The bloom continued to collapse during the subsequent three to four days so that by March 11-12 surface concentrations of chlorophyll a had decreased by 50 percent near the mouth of the estuary and by an order of magnitude along the southern boundary of the plume (Fig. 12). High concentrations were still found in the bottom layer (Fig. 11), suggesting that much of the decline was due to sinking. More recent observations (Malone et al. in press, a, b) indicate that most of the diatom biomass produced during the diatom bloom period sinks from the euphotic zone but does not accumulate in the benthos. Rather, most remains in suspension and is distributed across the shelf during alternating episodes of mixing and sinking.

May 1977: Chlorophyll a concentrations varied from 0.5 to 27.5  $\mu\text{g liter}^{-1}$  in the surface layer and from 0.5 to 6.0  $\mu\text{g liter}^{-1}$  in the

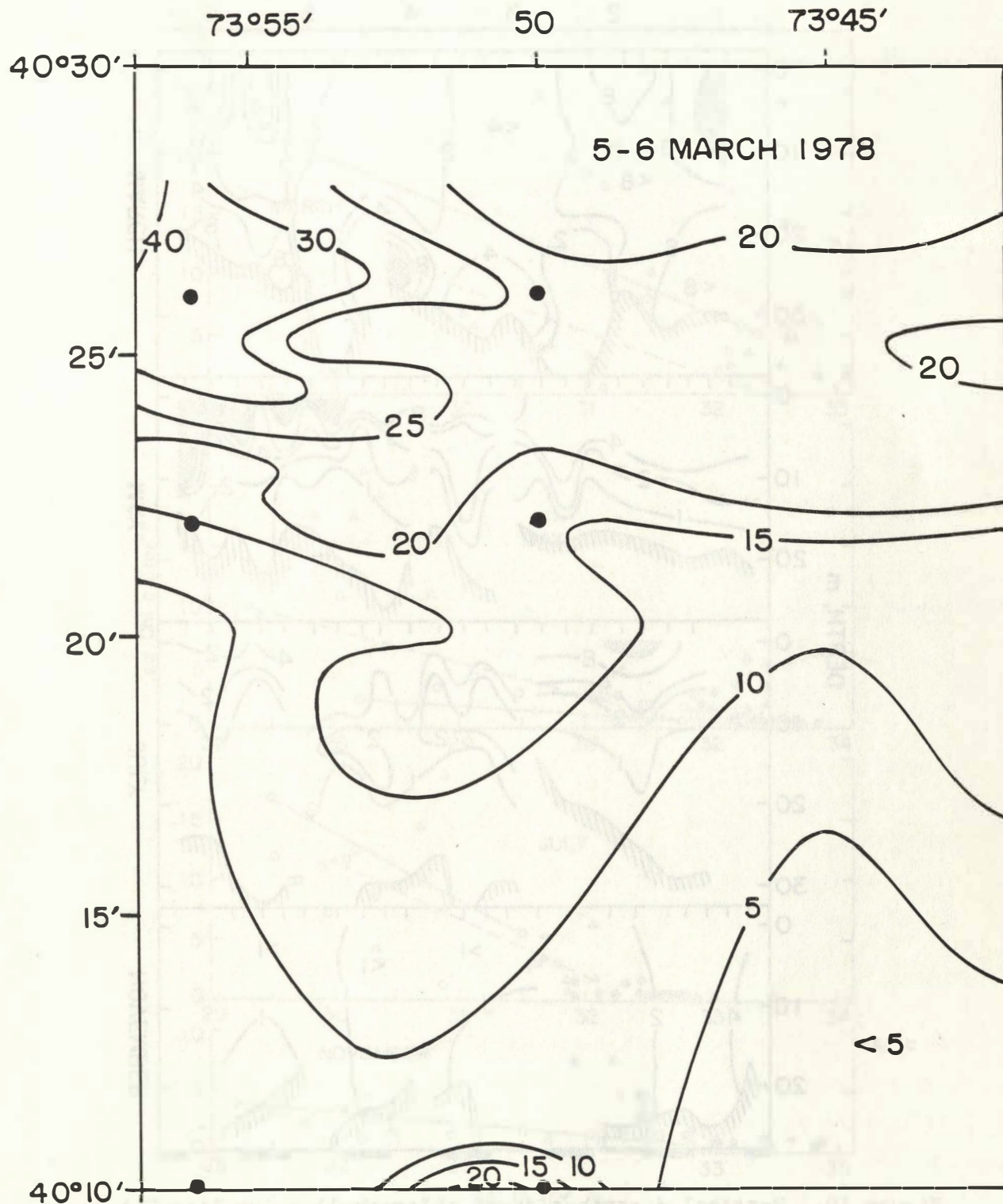


Figure 9. Distribution of surface chlorophyll *a* ( $\mu\text{g liter}^{-1}$ ) before drogue studies.

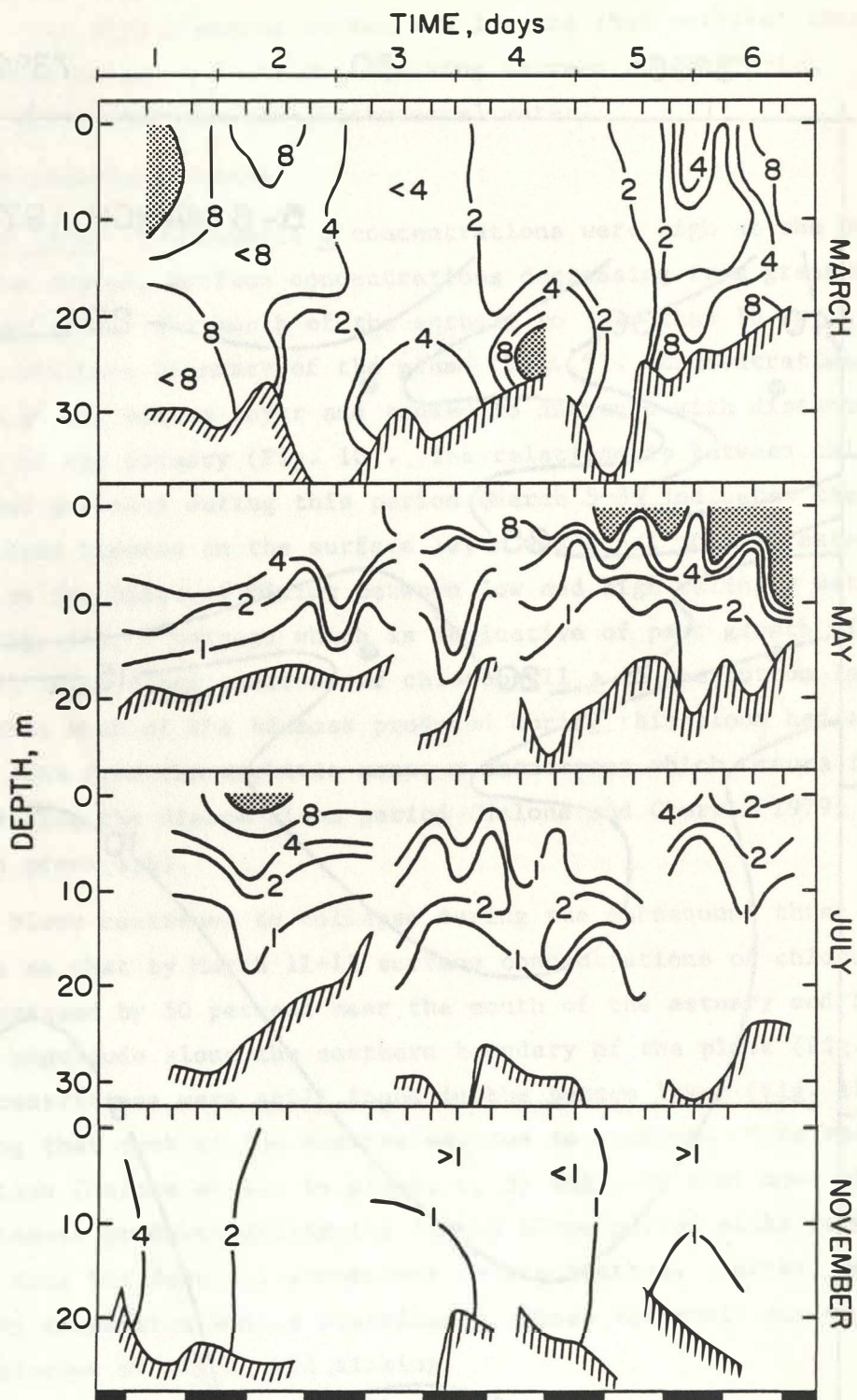


Figure 10. Vertical distribution of chlorophyll a (µg liter<sup>-1</sup>) as in Fig. 5; hatched areas indicate chlorophyll a concentrations greater than 16 µg liter<sup>-1</sup>.

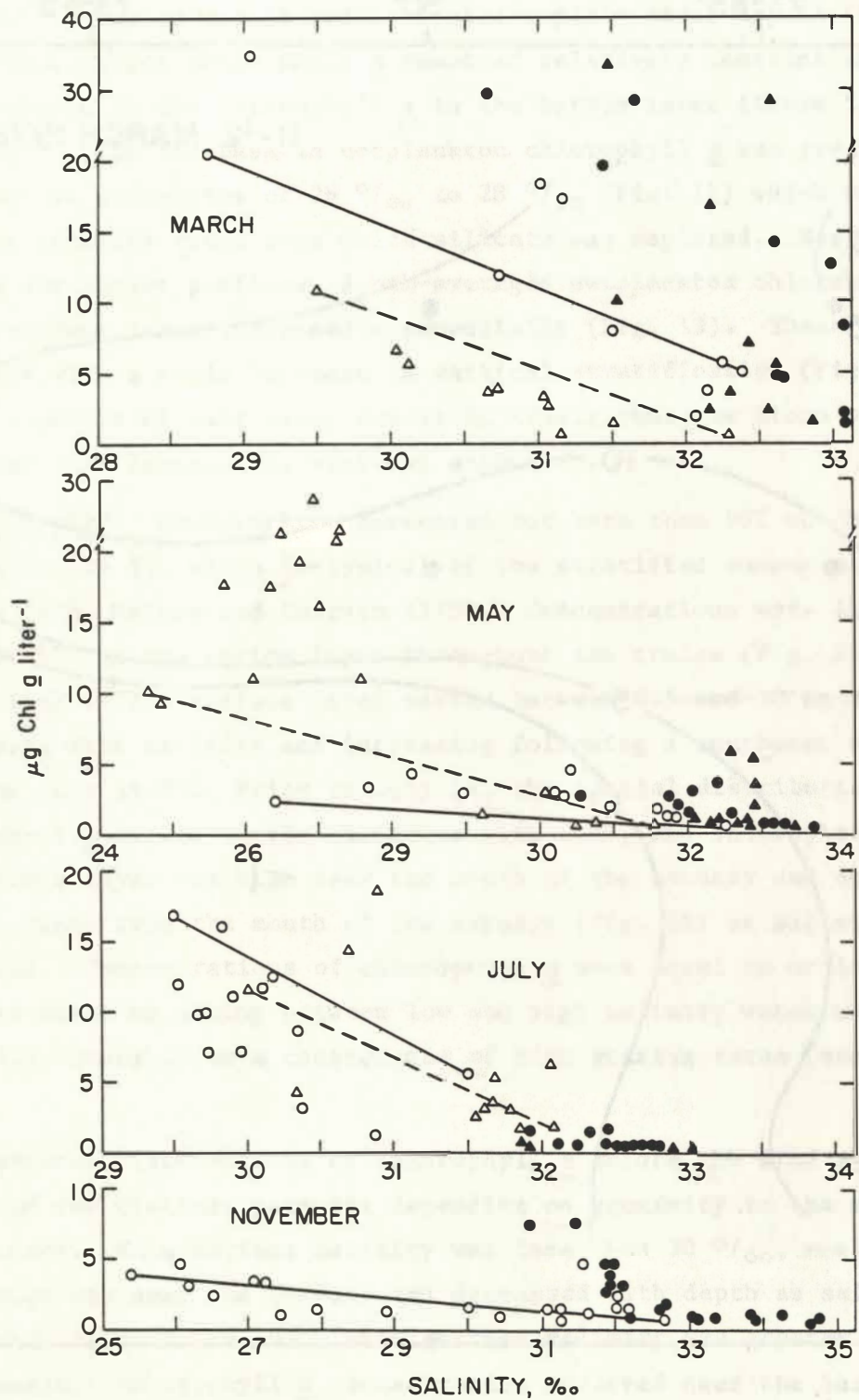


Figure 11. Chlorophyll *a*-salinity relationships; symbols as in Fig. 7.

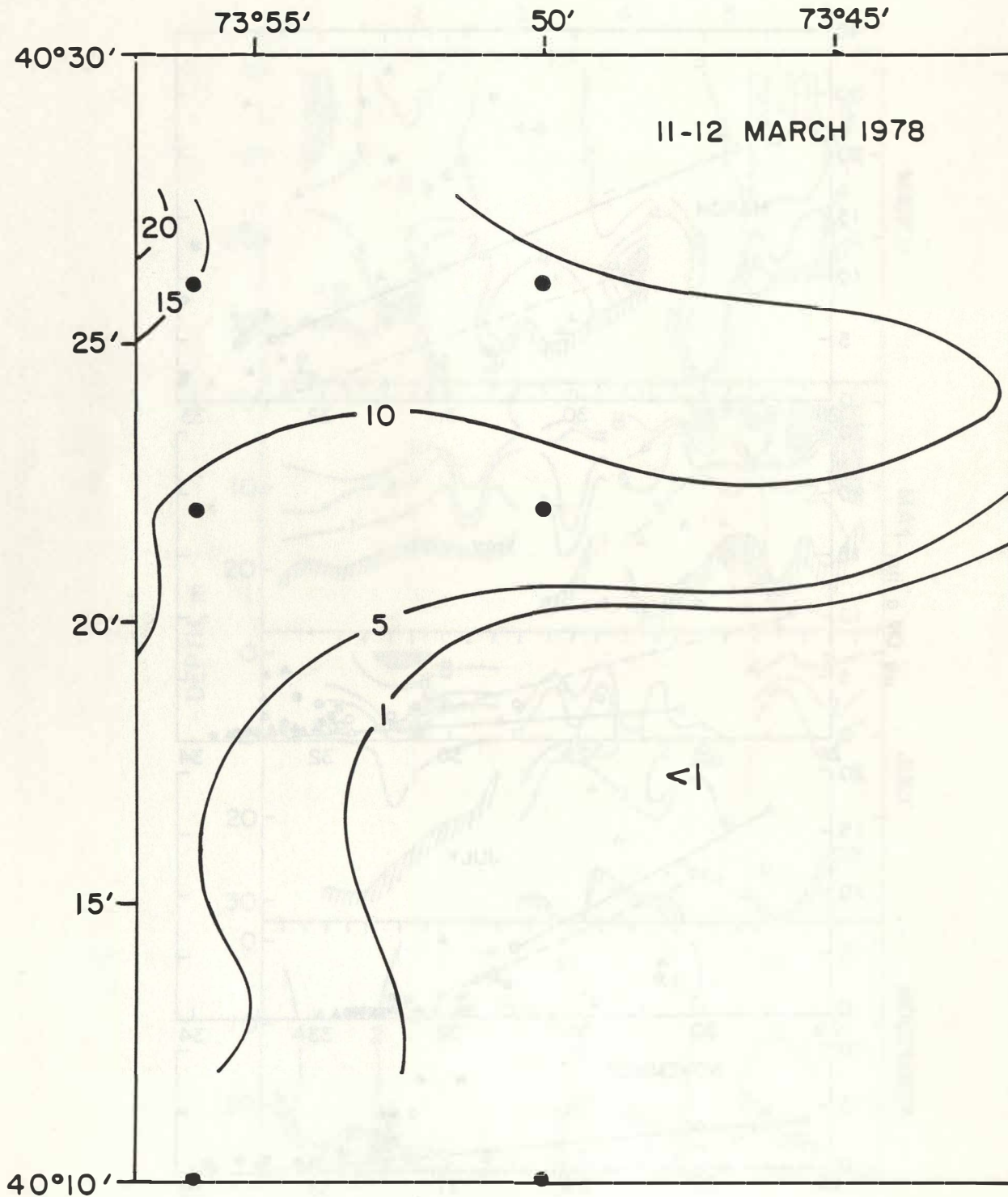


Figure 12. Distribution of surface chlorophyll *a* ( $\mu\text{g liter}^{-1}$ ) after drogue study 2.

bottom layer (Fig. 11). Concentrations greater than  $2 \mu\text{g liter}^{-1}$  in the bottom layer were only observed near shore in water columns less than 15 m deep. Concentrations in the surface layer were less than  $5 \mu\text{g liter}^{-1}$  prior to May 14 and increased rapidly after May 14 (Fig. 10). Nanoplankton chlorophyll a remained relatively constant throughout the bloom as did chlorophyll a in the bottom layer (Table 5, Figs. 10 and 11). The increase in netplankton chlorophyll a was greatest in magnitude at salinities of  $26 \text{ ‰}$  to  $28 \text{ ‰}$  (Fig. 11) which coincided with the salinity range over which silicate was depleted. Based on sunrise and sunset profiles, depth-averaged netplankton chlorophyll a in the surface layer increased exponentially (Fig. 13). These changes coincided with a rapid increase in vertical stratification (Fig. 6) during a period of calm wind, and it is likely that the bloom was stimulated by this increase in vertical stability.

July 1977: Nanoplankton accounted for more than 90% of chlorophyll a (Table 5), which is typical of the stratified summer period (Malone 1976; Malone and Chervin 1979). Concentrations were less than  $2 \mu\text{g liter}^{-1}$  in the bottom layer throughout the cruise (Fig. 11). Concentrations in the surface layer varied between 0.5 and  $20 \mu\text{g liter}^{-1}$ , decreasing with salinity and increasing following a southwest wind event on July 24-25. Prior to July 24, the spatial distribution of chlorophyll a showed little variation with time, and chlorophyll a in the surface layer was high near the mouth of the estuary and decreased with distance from the mouth of the estuary (Fig. 14) as salinity increased. Concentrations of chlorophyll a were equal to or less than expected based on mixing between low and high salinity water masses (Fig. 11), probably as a consequence of high grazing rates (section 3.11).

Vertical distributions of chlorophyll a before the wind event exhibited two distinct patterns depending on proximity to the mouth of the estuary. When surface salinity was less than  $30 \text{ ‰}$ , maximum concentration was near the surface and decreased with depth as salinity increased (Figs. 5 and 10). When surface salinity was greater than  $31 \text{ ‰}$ , maximum chlorophyll a concentration occurred near the base of the surface layer in association with a salinity minimum (Figs. 5 and 10).

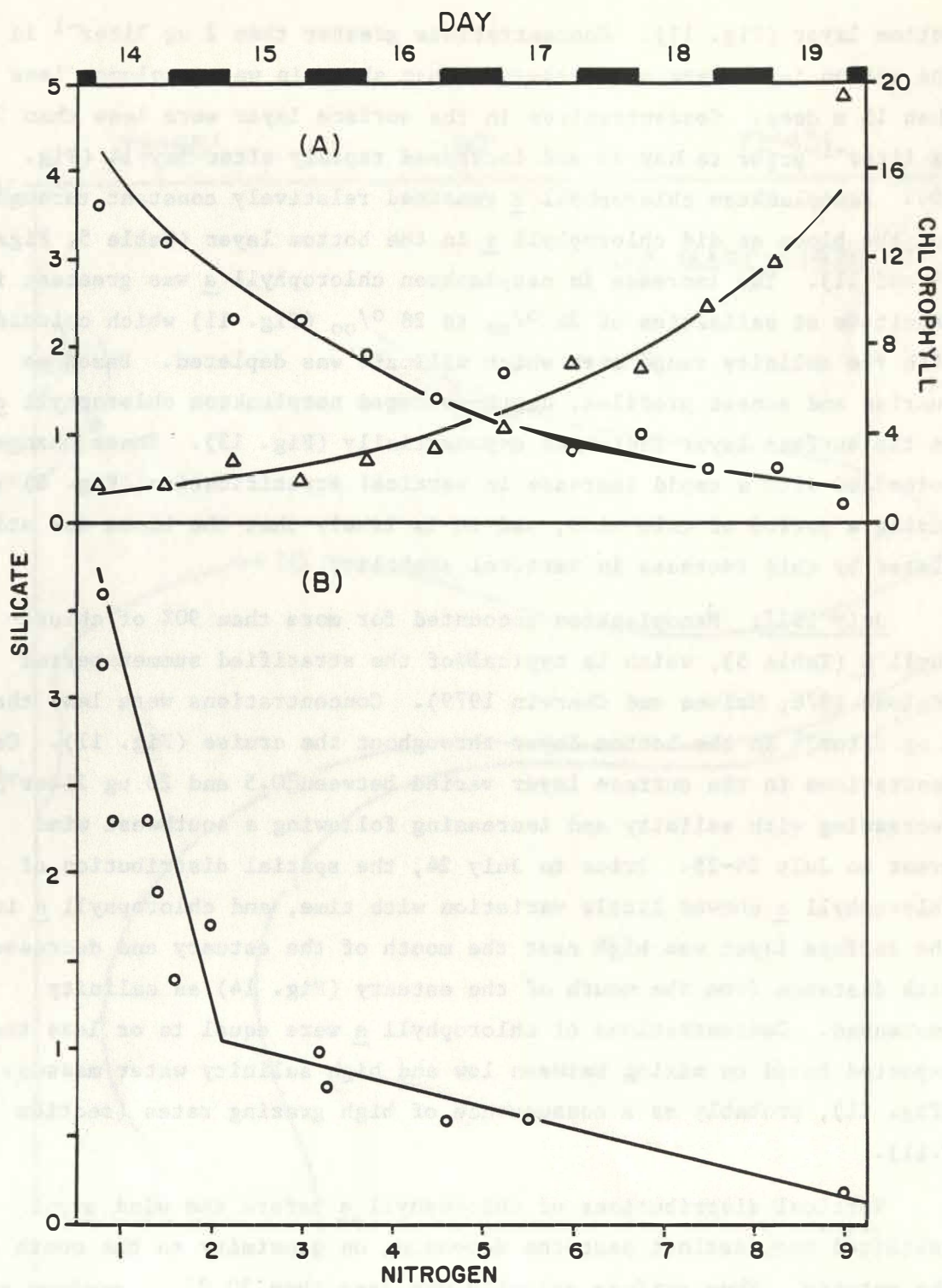


Figure 13. (A) sunrise and sunset concentrations (mean surface layer) of netplankton chlorophyll *a* (triangles,  $\mu\text{g liter}^{-1}$ ) and  $\text{SiO}_4\text{-Si}$  (circles,  $\mu\text{g-at liter}^{-1}$ ) during May 14-19; (B) relationship between concentrations of ambient  $\text{SiO}_4\text{-Si}$  (circles,  $\mu\text{g-at liter}^{-1}$ ) and netplankton biomass as particulate nitrogen at sunrise and sunset during May 14-19.

The southwest gale perturbed this steady-state distribution. Surface chlorophyll a near the mouth of the estuary was reduced from greater than 15  $\mu\text{g liter}^{-1}$  (Fig. 14) to less than 5  $\mu\text{g liter}^{-1}$  (Fig. 15), and the salinity minimum, with its chlorophyll a maximum, was moved nearer to the surface (Figs. 5 and 10). During the subsequent three days, surface chlorophyll a more than doubled over much of the study area (Fig. 16), especially at intermediate salinities of 30.5 ‰ to 31.0 ‰ where chlorophyll a was higher than expected on the basis of mixing (Fig. 11).

November 1977: Chlorophyll a concentrations decreased with distance from the mouth of the estuary at the beginning of the study period and with time during the study period (Fig. 10 and Table 5). Concentrations in the surface layer decreased with increasing salinity as would be expected if the chlorophyll a distribution was mainly determined by mixing between low and high salinity water masses (Fig. 11), i.e., phytoplankton growth rate must have been low relative to dilution (flushing) rate of water in the study area.

Vertical profiles were either uniform with depth or characterized by high concentrations near the bottom (Figs. 10 and 11). High near-bottom concentrations were observed most frequently early in the cruise and were composed mostly of netplankton dominated by the diatom S. costatum. Such changes in the chlorophyll a field indicate that a bloom of S. costatum had developed and had been dissipated by sinking and mixing prior to our observations.

### 3.05 Suspended and Dissolved Organic Matter

Variations in dissolved organic carbon (DOC) were generally related to salinity while variations in particulate organic carbon (POC) were generally related to chlorophyll a. DOC tended to be higher in the surface layer than in the bottom layer, and the relationship between DOC and salinity showed little variability during any given cruise except during May (Fig. 17). DOC was significantly correlated with salinity over the entire water column at the beginning of the May cruise (Table 13). By the end of the cruise, DOC had increased in the bottom layer and was poorly correlated with salinity in the surface

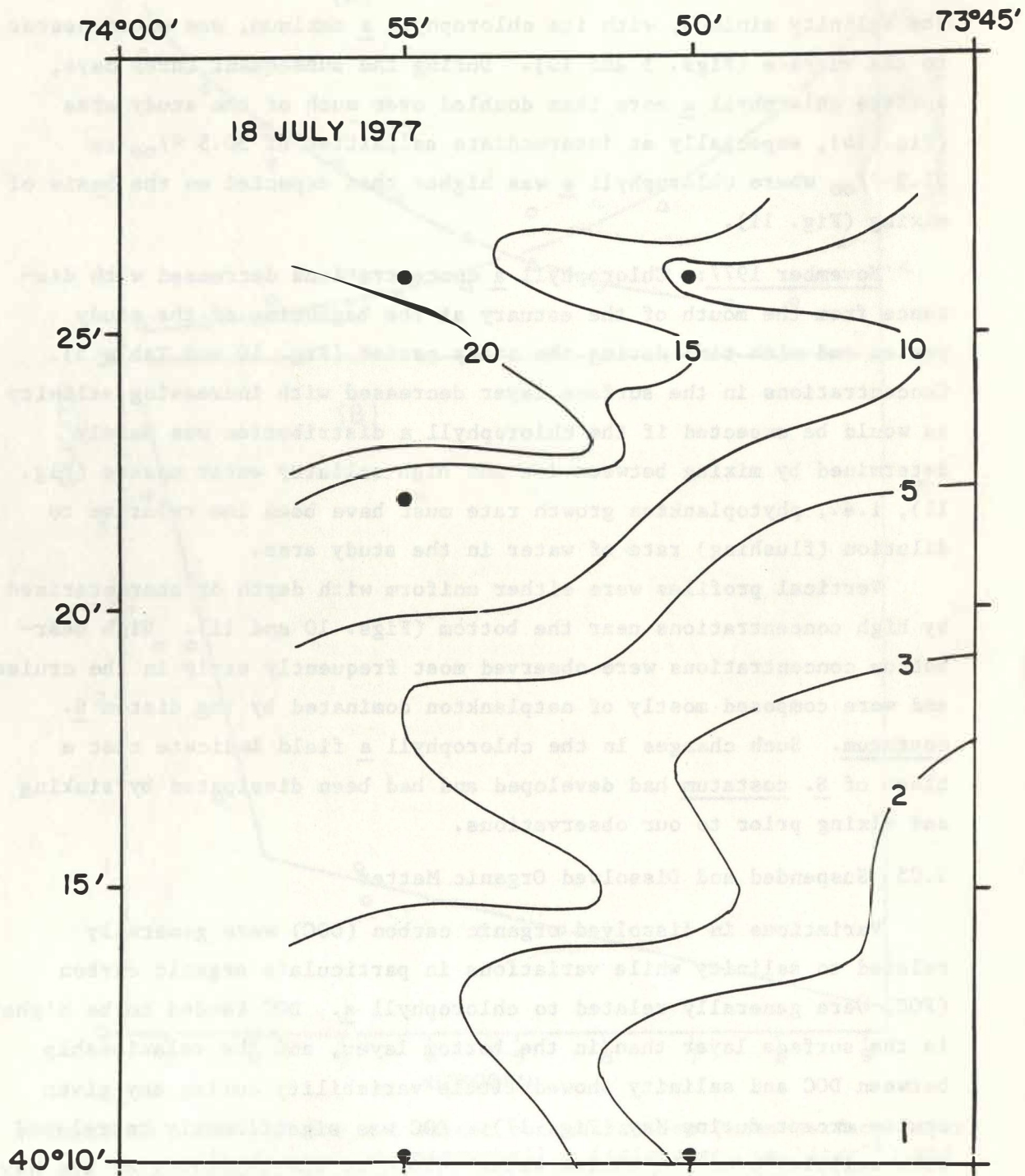


Figure 14. Distribution of surface chlorophyll a ( $\mu\text{g liter}^{-1}$ ) before drogue studies.

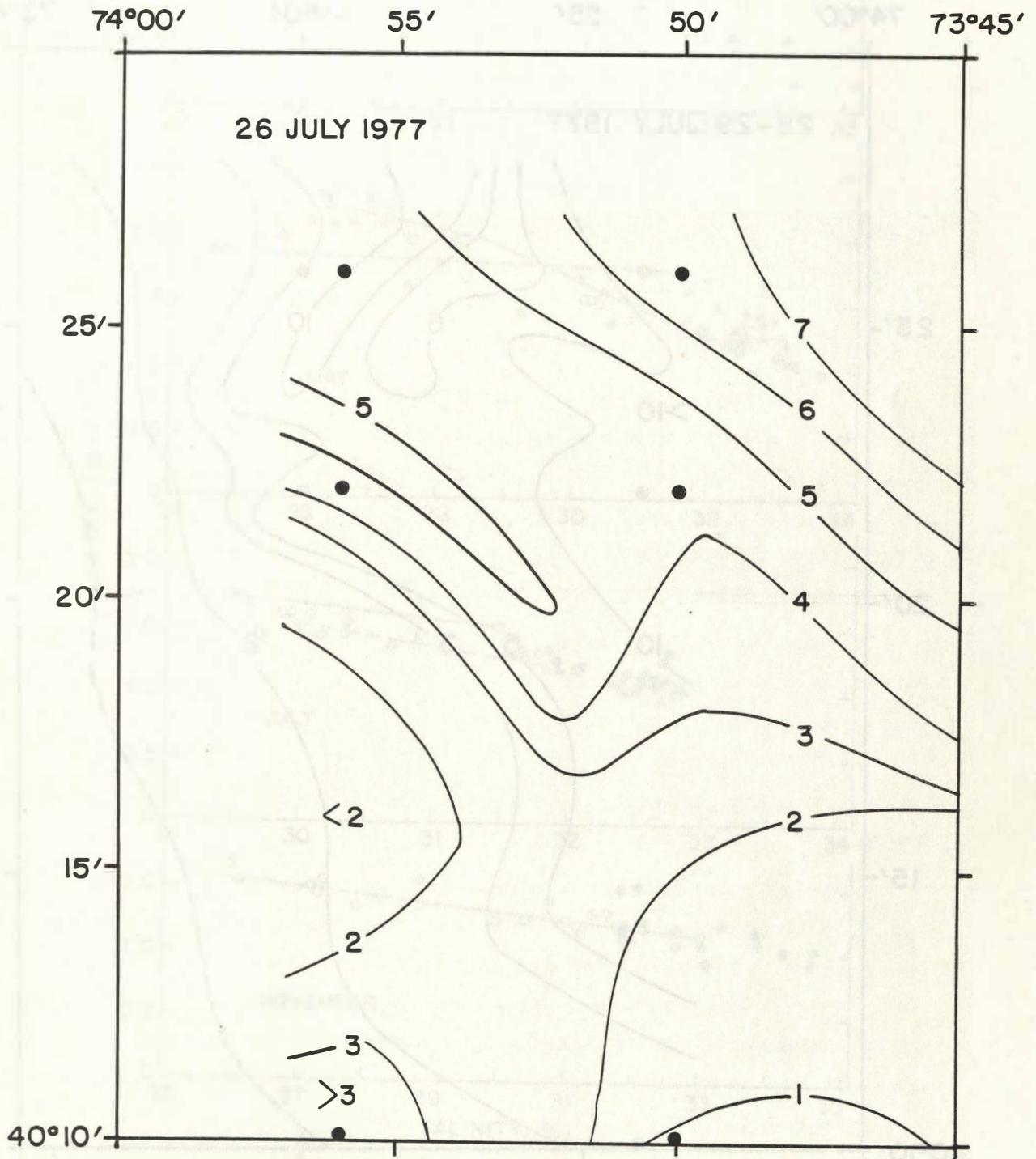


Figure 15. Distribution of surface chlorophyll a between drogue studies 3 and 4 immediately after (within 24 hours) a wind event.

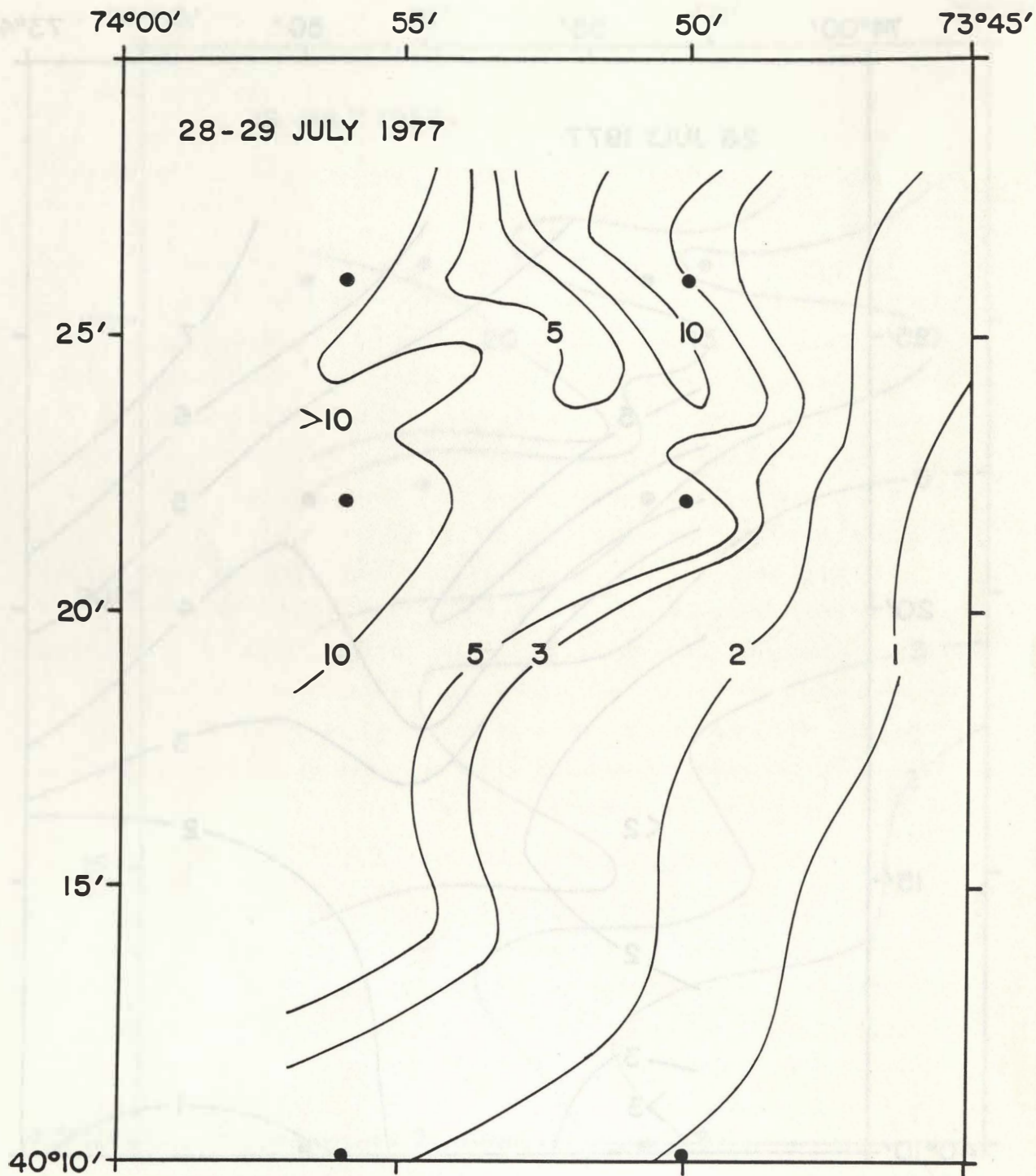


Figure 16. Distribution of surface chlorophyll a four days after the wind event.

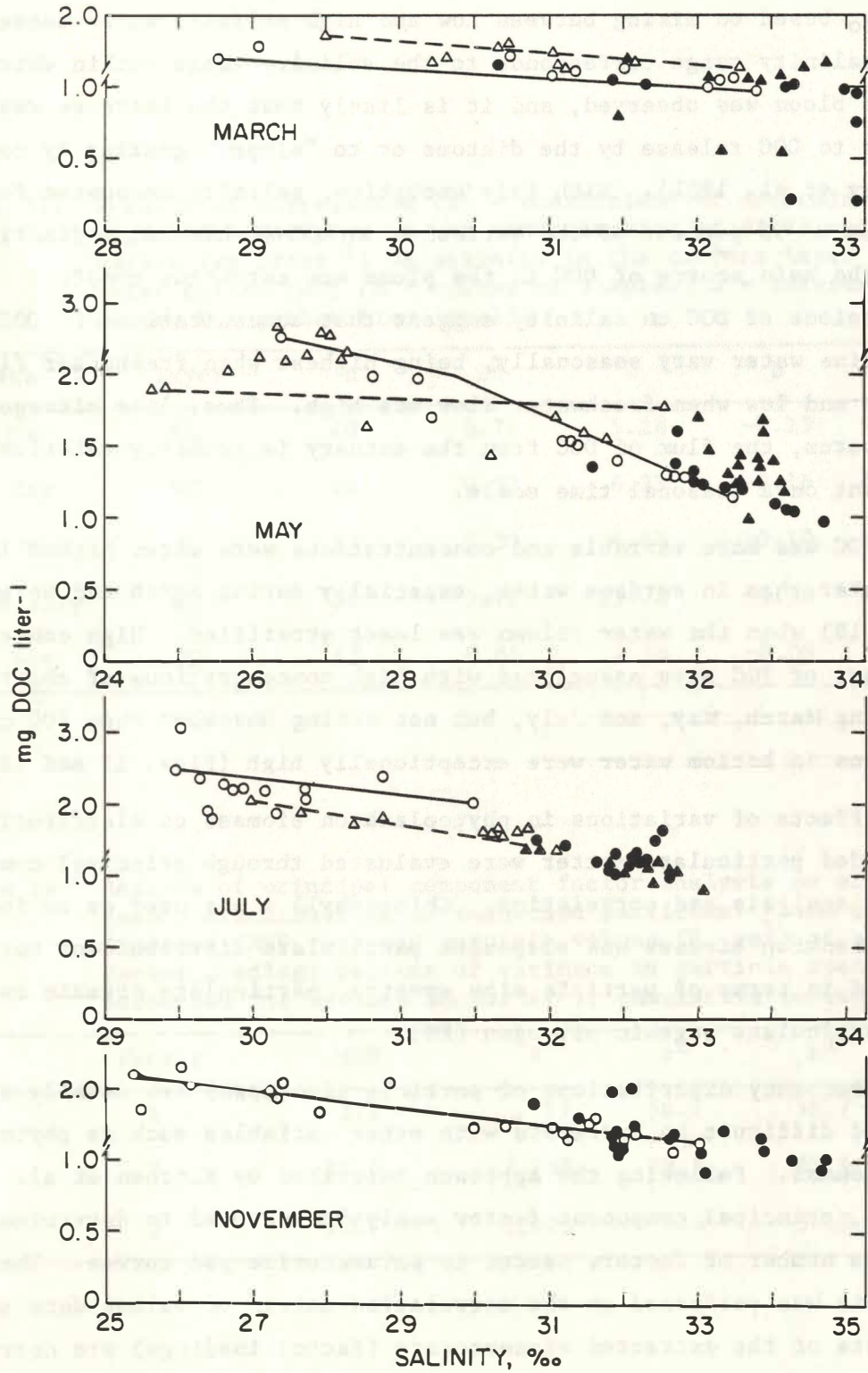


Figure 17. Dissolved organic carbon (DOC)-salinity relationships; symbols as in Fig. 7; note change in scale along the ordinate.

layer. DOC was higher than expected at salinities of 26 ‰ to 28 ‰ based on mixing between low and high salinity water masses. This salinity range corresponds to the salinity range within which the diatom bloom was observed, and it is likely that the increase was due either to DOC release by the diatoms or to "sloppy" grazing by copepods (Eppley et al. 1981). With this exception, salinity accounted for 65 percent to 93 percent of the variation in DOC (Table 13) indicating that the main source of DOC in the plume was estuarine runoff. Regressions of DOC on salinity suggest that concentrations of DOC in estuarine water vary seasonally, being highest when freshwater flow was lowest and low when freshwater flow was high. Thus, like nitrogen and phosphorus, the flux of DOC from the estuary is probably relatively constant on a seasonal time scale.

POC was more variable and concentrations were often higher in bottom water than in surface water, especially during March and November (Fig. 18) when the water column was least stratified. High concentrations of POC were associated with high concentrations of chlorophyll a during March, May, and July, but not during November when POC concentrations in bottom water were exceptionally high (Figs. 11 and 18).

Effects of variations in phytoplankton biomass on distributions of suspended particulate matter were evaluated through principal component factor analysis and correlation. Chlorophyll a was used as an index of phytoplankton biomass and suspended particulate distributions were defined in terms of particle size spectra, particulate organic carbon, and particulate organic nitrogen (PN).

Frequency distributions of particle size (psd) are usually irregular and difficult to correlate with other variables such as phytoplankton biomass. Following the approach described by Kitchen et al. (1975), principal component factor analysis was used to determine the minimum number of factors needed to parameterize psd curves. The analysis was performed on the correlation matrix of volume data so that elements of the extracted eigenvectors (factor loadings) are correlations between the original variables and the eigenvectors or factors.

Table 13. Results of correlation ( $r^2$  = coefficient of determination) and regression analyses of the concentration of dissolved organic carbon ( $\text{mg liter}^{-1}$ ) on salinity in the surface layer (SL) or water column (WC) ( $n$  = number of samples,  $a$  = intercept,  $b$  = slope,  $P$  = probability level).

Date	Layer	n	$r^2$	a	b	P
6-15 Mar	SL	40	0.77	5.28	-0.13	<0.001
9-12 May	WC	24	0.93	6.33	-0.16	<0.001
17-19 May	SL	17	0.32	4.68	-0.10	<0.05
19-28 July	WC	36	0.78	13.78	-0.39	<0.001
9-20 Nov	WC	42	0.65	4.16	-0.09	<0.001

Table 14. Results of principal component factor analysis on size frequency distributions of suspended particles: mean spherical diameter (MSD,  $\mu\text{m}$ ) and particle volume ( $V$ ,  $\mu\text{m}^3$ ) of maximum factor loading; percent of variance in particle spectra accounted for by each factor ( $r^2$ ); cumulative percent ( $R^2$ ).

Factor	MSD	V	$r^2$	$R^2$
1	3.2	17	56.7	56.7
2	32.0	17,158	28.9	85.6
3	12.7	1,073	5.4	91.0

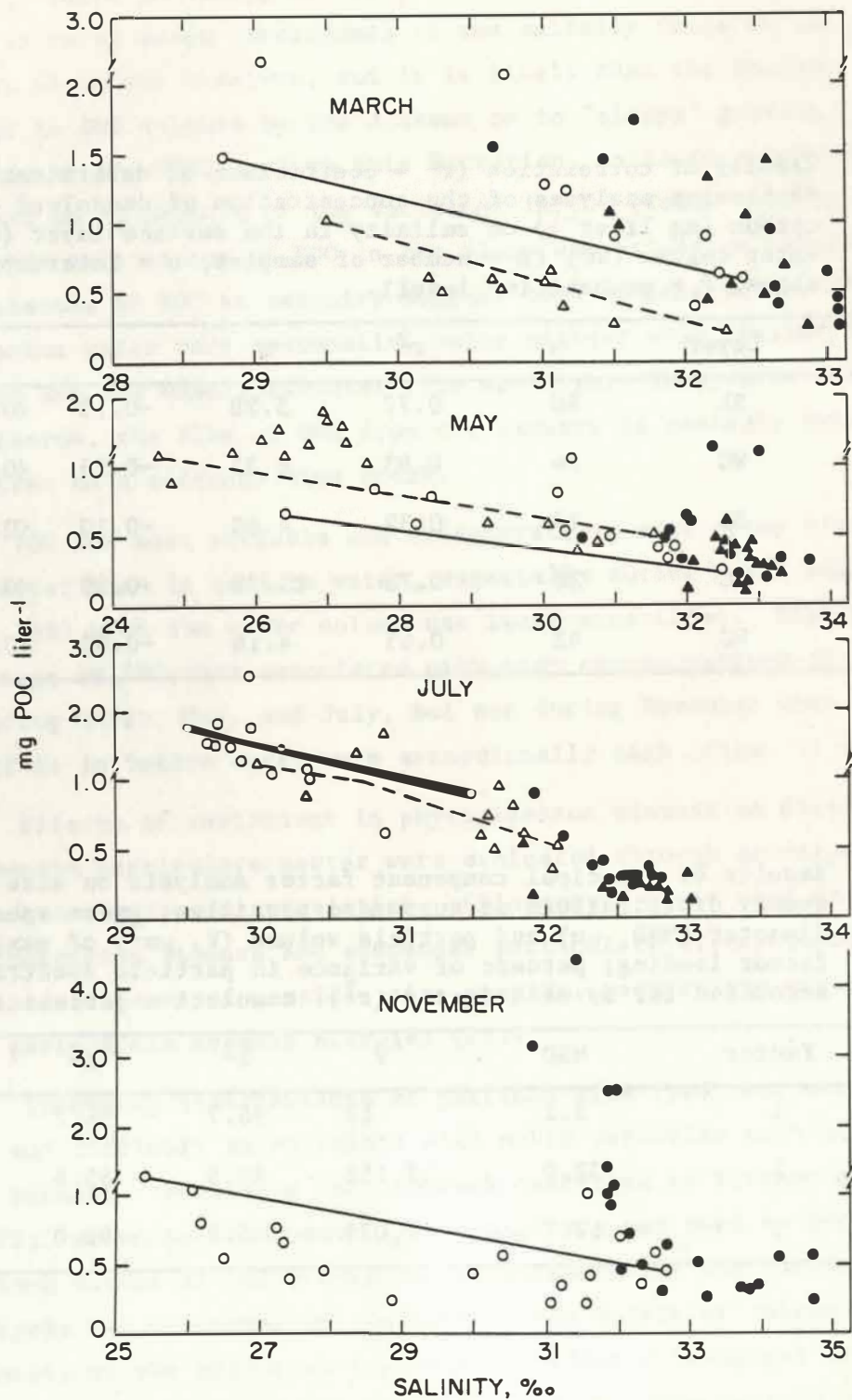


Figure 18. Particulate organic carbon (POC)-salinity relationships; symbols as in Fig. 7; note change in scale along the ordinate.

The final factor loading matrix is obtained by orthogonal varimax rotation of the factor scores to maximize the number of correlations close to 1.0 and 0.0. This helps to define sets of independent variables. Factor scores, which weight each factor by channel, are calculated to have mean zero or unit variance. Thus, psd curves can be approximated as follows:

$$V_x = \bar{V}_x + S_{Vx} (aF1_x + bF2_x + cF3_x \dots)$$

where  $V_x$  = volume of particles in channel x for a given sample,  
 $\bar{V}_x$  = mean volume of particles in channel x,  
 $S_{Vx}$  = standard deviation in channel x,  
a,b,c,... = factor scores for factors 1,2,3,... for a given sample and,  
 $F1_x, F2_x, F3_x, \dots$  = factor loadings for channel x on factors 1,2,3...

Factor scores can be used to relate psd curves to other properties, such as chlorophyll a concentration.

Three factors, each associated with different but overlapping ranges of the particle spectrum, accounted for 91 percent of the variance in psd curves (Table 14). Factors 1 and 2 accounted for 86 percent of the variance and loaded primarily on small volume channels (less than 8.0  $\mu\text{m}$ ) and large volume channels (greater than 20.2  $\mu\text{m}$ ), respectively. Factor 3, which had high factor loadings at intermediate channels (10.1 to 16.0  $\mu\text{m}$ ), accounted for an additional 5 percent of the variance and was important because phytoplankton in the netplankton fraction were dominated by chain-forming diatoms with small cells. Consequently, a given species can be found in a wide range of size classes depending on chain length (cf. Malone et al. 1979).

Peaks in psd curves were caused by phytoplankton and shifted from intermediate to large volumes in March and May to small volumes in July and November as the proportion of chlorophyll a accounted for by netplankton changed (Table 15). High chlorophyll a concentrations were due to netplankton diatoms in March (mostly Skeletonema costatum and Thalassiosira nordenskioldii) and in May (mostly Asterionella japonica) when chlorophyll a concentration was best correlated with factors 3 and

Table 15. Correlation coefficients between chlorophyll a concentration and factor scores for suspended particles in the water column (ambient) and between decreases in chlorophyll a and the difference between factor scores for particle size distributions before and after grazing (n = number of samples, % Net = mean proportion of chlorophyll a accounted for by netplankton).

Conditions	Month	n	Factors			% Net
			1	3	2	
Ambient	March	34	-0.77 <sup>c</sup>	0.88 <sup>c</sup>	-0.24	66
	May	19	-0.05	0.71 <sup>c</sup>	0.76 <sup>c</sup>	64
	July	24	0.96 <sup>c</sup>	0.52 <sup>b</sup>	0.34	2
	Nov	26	0.55 <sup>b</sup>	0.15	-0.35	35
Grazed	March	5	-0.73	0.83 <sup>a</sup>	0.91 <sup>a</sup>	67
	May	5	0.08	0.84 <sup>a,d</sup>	-	79
	July	5	0.95 <sup>b</sup>	0.88 <sup>a</sup>	-0.87 <sup>a</sup>	0
	Nov	5	0.81 <sup>a</sup>	0.25	-0.34	30

a p < 0.05

b p < 0.01

c p < 0.001

d Factors 2 and 3 were combined because Asterionella japonica, which dominated during this period, was abundant in size classes from about 8.0  $\mu$ m to 25.4  $\mu$ m (cf. Malone et al. 1979).

2, respectively. During July, when chlorophyll a was best correlated with factor 1, nanoplankton (solitary cells less than 8  $\mu\text{m}$  in mean spherical diameter) accounted for most chlorophyll a. Chlorophyll a was not well correlated with any factor during November, when concentrations were low and neither size fraction was clearly dominant, i.e., most suspended particles were not phytoplankton cells.

Variations in POC and PN were significantly correlated ( $P < 0.01$ ) with chlorophyll a and with each other during all cruises (Table 16). Chlorophyll a accounted for 74 percent to 81 percent of variations in POC and PN during March and May, for 66 percent to 72 percent during July, and for 55 percent to 59 percent during November. Variations in phytoplankton biomass are most pronounced and are best correlated with POC and PN when residence times of phytoplankton in the water column are long (low rates of grazing and decomposition) and least pronounced and poorly correlated with POC when residence times are short (high rates of grazing or dilution) or when phytoplankton production does not account for most of the input of particulate organic matter (Malone and Chervin 1979). Residence time in the water column was longest during March and May, when biomass and productivity were respectively highest, and shortest during November when biomass and productivity were lowest (Fig. 4).

Phytoplankton biomass as carbon (Ph-C) and nitrogen (Ph-N) were calculated from chlorophyll a concentration (Chl) using biomass ratios estimated from linear regressions of POC and PN on chlorophyll a (Table 17). C:Chl based on direct measurements decreased exponentially as Chl increased except in November when Chl was low (Fig. 19). These relationships reflect the presence of proportionately larger amounts of nonphytoplankton carbon (NPh-C) and nitrogen (NPh-N) at low Chl (cf. Eppley et al. 1977). To minimize the resulting bias, biomass ratios in Table 17 were derived for Chl gradients when Chl increased above  $4 \text{ mg m}^{-3}$ . C:Chl estimated in this way agree well with ratios reported earlier for similar times of year (Malone 1977; Malone and Chervin 1979) except in November when Chl was low and variations in C:Chl were poorly related to Chl (Fig. 19C). November was also unique in that concentration gradients of Chl were not observed in time or space, cell

Table 16. Results of correlation ( $r^2$  = coefficient of determination) and regression analyses between concentrations ( $\mu\text{g liter}^{-1}$ ) of particulate organic carbon (POC), nitrogen (PON), and chlorophyll a (Chl) during drogue studies (n = number of samples, a = intercept, b = slope).

Month	Y	X	n	$r^2$	a	b
March	POC	Chl	214	0.77	301	52
	PON	Chl	214	0.81	38	6.0
	POC	PON	214	0.87	26	7.8
May	POC	Chl	262	0.74	355	61
	PON	Chl	262	0.81	42	11
	POC	PON	262	0.88	135	5.3
July	POC	Chl	125	0.66	340	87
	PON	Chl	125	0.72	44	14
	POC	PON	125	0.88	120	6.0
Nov	POC	Chl	133	0.59	27	313
	PON	Chl	133	0.55	10	33
	POC	PON	133	0.94	27	9.0

Table 17. Results of linear regression and correlation analysis between concentrations ( $\text{mg m}^{-3}$ ) of particulate organic carbon (POC), nitrogen (PN) and chlorophyll a (Chl), when chlorophyll a concentration exceeded  $4 \text{ mg m}^{-3}$  ( $\bar{Y} = a + bX$ ,  $n$  = number of samples,  $r^2$  = coefficient of determination).

Month	Y	X	n	$r^2$	a	b
March	POC	Chl	104	0.71	331	50
	PN	Chl	104	0.74	43	5.7
	POC	PN	104	0.86	148	6.6
May	POC	Chl	96	0.69	506	49
	PN	Chl	96	0.77	63	9.7
	POC	PN	96	0.79	234	4.7
July	POC	Chl	44	0.56	541	72
	PN	Chl	44	0.63	74	12
	POC	PN	44	0.76	108	6.1
Nov	POC	Chl <sup>1</sup>	10	0.58	27	313
	PN	Chl <sup>1</sup>	10	0.64	10	33
	POC	PN	10	0.99	244	8.0

<sup>1</sup> Concentration gradients of chlorophyll a were not observed to develop during November, and chlorophyll a concentrations were too low relative to POC and PN to give realistic estimates of C:Chl and N:Chl for phytoplankton.

density was consistently low ( $<10^9 \text{ m}^{-3}$ ), and variations in particle size spectra were poorly correlated with Chl. Thus, even though significant correlations were found between POC, PN, and Chl, biomass ratios were probably overestimated in November (Table 17). For lack of better estimates, C:Chl and N:Chl for November were assumed to be the means of biomass ratios found during seasonal extremes in terms of vertical mixing, temperature, and the relative biomass of netplankton diatoms (March and July).

Seasonal variations in particulate organic matter and phytoplankton biomass were similar to previous years (Malone 1976, 1977; Malone and Chervin 1979) and were significant relative to daily variations during each cruise (F test:  $P = 0.03$  for POC,  $0.02$  for Ph-C, and  $0.01$  for NPh-C). High POC was associated with high Ph-C in March and with high NPh-C in November (Table 18). As a proportion of POC, Ph-C decreased from a mean of 49 percent in March to 38 percent in May, 35 percent in July, and 18 percent in November. Ph-N remained near 50 percent of PN in March, May, and July, but dropped to 23 percent in November. A positive correlation was also found between PN:POC and Ph-C:POC ( $r = 0.58$ ,  $n = 44$ ,  $P < 0.01$ ), which suggests that these trends reflect the tendency for phytoplankton to be richer in nitrogen than nonphytoplankton material.

### 3.06 Photosynthetic Production of Organic Matter

Rates of particulate carbon production estimated by direct measurement of filterable  $^{14}\text{C}$  and by difference between total organic  $^{14}\text{C}$  and dissolved organic  $^{14}\text{C}$  were significantly correlated ( $r = 0.98$ ,  $P < 0.001$ ) by the regression equation  $\text{PP}_d = 1.17 + 1.00 \text{PP}_f$ , where  $\text{PP}_d = \mu\text{g C liter}^{-1} \text{ day}^{-1}$  by difference and  $\text{PP}_f = \mu\text{g C liter}^{-1} \text{ day}^{-1}$  by direct measurement. Thus, fractionation and filtration had no systematic effect on estimates of particulate carbon fixation (slope = 1), and cell breakage as a consequence of filtration was minimal (intercept of  $1.17 \mu\text{g C liter}^{-1} \text{ day}^{-1}$  is low relative to measured rates, which varied from 40 to  $1280 \mu\text{g C liter}^{-1} \text{ d}^{-1}$  at the 100 percent light level).

Rates of DOC release by phytoplankton varied from a mean of 7 percent of total carbon fixation (particulate + dissolved from 24-hr

Table 18. Mean and range of concentrations ( $\text{g m}^{-2}$ ) of particulate organic carbon (POC) and nitrogen (PN) and the proportion of each due to phytoplankton at stations where copepods were collected (n = 11).

Date		POC	% Ph-C	PN	% Ph-N
Mar 6-15	Mean	9.06	18	1.18	21
		15.34	49	1.84	46
		29.53	80	4.78	86
May 9-19	Mean	4.78	18	0.77	24
		8.67	38	1.28	50
		13.90	69	2.55	72
Jul 19-28	Mean	7.03	9	1.13	10
		10.05	35	1.41	47
		14.52	82	2.24	93
Nov 9-20	Mean	5.34	9	0.64	8
		12.53	18	1.46	23
		26.95	29	2.57	36

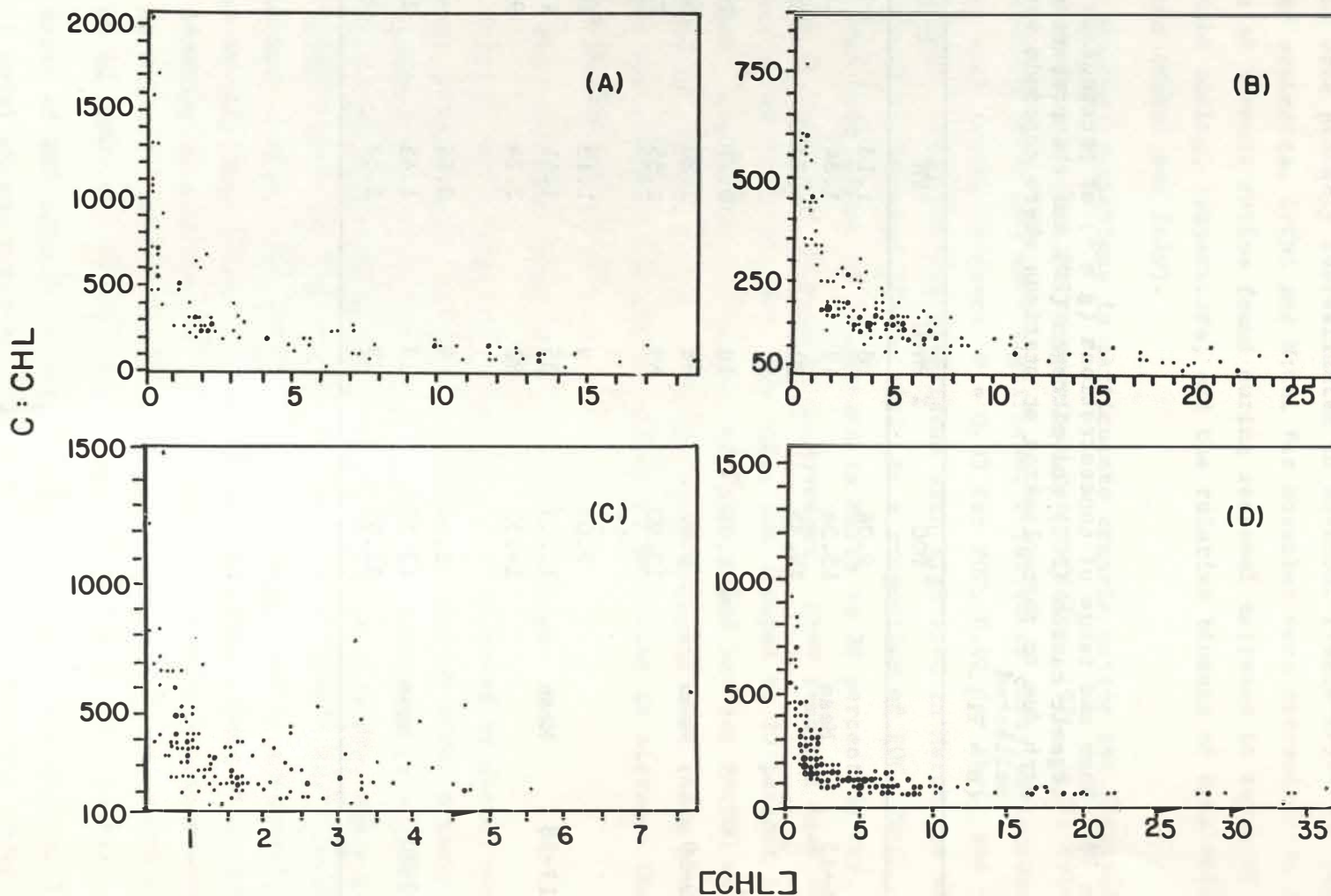


Figure 19. Ratio of particulate organic carbon to chlorophyll a concentration (C:Chl,  $\mu\text{g}:\mu\text{g}$ ) as a function of the concentration of chlorophyll a ( $\mu\text{g liter}^{-1}$ ) during drogue studies (A, May; B, July; C, November; D, March).

sunlight incubations) during May to 16 percent during November (Table 19). Release rates were low during May and July when phytoplankton growth rates were highest and were high during March and November following the collapse of diatom blooms when growth rates were low. Release rates were less than 12 percent when particulate carbon fixation was greater than  $1 \text{ g C m}^{-2} \text{ d}^{-1}$ . Below  $1 \text{ g C m}^{-2} \text{ d}^{-1}$ , percent release tended to increase as productivity decreased. This trend was especially pronounced during March and could be indicative of physiological stress.

Euphotic zone primary productivity (particulate) ranged from  $0.1 \text{ g C m}^{-2} \text{ d}^{-1}$  in November to  $5.0 \text{ g C m}^{-2} \text{ d}^{-1}$  in May (Table 19). Time averaged productivity for each cruise exceeded  $1.0 \text{ g C m}^{-2} \text{ d}^{-1}$  except during November when productivity averaged  $0.2 \text{ g C m}^{-2} \text{ d}^{-1}$ . Given an allochthonous input of  $0.5 \text{ g C m}^{-2} \text{ d}^{-1}$  (apex area =  $1250 \text{ km}^2$ ; input due to estuarine runoff and ocean dumping of sludge and dredge spoils of  $2.2 \times 10^8 \text{ kg C yr}^{-1}$  from Thomas et al. 1976 and Garside and Malone 1978, after subtracting the DOC input), phytoplankton productivity in the plume accounted for 72, 87, 76, and 28 percent of identified POC inputs during March, May, July, and November, respectively.

Variations of chlorophyll a content of the euphotic zone accounted for most of the variance in primary productivity during each cruise (Table 20). Chlorophyll a specific productivity (PPChl), estimated by the slope of the regression lines, was highest during May when diatoms were growing exponentially and lowest during November when chlorophyll a concentrations were low and inversely related to salinity (Fig. 11). With the notable exception of March, differences in PPChl between the nanoplankton and netplankton fractions were consistent with their relative biomass. Thus, netplankton PPChl was  $123 \text{ g C [g Chl} \cdot \text{d]}^{-1}$  during the May diatom bloom compared to the nanoplankton PPChl of  $79 \text{ g C [g Chl} \cdot \text{d]}^{-1}$ . During July when nanoplankton dominated and the spatial distribution of chlorophyll was relatively stationary in time prior to the southwest wind event, nanoplankton PPChl was  $94 \text{ g C [g Chl} \cdot \text{d]}^{-1}$  compared to  $42 \text{ g C [g Chl} \cdot \text{d]}^{-1}$  for netplankton. Neither fraction clearly dominated during November when both chlorophyll a and PPChl were low. Although netplankton dominated during March, PPChl was similar in both fractions. However,

Table 19. Primary productivity of particulate organic carbon (PP, mg C m<sup>-2</sup> d<sup>-1</sup>), the proportion of PP accounted for by netplankton (% Net), proportion of total productivity released as dissolved organic carbon (% DOC), and incident radiation (I<sub>0</sub>, E m<sup>-2</sup> d<sup>-1</sup>) (C = coefficient of variation).

Date	PP	% Net	% DOC	I <sub>0</sub>	Date	PP	% Net	% DOC	I <sub>0</sub>
7 Mar	3.27	86	6	28	11 May	1.76	57	9	46
8	1.84	83	10	9	12	1.33	46	9	47
9	0.76	50	26	14	13	2.05	65	11	48
10	1.23	75	5	7	14	3.90	82	8	49
11	0.68	50	20	20	15	4.49	74	7	40
12	1.15	71	27	25	16	4.97	76	4	38
13	0.12	21	45	11	17	4.87	78	6	34
Mean	1.29	62	13	16	Mean	3.34	68	7	43
C	79%			51%	C	47%			13%
20 July	2.26	1	7	35	11 Nov	0.21	47	29	12
21	3.47	1	8	41	16	0.22	26	8	13
23	0.60	4	7	47	17	0.24	21	10	8
24	0.55	12	12	39	18	0.19	24	10	12
27	1.09	5	8	47	19	0.12	33	21	11
Mean	1.59	5	8	42	Mean	0.20	30	16	11
C	79%			12%	C	25%			17%

Table 20. Linear regression and correlation analyses of phytoplankton productivity ( $\text{mg C m}^{-2} \text{d}^{-1}$ ) on chlorophyll *a* ( $\text{mg m}^{-2}$ ) in the euphotic zone during each cruise (Net = netplankton, Nano = nanoplankton, Whl = unfractionated, a = intercept, b = slope,  $r^2$  = coefficient of determination, n = number of measurements).

Cruise	Fraction	n	$r^2$	a	b
March	Nano	7	0.74	- 39	35
	Net	7	0.90	- 56	37
	Whl	7	0.90	- 26	37
May	Nano	7	0.94	- 462	79
	Net	6 <sup>1</sup>	0.99	- 474	123
	Whl	6 <sup>1</sup>	0.99	-1384	116
July	Nano	5	0.95	- 412	94
	Net	5	0.81	4	42
	Whl	5	0.95	- 480	96
Nov.	Nano	5	0.92	8	23
	Net	5	0.99	2	20
	Whl	5	0.96	- 3	24

<sup>1</sup> Productivity on May 17 was deleted because it was low, probably as a consequence of silicate limitation.

measurements were made during the collapse of a netplankton bloom when nanoplankton chlorophyll a was increasing relative to netplankton chlorophyll a (Table 5) and, therefore, PPChl would not be expected to be expressed in the relative biomass of the two size fractions.

Nanoplankton PPChl varied between cruises and was highly correlated ( $R^2 = 0.97$ ) with incident radiation ( $I_0$ ) and temperature (T) by the multiple regression equation

$$ppChl = -0.14 + 1.82 (I_0) + 0.58 (T) .$$

Netplankton PPChl was less predictable in terms of synoptic environmental parameters (light, temperature, nutrients, vertical stability) but was related to time-dependent variations in netplankton chlorophyll a, i.e., PPChl was highest during exponential growth (May) and lowest when biomass was low (November) and declining (March). These findings are consistent with the conclusion that nanoplankton growth varies on a seasonal time scale while netplankton growth varies episodically. This suggests that diatom populations are more responsive to storm events which generate vertical mixing and upwelling (Malone 1982b; Malone et al. in press b).

The importance of light attenuation by chlorophyll a relative to nonphotosynthetic materials in the euphotic zone is illustrated by the relationship between productivity and the proportion of light attenuated by phytoplankton (Fig. 20). Light attenuation by phytoplankton ( $I_{Chl}$ ) was calculated from Morel (1978) as  $I_{Chl} = k_c [Chl]$  where  $k_c$  is the mean absorption coefficient per unit chlorophyll a ( $0.015 \text{ m}^{-1} [\text{mg Chl m}^{-3}]^{-1}$ ) and  $[Chl]$  is the mean concentration of chlorophyll a ( $\text{mg m}^{-3}$ ) in the euphotic zone. Phytoplankton accounted for 1-26 percent of light attenuation in the euphotic zone, with values of less than 5 percent typical of November and rates above 15 percent limited to March and May. Maximum productivity (%  $I_{Chl} = 100$ ) would be  $30 \text{ g C m}^{-2} \text{ d}^{-1}$  during May and July compared to  $11 \text{ g C m}^{-2} \text{ d}^{-1}$  during March. Ryther (1959) estimated a theoretical maximum of  $25 \text{ g C m}^{-2} \text{ d}^{-1}$  given incident radiation of  $50 \text{ E m}^{-2} \text{ d}^{-1}$  (maximum for summer at temperature latitudes). Low maximum productivity during March is probably a consequence of more uniform distributions of chlorophyll a

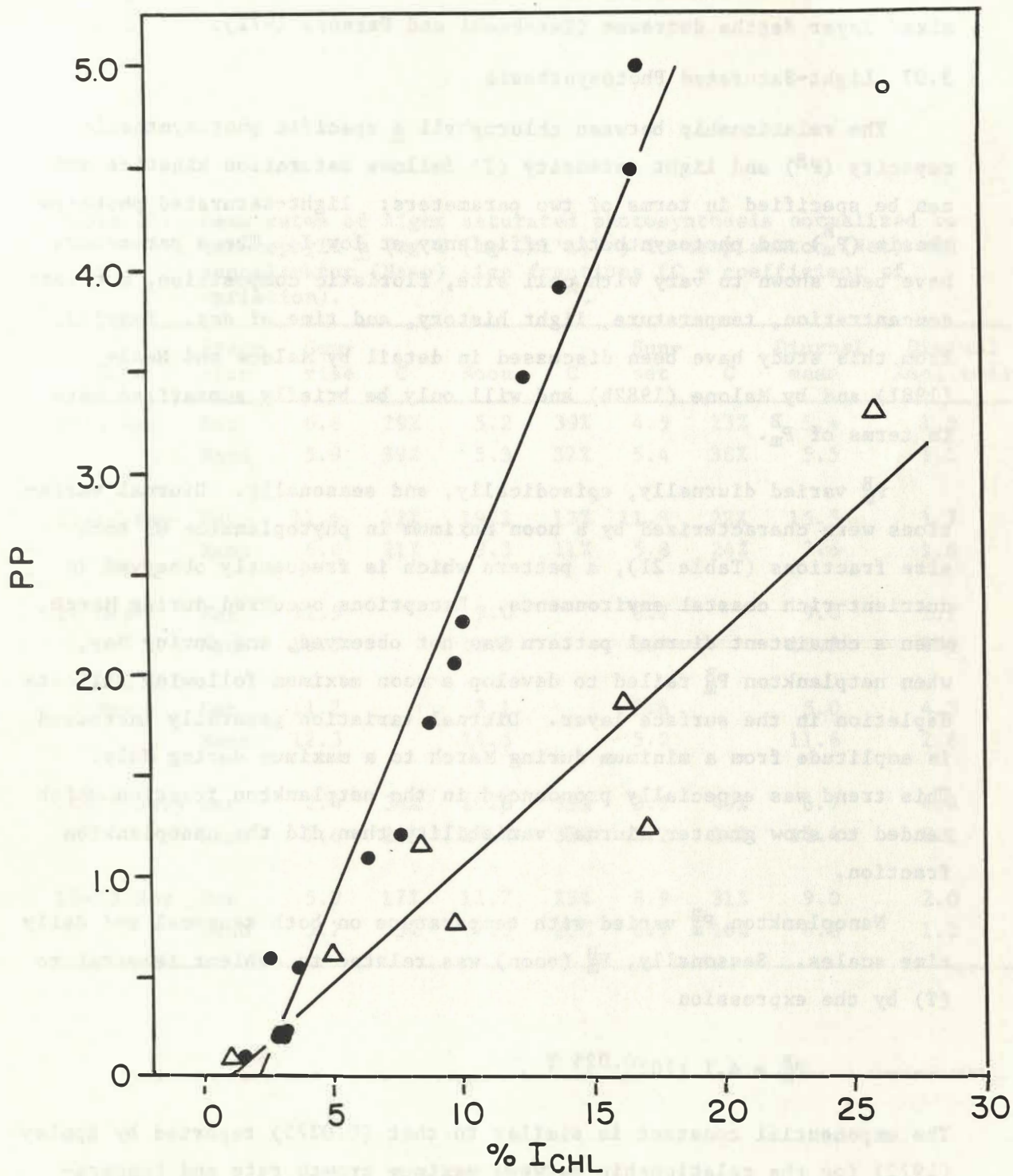


Figure 20. Primary productivity (PP,  $\mu\text{g C m}^{-2} \text{d}^{-1}$ ) as a function of the proportion of light attenuation due to chlorophyll a (% I<sub>chl</sub>) (Δ, March; ● May, June and July; ○ at peak of bloom during May after silicate depletion).

with depth (Fig. 10) and weaker stratification of the water column (Fig. 6), since maximum productivity increases as euphotic zone and mixed layer depths decrease (Takahashi and Parsons 1972).

### 3.07 Light-Saturated Photosynthesis

The relationship between chlorophyll a specific photosynthetic capacity ( $P^B$ ) and light intensity ( $I$ ) follows saturation kinetics and can be specified in terms of two parameters: light-saturated photosynthesis ( $P_m^B$ ) and photosynthetic efficiency at low  $I$ . These parameters have been shown to vary with cell size, floristic composition, nutrient concentration, temperature, light history, and time of day. Results from this study have been discussed in detail by Malone and Neale (1981) and by Malone (1982b) and will only be briefly summarized here in terms of  $P_m^B$ .

$P_m^B$  varied diurnally, episodically, and seasonally. Diurnal variations were characterized by a noon maximum in phytoplankton of both size fractions (Table 21), a pattern which is frequently observed in nutrient-rich coastal environments. Exceptions occurred during March, when a consistent diurnal pattern was not observed, and during May, when netplankton  $P_m^B$  failed to develop a noon maximum following silicate depletion in the surface layer. Diurnal variation generally increased in amplitude from a minimum during March to a maximum during July. This trend was especially pronounced in the netplankton fraction which tended to show greater diurnal variability than did the nanoplankton fraction.

Nanoplankton  $P_m^B$  varied with temperature on both seasonal and daily time scales. Seasonally,  $P_m^B$  (noon) was related to ambient temperature ( $T$ ) by the expression

$$P_m^B = 4.1 (10)^{0.025 T} .$$

The exponential constant is similar to that (0.0275) reported by Eppley (1972) for the relationship between maximum growth rate and temperature, which suggests that photosynthesis and growth are in approximate steady-state in the nanoplankton fraction on a seasonal time scale.

Table 21. Mean rates of light saturated photosynthesis normalized to chlorophyll a ( $\text{mg C} [\text{mg Chl}\cdot\text{n}]^{-1}$ ) in netplankton (Net) and nanoplankton (Nano) size fractions (C = coefficient of variation).

Date	Fraction	Sun-rise	C	Noon	C	Sun-set	C	Diurnal mean	Diurnal Amplitude
6-14 Mar	Net	6.6	29%	5.2	39%	4.5	23%	5.4	1.5
	Nano	5.9	39%	5.3	37%	5.4	38%	5.5	1.1
11-17 May	Net	11.6	12%	19.2	13%	11.9	22%	15.5	1.7
	Nano	6.0	21%	9.3	11%	5.8	24%	7.6	1.6
18 May	Net	11.5		9.0		6.7		9.0	1.7
	Nano	10.5		12.0		6.4		10.2	1.9
19 May	Net	11.2		3.1		2.6		5.0	4.3
	Nano	12.3		14.5		5.2		11.6	2.8
20-28 July	Net	2.4	34%	10.6	39%	3.2	49%	6.7	4.4
	Nano	7.6	24%	15.4	33%	7.2	34%	11.4	2.1
10-19 Nov	Net	5.9	17%	11.7	23%	6.9	31%	9.0	2.0
	Nano	5.7	23%	7.5	20%	6.7	16%	6.8	1.3

Nanoplankton  $P_m^B$  also responded to the rapid temperature increase observed during the May diatom bloom.  $P_m^B$  was related to temperature depending on time of day as follows:

$$P_m^B = 0.58 (10)^{0.10} T \quad (\text{sunrise});$$

$$P_m^B = 0.34 (10)^{0.11} T \quad (\text{noon}); \text{ and}$$

$$P_m^B = 0.21 (10)^{0.05} T \quad (\text{sunset}).$$

Thus, nanoplankton  $P_m^B$  was more sensitive to daily increases in temperature ( $0.5 \text{ }^\circ\text{C d}^{-1}$ ) than to seasonal increases ( $0.17 \text{ }^\circ\text{C d}^{-1}$ ), especially during the first half of the photoperiod.

Like  $PP^{Ch1}$ , variations in netplankton  $P_m^B$  were less predictable and were not correlated with temperature, nutrients, or vertical stability on a seasonal time scale (Malone and Neale 1981). Seasonal variations in netplankton  $P_m^B$  appear to be more related to environmental history and species composition than to ambient environmental conditions.

However, an important exception was documented during the May diatom bloom when  $P_m^B$  was influenced by silicate depletion (Table 21). Netplankton  $P_m^B$  was high during the first few days of the bloom when  $P_m^B$  had a noon maximum.  $P_m^B$  failed to develop a noon maximum on May 18-19 as noon and sunset rates showed a marked decline. This change in the diurnal phasing of  $P_m^B$  and the decrease in noon and sunset rates occurred 24 hours after silicate depletion was first observed in the surface layer. This was the only clear case of nutrient limitation observed (Fig. 8) and is consistent with the conclusion that phytoplankton growth is not nutrient limited on a seasonal time scale but can experience transient nutrient limitation on the event time scale (Malone 1977). Variations in netplankton  $P_m^B$  appear to be more related to how physical processes distribute cells with respect to the euphotic zone than are variations in nanoplankton  $P_m^B$ .

### 3.08 Uptake of Nitrate and Ammonium by Phytoplankton

Uptake rates ( $\mu\text{g-at liter}^{-1} \text{ h}^{-1}$ ), a function of uptake velocity and particulate nitrogen concentration, were low during March and November ( $<0.05 \mu\text{g-at liter}^{-1} \text{ h}^{-1}$ ) and high during May and July

(Table 22). During May, uptake rate increased from less than  $0.1 \mu\text{g-at liter}^{-1} \text{ h}^{-1}$  to greater than  $0.5 \mu\text{g-at liter}^{-1} \text{ h}^{-1}$  as the diatom bloom developed. During July, uptake rates were highest ( $>0.1 \mu\text{g-at liter}^{-1} \text{ h}^{-1}$ ) near the mouth of the estuary prior to the southwest wind event and during the nanoplankton bloom which followed the wind event.

Velocities of nitrate and ammonium uptake ( $\text{h}^{-1}$ ) were saturated at less than 10 percent of incident radiation and showed inhibition at light levels greater than 40 percent of incident (Garside 1981). Uptake velocity of nitrate and ammonium as a function of light varied, but the velocity of total inorganic nitrogen uptake as a function of light was adequately described by a single curve during March and November and by two curves during July (Garside 1981). Maximum uptake velocities (at light saturation) were low ( $<0.007 \text{ h}^{-1}$ ) during March and November and high ( $>0.02 \text{ h}^{-1}$ ) during May and July when chlorophyll a concentrations were high. High velocities of nitrate and ammonium uptake were observed simultaneously only when chlorophyll a exceeded  $10 \mu\text{g liter}^{-1}$  and ammonium concentration was less than  $2 \mu\text{g-at liter}^{-1}$ , i.e., when phytoplankton uptake was high and substrate concentrations of nitrogen were low. Given the concentrations of nitrate and ammonium typical of the plume (Tables 7 and 22), these results indicate that uptake velocities are usually independent of substrate concentration in the plume. Garside (1981) concluded that uptake velocities were light-dependent under most conditions.

Ammonium uptake exceeded nitrate uptake except when ambient ammonium concentration was less than  $2 \mu\text{g-at liter}^{-1}$  (Fig. 21). The general preference for ammonium over nitrate is consistent with the concept of ammonium inhibition of nitrate uptake, and our results are similar to those reported by McCarthy et al. (1977) for phytoplankton in Chesapeake Bay. It should be noted that light intensity did not influence this preference (Fig. 21) so that, while total uptake was light-dependent, the form taken up was dependent on the concentration of ammonium.

Table 22. Seasonal ranges of ambient concentrations of particulate nitrogen (PN), nitrate, and ammonium, and maximum uptake velocities ( $\text{h}^{-1}$ ) and rates ( $\mu\text{g-at liter}^{-1} \text{h}^{-1}$ ) of nitrate and ammonium uptake.

Month	$\mu\text{g-at liter}^{-1}$			$\text{h}^{-1}$		$\mu\text{g-at liter}^{-1} \text{h}^{-1}$	
	PN	$\text{NO}_3$	$\text{NH}_4$	$\text{NO}_3$	$\text{NH}_4$	$\text{NO}_3$	$\text{NH}_4$
March	4.9	1.9	0.5	0.001	0.002	0.01	0.01
	6.1	5.5	2.2	0.006	0.006	0.03	0.03
May	7.1	2.7	0.6	0.000	0.001	0.00	0.01
	19.3	13.4	11.2	0.025	0.036	0.48	0.75
July	6.5	0.0	0.3	0.003	0.005	0.02	0.04
	18.3	3.0	8.3	0.027	0.052	0.46	0.85
Nov	3.8	3.1	3.4	0.001	0.006	0.01	0.02
	3.9	3.6	3.8	0.001	0.008	0.01	0.03

and July (Table 22). During May, uptake rate increased from less than  $0.1 \mu\text{g-at liter}^{-1} \text{ h}^{-1}$  to greater than  $0.5 \mu\text{g-at liter}^{-1} \text{ h}^{-1}$  as the diatom bloom developed. During July, uptake rates were highest ( $>0.1 \mu\text{g-at liter}^{-1} \text{ h}^{-1}$ ) near the mouth of the estuary prior to the southwest wind event and during the nanoplankton bloom which followed the wind event.

Velocities of nitrate and ammonium uptake ( $\text{h}^{-1}$ ) were saturated at less than 10 percent of incident radiation and showed inhibition at light levels greater than 40 percent of incident (Garside 1981). Uptake velocity of nitrate and ammonium as a function of light varied, but the velocity of total inorganic nitrogen uptake as a function of light was adequately described by a single curve during March and November and by two curves during July (Garside 1981). Maximum uptake velocities (at light saturation) were low ( $<0.007 \text{ h}^{-1}$ ) during March and November and high ( $>0.02 \text{ h}^{-1}$ ) during May and July when chlorophyll a concentrations were high. High velocities of nitrate and ammonium uptake were observed simultaneously only when chlorophyll a exceeded  $10 \mu\text{g liter}^{-1}$  and ammonium concentration was less than  $2 \mu\text{g-at liter}^{-1}$ , i.e., when phytoplankton uptake was high and substrate concentrations of nitrogen were low. Given the concentrations of nitrate and ammonium typical of the plume (Tables 7 and 22), these results indicate that uptake velocities are usually independent of substrate concentration in the plume. Garside (1981) concluded that uptake velocities were light-dependent under most conditions.

Ammonium uptake exceeded nitrate uptake except when ambient ammonium concentration was less than  $2 \mu\text{g-at liter}^{-1}$  (Fig. 21). The general preference for ammonium over nitrate is consistent with the concept of ammonium inhibition of nitrate uptake, and our results are similar to those reported by McCarthy et al. (1977) for phytoplankton in Chesapeake Bay. It should be noted that light intensity did not influence this preference (Fig. 21) so that, while total uptake was light-dependent, the form taken up was dependent on the concentration of ammonium.

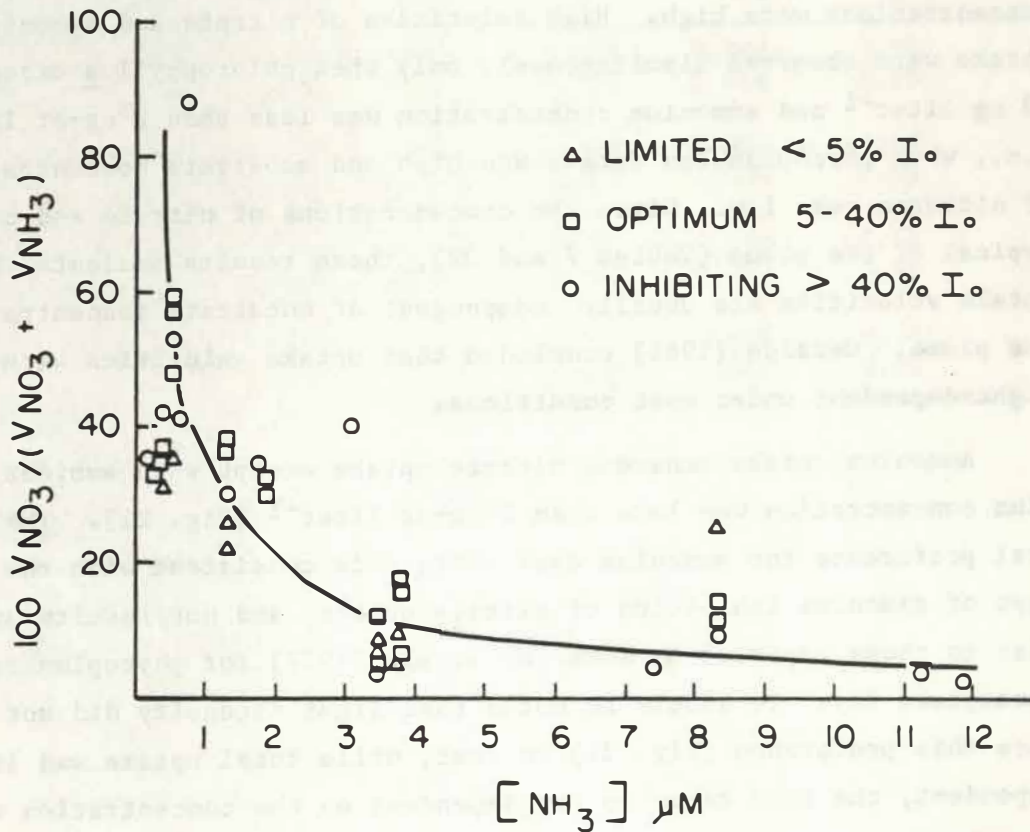


Figure 21. Percentage of total nitrogen uptake velocity as nitrate at different substrate concentrations ( $\mu\text{g-at liter}^{-1}$ ) of ammonium.

Estimates of mean seasonal uptake rates varied from  $125 \text{ mg N m}^{-2} \text{ d}^{-1}$  during July to  $82 \text{ mg N m}^{-2} \text{ d}^{-1}$  during March and  $22 \text{ mg N m}^{-2} \text{ d}^{-1}$  during November. These seasonal trends are similar to those for primary productivity (Table 19) but yield C:N assimilation ratios that are high (March C:N = 16, July C:N = 13, November C:N = 9 by weight) compared to biomass ratios (Table 17). This may reflect the assumption that nitrogen was only assimilated during the photoperiod or differential metabolism of C and N during respiration when phytoplankton might be expected to retain more N than C.

### 3.09 Biomass and Abundance of Copepods

Copepods were the most abundant group of macrozooplankton, accounting for 87, 90, 82, and 65 percent of individuals during March, May, July, and November, respectively. Other abundant organisms included barnacle larvae (March), polychaete larvae (May), bivalve larvae (July and November), doliolids (July and November), cladocera (May, July, and November), gastropods (July), and chaetognaths (March and May). A total of 29 species of copepods and 23 other taxa were identified, the number of species present during any given cruise being highest during November when a variety of offshore forms were present. Such an influx of offshore forms occurs annually during November (Judkins et al. 1980; Stepien et al. 1981).

Mean copepod abundance increased by an order of magnitude from less than  $2.0 \times 10^3 \text{ m}^{-3}$  during March and November to nearly  $2.0 \times 10^4 \text{ m}^{-3}$  during July (Table 23). Variations in abundance were significant between months relative to daily variations (F test,  $P < 0.001$ ) and were consistent with the seasonal cycle of abundance described for previous years (Chervin 1978; Malone and Chervin 1979). Copepod biomass (dry weight) was significantly correlated with abundance during each cruise (Table 24). The six copepod species listed in Table 23 dominated the macrozooplankton during all four cruises, i.e., various combinations of these species accounted for more than 75 percent of total copepods. A more complete discussion of copepod communities in the estuary and coastal plume of the Hudson River is given by Stepien et al. (1981).

Table 23. Mean abundance ( $10^3 \text{ m}^{-3}$ ) and frequency of occurrence (percent of total samples) of the most abundant species of copepods.

Species	March	%	May	%	July	%	Nov	%
<u>Pseudocalanus minutus</u>	0.65	100	1.01	100	7.86	100	0.02	76
<u>Centropages typicus</u>	0.01	77	0.01	54	2.65	100	0.61	100
<u>Oithona similis</u>	0.16	100	1.77	100	1.93	100	0.09	95
<u>Temora longicornis</u>	0.01	65	0.77	100	1.24	100	0.00	52
<u>Paracalanus parvus</u>	0.00	8	0.00	0	0.26	88	0.19	95
<u>Acartia tonsa</u>	0.00	15	0.00	8	0.31	92	0.15	100
Total copepods	1.94		5.30		18.85		1.77	
Number of samples	26		24		25		21	

Table 24. Linear regression and correlation analysis of copepod biomass (mg of adult copepods  $\text{m}^{-3}$ ) on abundance (no. of adult copepods  $\text{m}^{-3}$ ) n = number of observations, r = correlation coefficient, a = intercept, b = slope; all correlations were significant,  $P < 0.01$ .

Month	n	r	a	b
March	23	0.73	-0.54	0.004
May	26	0.86	-6.66	0.02
July	25	0.96	3.91	0.005
Nov	21	0.97	0.36	0.01

### 3.10 Plankton Respiration

Microbial Respiration: Rates of respiration by microplankton ( $R_m$ ) in carbon equivalents ( $RQ = 1$ ) ranged from 0.4 to 10.0 g C m<sup>-2</sup> d<sup>-1</sup>, with low rates during November and high rates during July (Table 25). There is some question as to whether  $R_m$  included the respiration of copepods during July. Copepods were abundant at this time and were frequently observed in BOD bottles. However, Niskin bottles do not sample copepods quantitatively, and it is likely that  $R_m$  overestimated microbial respiration but underestimated total plankton respiration.

Vertical gradients were most pronounced during May and July when the water column was well stratified and most respiration occurred in the surface layer (Table 25). Respiration was more evenly distributed between layers during March and November when vertical mixing was greatest. These patterns paralleled the distribution of chlorophyll a, and respiration was significantly correlated with chlorophyll a in the surface layer during May and July and in the water column during March and November (Table 26). Poor correlations in the bottom layer during May and July were partly due to low chlorophyll a concentrations and reflected the importance of organic substrates other than those associated with phytoplankton. Positive correlations during May and July were probably a consequence of respiration by both phytoplankton and microheterotrophs. Chlorophyll a specific respiration increased from May to July (slope of the regression equations in Table 26), suggesting that microheterotrophs accounted for a greater proportion of respiration during July than during May.

Respiration and chlorophyll a were inversely related during March (Table 26). This coincided with the collapse of a diatom bloom and implies that the respiration of phytoplankton or microheterotrophs increased as the bloom collapsed. We have no evidence to resolve the two processes, but it is likely that both were involved.

Seasonal variations in chlorophyll a specific respiration ( $R_m^B$ ) in surface (s) and bottom (b) layers were correlated with temperature (T) by the least square regressions

Table 25. Mean and range of respiration rates (in carbon equivalents,  $\text{g C m}^{-2} \text{d}^{-1}$ ) for microplankton ( $R_m$ ) and copepods ( $R_c$ ); T = surface temperature ( $^{\circ}\text{C}$ ) and % SL = proportion of microbial respiration in the surface layer.

Month		T	$R_m$	% SL	$R_c$
			9.96	79	0.03
March	mean	1.8	1.81	48	0.02
			3.05	20	0.00
			3.21	94	0.56
May	mean	11.1	1.92	76	0.23
			0.89	69	0.03
			9.23	96	3.44
July	mean	20.8	3.16	85	1.64
			1.75	71	0.46
			2.10	72	0.59
Nov	mean	12.7	0.91	57	0.24
			0.38	38	0.05

Table 26. Correlation and regression analysis of depth integrated respiration ( $\text{mg C m}^{-2} \text{d}^{-1}$ ) on chlorophyll a ( $\text{mg m}^{-2}$ ) (SL = surface layer, BL = bottom layer, WC = water column, r = correlation coefficient, a = intercept, b = slope, NS = not significant).

Month	Layer	n	r	a	b
May	SL	15	0.71**	712	18
	BL	15	NS	254	12
July	SL	12	0.95**	407	61
	BL	12	NS	357	13
Nov	WC	10	0.68*	328	26
March	WC	14	-0.61*	2623	-7

\* P < 0.05

\*\* P < 0.01

$$(R_m^B)_s = 11.5 + 2.5 T \quad (r=0.77, n=48, P<0.01)$$

and  $(R_m^B)_b = 13.6 + 2.7 T \quad (r=0.47, n=48, P<0.01),$

where  $R_m^B$  = depth integrated respiration per unit chlorophyll a.

Copepod Respiration: Respiration by copepods ( $R_C$ ) varied from 0.00 to 3.44 g C m<sup>-2</sup> d<sup>-1</sup> with rates being highest during July and lowest during March (Table 25).  $R_C$ , as a proportion of total respiration in the water column ( $R_C + R_m$ ), ranged from a mean of 1 percent during March to 34 percent during July. These variations reflected changes in the abundance of copepods (section 3.09) and copepod specific respiration ( $R$ , Table 27), both of which were low during March and high during July. Variations in  $R$  were positively correlated with temperature and with assimilation rates of organic substrates other than phytoplankton (section 3.11; Chervin et al. 1981).

### 3.11 Assimilation of Particle Organic Matter by Copepods

Copepod biomass, assimilation, and respiration exhibited similar patterns of variation. As a proportion of phytoplankton biomass, copepod biomass increased from a mean of 0.4 percent in March to 6 percent in May and 24 percent in July. By November this proportion had dropped to 5 percent. Mean assimilation rates of POC ( $A_{POC}$ ) and PN ( $A_{PN}$ ) increased from 0.7  $\mu$ g C copepod<sup>-1</sup> d<sup>-1</sup> and 0.1  $\mu$ g N copepod<sup>-1</sup> d<sup>-1</sup> in March to 10.5  $\mu$ g C copepod<sup>-1</sup> d<sup>-1</sup> and 1.6  $\mu$ g N copepod<sup>-1</sup> d<sup>-1</sup> in July (Table 27). Likewise, respiration ( $R$ ) increased from 0.5  $\mu$ g C copepod<sup>-1</sup> d<sup>-1</sup> in March to 7.8  $\mu$ g C copepod<sup>-1</sup> d<sup>-1</sup> in July. Net growth efficiency was in the range of efficiencies reported for copepods (20 to 60 percent; Tranter 1976) except in November when efficiency averaged only 6 percent and N:C assimilation ratios were low (Table 27).

Assimilation rates of phytoplankton ( $A_{Ph}$ ) did not parallel variations in total assimilation in that absolute rates were lowest in

Table 27. Mean and range of incubation temperature (T, C), rates of assimilation ( $\mu\text{g copepod}^{-1} \text{d}^{-1}$ ), proportion of assimilation accounted for by phytoplankton (%Ph-C, %Ph-N), PN:POC assimilation ratio (N:C by weight), respiration (R,  $\mu\text{g C copepod}^{-1} \text{d}^{-1}$ ), and growth efficiency ( $K = (A-R)/A$ ).

Date	T	Assimilation					R	K
		POC	%Ph-C	PN	%Ph-N	N:C		
8-12 Mar	4.5	0.50	51	0.07	33	0.14	0.40	0.12
	5.7	0.72	75	0.11	56	0.15	0.47	0.35
	7.2	0.94	100	0.14	87	0.17	0.62	0.52
11-19 May	13.9	3.12	11	0.43	17	0.13	1.81	0.15
	14.9	6.15	22	0.85	30	0.14	2.68	0.56
	16.0	9.51	34	1.27	44	0.15	5.02	0.75
20-27 July	23.0	5.47	1	1.09	2	0.12	2.93	0.01
	24.2	10.49	26	1.56	29	0.15	7.75	0.26
	25.0	17.22	97	2.43	84	0.20	11.36	0.61
10-18 Nov	13.0	3.67	2	0.40	2	0.10	3.65	-0.01
	13.7	5.02	3	0.53	4	0.11	4.71	0.06
	14.8	6.80	5	0.71	7	0.11	6.41	0.21

November and the proportion of phytoplankton assimilated was highest in March (Table 27). Mean assimilation rates of phytoplankton biomass as carbon ( $A_{Ph-C}$ ) and nitrogen ( $A_{Ph-N}$ ) increased from  $0.15 \mu\text{g C copepod}^{-1} \text{d}^{-1}$  and  $0.02 \mu\text{g N copepod}^{-1} \text{d}^{-1}$  in November to  $2.73 \mu\text{g C copepod}^{-1} \text{d}^{-1}$  and  $0.45 \mu\text{g N copepod}^{-1} \text{d}^{-1}$  in July. These rates are probably too high since they were calculated from changes in chlorophyll a concentration. However, the error is systematic and probably small since assimilation efficiencies are typically high (70 to 90 percent) and relatively constant over a wide range of algal concentration and temperature (Conover 1966), i.e., absolute rates may be overestimated depending on assimilation efficiency but patterns of variation should remain about the same.

Some circumstantial evidence is available to support the argument that the error associated with estimates of  $A_{Ph}$  were small. (1) The proportion of phytoplankton assimilated increased as the proportion available increased (Tables 18 and 27) and proportions of netplankton and nanoplankton assimilated parallel changes in the proportions available (Table 15). (2) More importantly, changes in factor scores for psd curves before and after grazing were significantly correlated with changes in chlorophyll a concentration (Table 15). Decreases in chlorophyll a during grazing experiments were best correlated with factors 3 and 2 when netplankton dominated and with factor 1 when nanoplankton dominated. Peaks in psd curves produced by phytoplankton were grazed as indicated by changes in both psd curves and chlorophyll a in phytoplankton size fractions.

Interactions between assimilation rates, respiration, temperature and food concentrations were evaluated by partial correlation and regression analyses (Table 28). Partial correlation revealed significant positive effects of temperature, phytoplankton-carbon (Ph-C), non-phytoplankton-carbon (NPh-C) and a negative effect of NPh-C assimilation ( $A_{NPh-C}$ ) on the assimilation of phytoplankton-carbon ( $A_{Ph-C}$ ). The minimum number of variables required to account for more than 50% of the variance in assimilation and respiration was determined by multiple correlation. Of the variables tested, only Ph-C had a

Table 28. Partial correlation coefficients and standard partial regression coefficients for interactions between copepod specific rates ( $\mu\text{g C copepod}^{-1} \text{d}^{-1}$ ) of assimilation (A) and respiration (R), temperature ( $^{\circ}\text{C}$ ), and concentrations ( $\mu\text{g l}^{-1}$ ) of phytoplankton-carbon (Ph-C) and nonphytoplankton-carbon (NPh-C);  $R^2$  = multiple coefficient of determination ( $n = 22$ ).

	A <sub>Ph-C</sub>	A <sub>NPh-C</sub>	R	T	Ph-C	NPh-C	$R^2$
<b>Correlation</b>							
A <sub>Ph-C</sub>	1.00	-0.52**	-0.18	0.64**	0.57**	0.50*	
A <sub>NPh-C</sub>		1.00	0.41*	0.30	0.38*	0.16	
R			1.00	0.63**	-0.43*	0.05	
T				1.00	0.03	0.02	
Ph-C					1.00	-0.39*	
NPh-C						1.00	
<b>Regression</b>							
A <sub>Ph-C</sub>		-0.56		0.89	0.42		0.82
A <sub>NPh-C</sub>	-0.34		0.99		0.31		0.76
R		0.38		0.53	-0.33		0.89

\*  $P < 0.05$

\*\*  $P < 0.01$

significant effect on all copepod specific rates. Temperature,  $A_{NPh-C}$ , and Ph-C accounted for 82 percent of the variance in  $A_{Ph-C}$ . The positive effects of temperature and Ph-C are clearly shown in Figure 22.  $A_{Ph-C}$  increased as Ph-C increased and exhibited steeper response curves over similar ranges of Ph-C as temperature increased. Increases in phytoplankton biomass were also associated with increases in N:C assimilation ratios (Fig. 22) suggesting that phytoplankton are more important than nonphytoplankton material as a source of protein. The negative effect of  $A_{NPh-C}$  on  $A_{Ph-C}$  (Table 25) may be indicative of an inhibitory effect or a tendency to increase  $A_{Ph-C}$  as a proportion of total assimilation in response to peaks in phytoplankton biomass.

Unlike  $A_{Ph-C}$  which was correlated with its substrate,  $A_{NPh-C}$  was unrelated to  $N_{Ph-C}$  (Table 28). Respiration (R),  $A_{Ph-C}$ , and Ph-C accounted for 76 percent of the variation in  $A_{NPh-C}$ . The positive interaction between R and  $A_{NPh-C}$  is intriguing and is consistent with the hypothesis that organic detritus can be used as an energy source but phytoplankton are required for nutrition (Heinle et al. 1974, 1977; Roman 1977; Chervin 1978). Interactions between  $A_{Ph-C}$ ,  $A_{NPh-C}$ , and their substrates suggest that the presence of phytoplankton stimulated assimilation rates in general, but that as phytoplankton biomass increased, assimilation rates of phytoplankton increased more rapidly than assimilation rates of nonphytoplankton. This was apparently the case for both POC and PN assimilation (Fig. 23). As Ph-C and Ph-N increased relative to POC and PN,  $A_{Ph-C}$  and  $A_{Ph-N}$  increased exponentially relative to total assimilation. The threshold concentration of phytoplankton below which phytoplankton assimilation was disproportionately low was about 50 percent of the total standing crop of particulate organic matter. Above 50 percent, assimilation of phytoplankton biomass increased rapidly and approached 100 percent of total assimilation when phytoplankton accounted for only 60 percent of suspended organic matter. Since phytoplankton seem to be richer in nitrogen than nonphytoplankton organic matter, N:C assimilation ratios generally increased as phytoplankton biomass increased (Fig. 22). Thus, growth efficiency increased as the N:C assimilation ratio

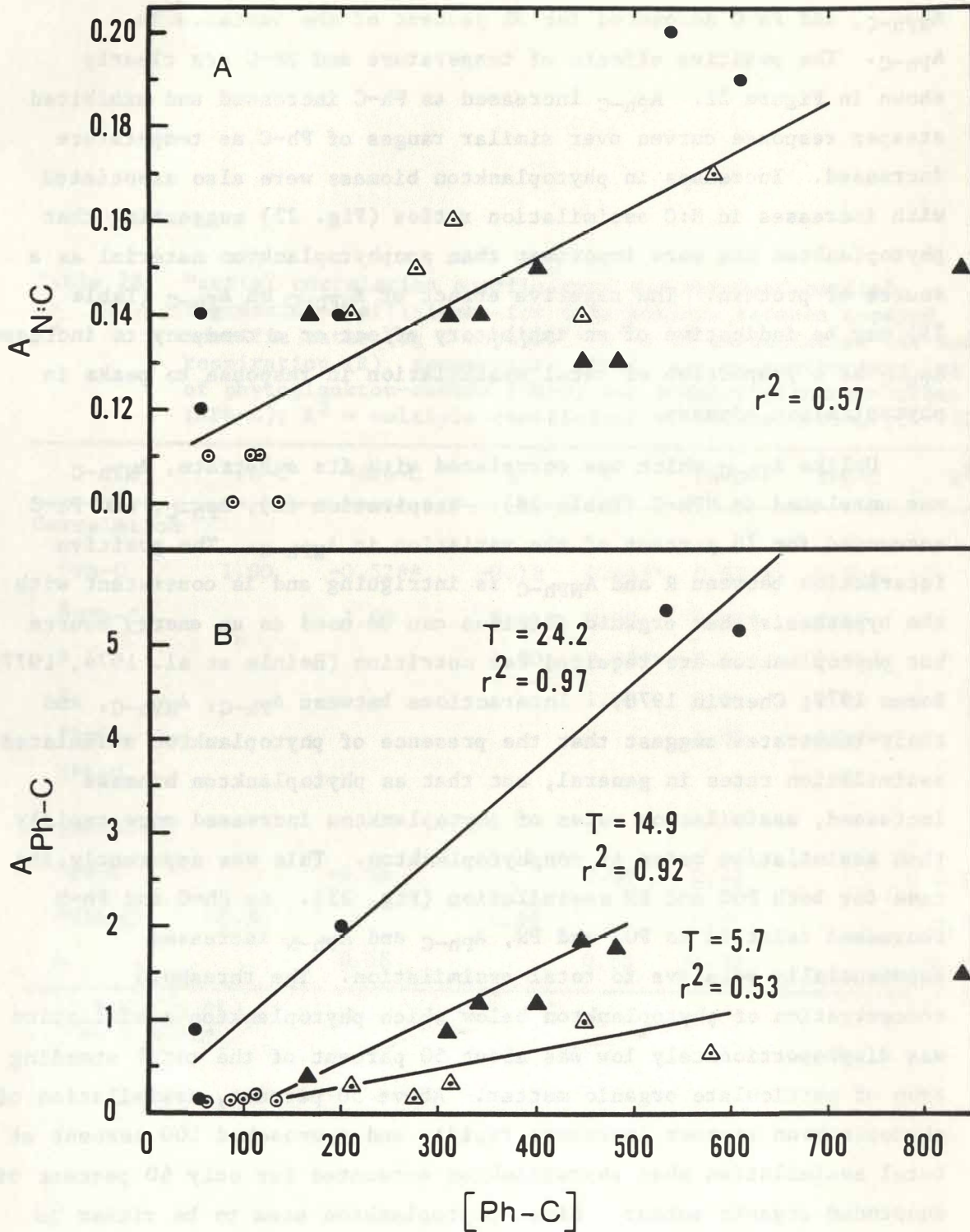


Figure 22. (A) ratio of nitrogen to carbon assimilation rates ( $A_{N:C}$ ) and (B) the assimilation rate of phytoplankton-carbon ( $A_{Ph-C}$ ,  $\mu\text{g C copepod}^{-1} \text{d}^{-1}$ ) as functions of Ph-C available ( $\mu\text{g liter}^{-1}$ ) during March ( $\Delta$ ), May ( $\blacktriangle$ ), July ( $\bullet$ ), and November ( $\circ$ ) ( $T = \text{°C}$ ,  $r^2 = \text{coefficient of determination}$ ).

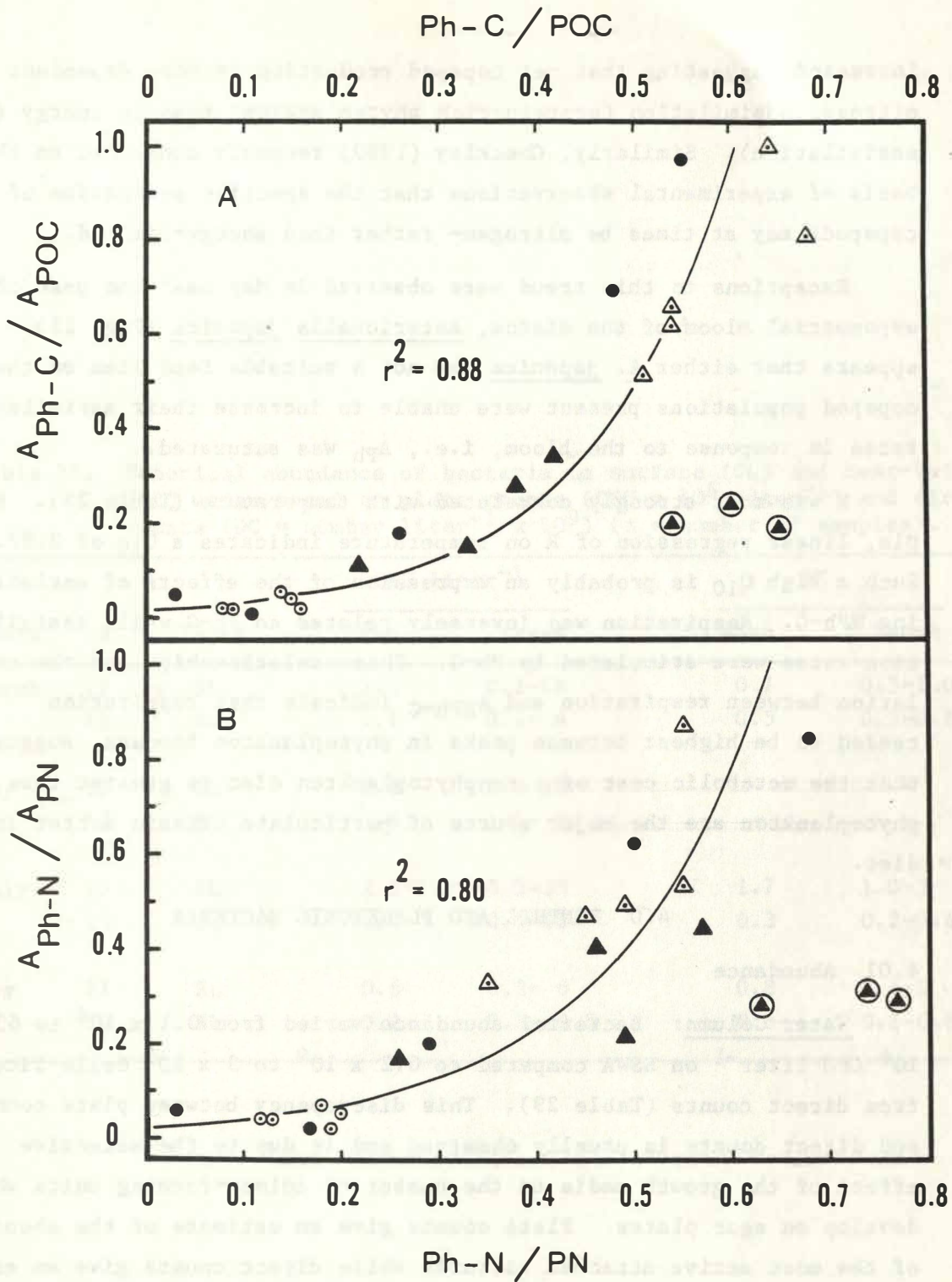


Figure 23. (A) Proportions of phytoplankton-carbon ( $A_{Ph-C}/A_{POC}$ ) and (B) nitrogen ( $A_{Ph-N}/A_{PN}$ ) assimilated relative to total assimilation as functions of the proportion of phytoplankton-carbon ( $Ph-C/POC$ ) and nitrogen ( $Ph-N/PN$ ) available during March ( $\Delta$ ), May ( $\blacktriangle$ ), July ( $\bullet$ ), and November ( $\circ$ ); circled triangles indicate ratios at peak of the May bloom not used in the regression-correlation analysis ( $r^2 =$  coefficient of determination).

increased suggesting that net copepod production is more dependent on nitrogen assimilation (protein-rich phytoplankton) than on energy (POC assimilation). Similarly, Checkley (1980) recently concluded on the basis of experimental observations that the specific production of copepods may at times be nitrogen- rather than energy-limited.

Exceptions to this trend were observed in May near the peak of an exponential bloom of the diatom, Asterionella japonica (Fig. 23). It appears that either A. japonica was not a suitable food item or the copepod populations present were unable to increase their assimilation rates in response to the bloom, i.e.,  $A_{Ph}$  was saturated.

R was most strongly correlated with temperature (Table 28). Simple, linear regression of R on temperature indicates a  $Q_{10}$  of 3.87. Such a high  $Q_{10}$  is probably an expression of the effects of assimilating NPh-C. Respiration was inversely related to Ph-C while assimilation rates were stimulated by Ph-C. These relationships and the correlation between respiration and  $A_{NPh-C}$  indicate that respiration tended to be highest between peaks in phytoplankton biomass, suggesting that the metabolic cost of a nonphytoplankton diet is greater than when phytoplankton are the major source of particulate organic matter in the diet.

#### 4.0 BENTHIC AND PLANKTONIC BACTERIA

##### 4.01 Abundance

Water Column: Bacterial abundance varied from  $0.1 \times 10^6$  to  $63 \times 10^6$  CFU liter<sup>-1</sup> on ESWA compared to  $0.2 \times 10^9$  to  $3 \times 10^9$  cells liter<sup>-1</sup> from direct counts (Table 29). This discrepancy between plate counts and direct counts is usually observed and is due to the selective effect of the growth media on the number of colony-forming units which develop on agar plates. Plate counts give an estimate of the abundance of the most active attached bacteria while direct counts give an estimate of total attached and free-living bacteria (Sieburth 1979). Thus, plate counts are indicative of a small and unknown proportion of total attached bacteria. At best, such counts can be used as a relative measure of the carrying capacity of a body of water for the most active attached bacteria.

Table 29. Numerical abundance of bacteria in surface (SL) and near-bottom (BL) water based on plate counts (CFU x 10<sup>6</sup> liter<sup>-1</sup>) and direct counts (DC = number liter<sup>-1</sup> x 10<sup>9</sup>) (n = number of samples).

Month	n	Layer	CFU liter <sup>-1</sup>		DC	
			Mean	Range	Mean	Range
March	17	SL	2.4	0.2-16	0.7	0.5-1.0
	12	BL	1.1	0.1- 4	0.5	0.3-0.6
May	17	SL	3.0	1.0-20	-	-
	17	BL	1.8	1.0- 8	-	-
July	17	SL	2.2	0.2-25	1.7	1.0-3
	16	BL	2.8	0.1-63	0.3	0.2-0.6
Nov	11	SL	0.6	0.2- 6	0.8	0.5-1
	14	BL	0.2	0.1- 0.5	0.6	0.2-0.8

Bacterial abundance in coastal water based on direct counts is usually in the range of  $1-10 \times 10^8$  cells liter<sup>-1</sup> (Ferguson and Rublee 1976; Fuhrman and Azam 1980; Fuhrman et al. 1980). Direct counts in the apex tended to be higher, ranging from  $2 \times 10^8$  to  $30 \times 10^8$  cells liter<sup>-1</sup>. This is probably related to the higher concentrations of organic substrates in the plume relative to most coastal environments (section 3.05).

Abundance based on plate counts was highest in the surface layer during March, May, and July, and lowest in the bottom layer during November (Table 29). High counts coincided with periods of high phytoplankton biomass, especially during May when a bloom of diatoms developed (section 3.04). Glycolytic and ureoclastic bacteria were also most abundant in the surface layer during May (Tables 30 and 31). Phytoplankton are known to release glycolic acid (e.g., Burris 1980) and DOC was observed to increase in association with the May diatom bloom (section 3.05). Thus, phytoplankton production appears to increase the ability of coastal water to support large populations of attached bacteria.

Benthic: Four reference stations were sampled (Fig. 1) in addition to those sampled in conjunction with water column studies. A summary of sediment characteristics is given in Table 32. Sediments at most stations sampled had a moisture content of less than 40 percent indicating that they mainly consisted of fine sand and silt. The most notable difference in sediment properties between cruises was the shift in redox potential from an oxidizing environment during May, July, and November to a reducing environment during March. This coincided with the accumulation of a large quantity of diatom biomass during March and could reflect an increase in the flux of organic matter (in the form of diatoms) from the water column.

Bacterial abundance varied from a mean of  $0.2 \times 10^5$  CFU g<sup>-1</sup> in March to  $1.5 \times 10^5$  CFU g<sup>-1</sup> dry weight in November (Table 33). Again, direct counts were two to four orders of magnitude higher than plate counts. Abundance generally decreased with distance from the mouth of

Table 30. Numerical abundance of glycolytic bacteria (CFU x 10<sup>6</sup> liter<sup>-1</sup>) and glycolate concentration (nM) in surface (SL) and near-bottom (BL) water (n = number of samples).

Month	n	Layer	CFU liter <sup>-1</sup>		Glycolate	
			Mean <sup>1</sup>	Range	Mean <sup>1</sup>	Range
March	17	SL	1.0	0.2- 5.0	122	13 -305
	12	BL	0.2	0.0- 1.5	135	13- 235
May	17	SL	3.1	1.0-11.0	208	57- 479
	17	BL	2.2	0.2-25.0	475	66-1341
July	17	SL	0.7	0.1- 3.0	278	45- 489
	16	BL	2.1	0.0-10.0	272	162- 493
Nov	11	SL	0.4	0.1- 6.5	198	30- 631
	14	BL	0.2	0.1- 0.3	145	10- 300

<sup>1</sup> Geometric mean

Table 31. Numerical abundance of ureoclastic bacteria (CFU x 10<sup>6</sup> liter<sup>-1</sup>) and urea concentration (nM) in surface (SL) and near-bottom (BL) water (n = number of samples).

Month	n	Layer	CFU liter <sup>-1</sup>		Urea	
			Mean <sup>1</sup>	Range	Mean <sup>1</sup>	Range
March	17	SL	2.7	0.5-16	32	18-47
	12	BL	1.3	0.0- 2	32	17-50
May	17	SL	4.1	1.0-20	37	36-40
	17	BL	1.4	2.5-12	34	28-56
July	17	SL	0.1	0.0- 1	39	25-50
	16	BL	0.5	0.5-79	41	28-57
Nov	11	SL	0.6	0.1- 4	39	28-57
	14	BL	0.3	0.1- 0.3	35	18-43

<sup>1</sup> Geometric mean

Table 32. Temperature (T°C), Eh, and percent water in benthic sediments within the SINC study area (n = number of samples).

Month	n	T°C		Eh		% H <sub>2</sub> O	
		Mean	Range	Mean	Range	Mean	Range
March	21	3.1	2.5- 4.0	- 49	-305-125	34	8-81
May	12	7.6	7.0-10.0	288	70-635	29	21-44
July	12	13.2	11.5-15.0	213	85-470	30	17-47
Nov.	8	12.6	11.0-14.2	268	205-405	34	16-58

Table 33. ATP (g/g dry wt.) and bacterial abundance (g<sup>-1</sup> dry wt. sediments) based on plate counts (CFU x 10<sup>5</sup>) and direct counts (DC, number x 10<sup>8</sup>) from samples collected in the apex (station R20 excluded).

Month	n	ATP		CFU		DC	
		Mean <sup>1</sup>	Range	Mean <sup>1</sup>	Range	Mean <sup>1</sup>	Range
March	21	18	6 - 48	0.2	0.0- 7.1	1.3	0.2- 7.1
May	12	8	0.3- 60	0.3	0.1- 1.2	16.6	2.8-31.6
July	12	245	82 -995	0.9	0.1-22.4	3.0	1.8- 6.4
Nov.	8	78	7 -247	1.5	0.0- 6.6	2.8	0.4- 7.4

<sup>1</sup> Geometric mean

the estuary (Fig. 24). ATP reached maximum concentration in July and minimum concentration in May (Table 33).

Glycolytic bacteria tended to be most abundant in July and November and least abundant in March and May; ureoclastic bacteria tended to be most abundant in November and least abundant in May (Table 34). In contrast to the water column where abundance and substrate concentration were not correlated, glycolytic bacteria and glycolate were significantly correlated ( $P < 0.05$ ) in July ( $r = 0.65$ ) and in March ( $r = 0.67$ ), while ureoclastic bacteria and urea were significantly correlated in July ( $r = -0.62$ ), November ( $r = 0.71$ ), and March ( $r = 0.98$ ). The negative correlation in July suggests that ureoclastic bacteria had a strong influence on the distribution of urea at this time. Positive correlations indicate either common sources for both bacteria and substrate or that bacterial abundance was substrate dependent.

#### 4.02 Heterotrophic Potential

Measurements of respired  $^{14}\text{CO}_2$  by glycolytic and ureoclastic microflora provide estimates of potential rates of glycolic acid and urea decomposition. Seasonal variations in the decomposition potential of these two components of the dissolved organic pool were not in phase (Table 35). Glycolic acid turnover times increased from a mean of 72 seconds in May when glycolytic bacteria were most abundant to 60 minutes in March when abundance was low (Table 35). In contrast, urea turnover times were shortest in November when abundance was lowest (mean = 31 minutes) and longest in March (7 hours, 18 minutes).

Measurements of  $^{14}\text{C}$  incorporated by glycolytic and ureoclastic microflora are estimates of glycolate- and urea-dependent growth potentials (Table 36).  $V_{\max}$  on glycolate was highest on average in July and lowest in March. The abundance of glycolytic bacteria followed a similar trend (Table 34) suggesting a correlation between growth and abundance except in November.  $V_{\max}$  on urea was high in July and low in May, November, and March (table 36).

Mean uptake rate of glycolic acid by benthic bacteria was high during May and July and low during November and March (Table 37). Urea

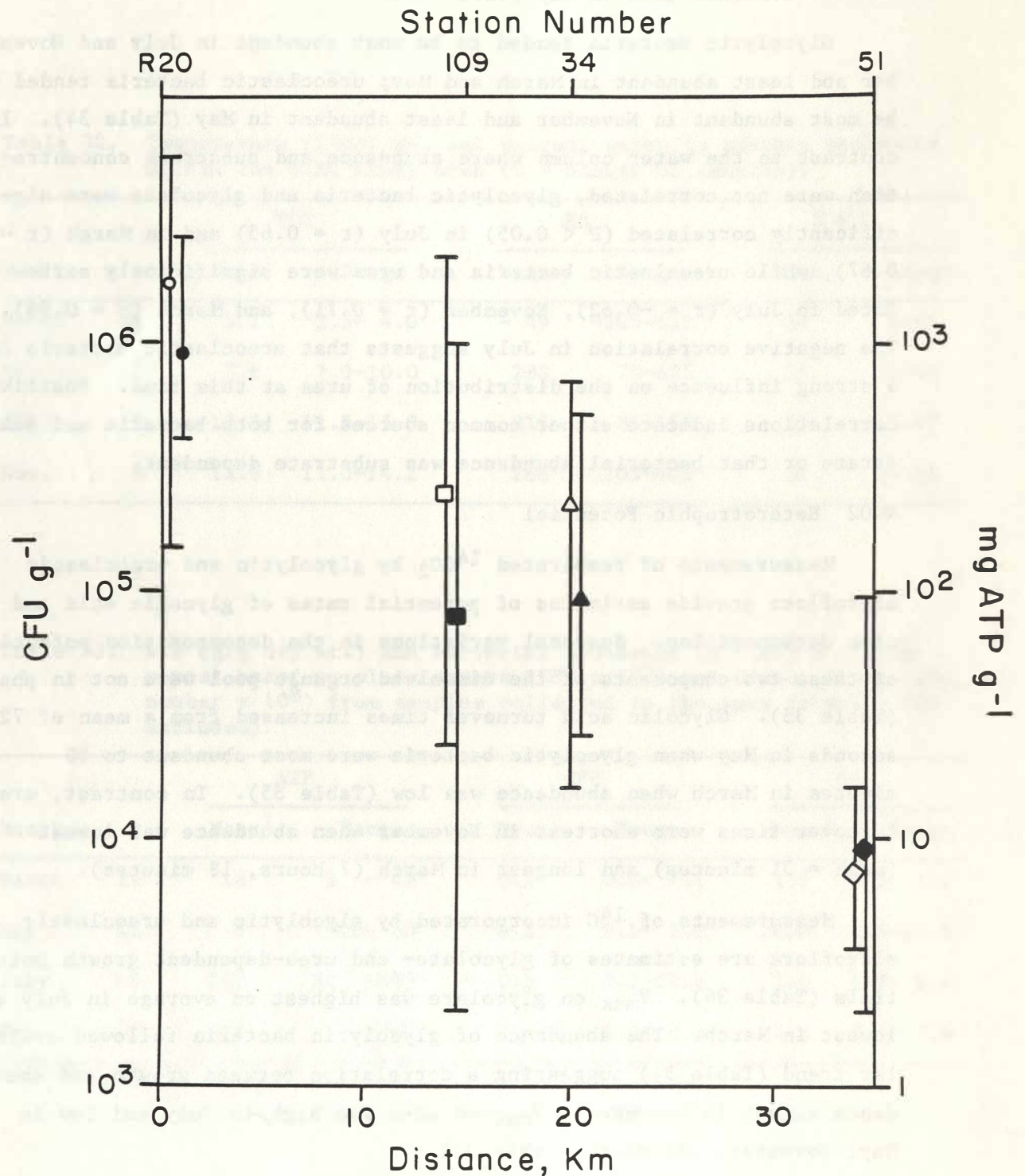


Figure 24. Bacterial abundance (open symbols, colony-forming units per gram of sediment) and ATP concentration (closed symbols) in surface sediments at reference stations shown in Fig. 1 (geometric means  $\pm$  range, n = 8).

Table 34. Abundance (CFU x 10<sup>4</sup> per gram dry wt. of sediment) of glycolytic (G) and ureoclastic (U) bacteria and respective substrate concentrations ( $\mu\text{g g}^{-1}$  dry wt. sediment) from samples collected in the apex (station R20 excluded).

Month	n	Type	Bacteria		Substrate	
			Mean <sup>1</sup>	Range	Mean <sup>1</sup>	Range
May	7	G	1.4	0.3- 2.9	47.3	7- 90
	7	U	2.1	0.1- 20.0	7.1	1- 32
July	7	G	17.3	0.3- 71.5	51.6	22-105
	7	U	2.2	0.2- 50.1	27.1	24- 32
Nov	4	G	19.4	< 0.0- 38.4	62.4	13-164
	4	U	5.0	< 0.2- 39.8	2.0	1- 3
March	11	G	2.6	0.0- 10.0	38.3	7-155
	11	U	3.2	0.2-158.5	3.1	1- 5

<sup>1</sup> Geometric mean

Table 35. Turnover times ( $T_t$ , hours) and maximum uptake rates ( $V_{\text{max}}$ , n moles liter<sup>-1</sup> hr<sup>-1</sup>) of respired CO<sub>2</sub> from glycolic acid (G) and urea (U) for those experiments that conformed to saturation kinetics (includes samples taken from the surface and bottom layers).

Month	Substrate	X/Y <sup>1</sup>	Water column					
			$T_t$			$V_{\text{max}}$		
			Low	Mean	High	Low	Mean	High
March	G	17/17	0.01	1.00	4.50	0.03	0.8	5.1
	U	10.12	0.90	7.30	11.30	0.14	0.8	8.6
May	G	17/17	0.01	0.02	0.06	4.40	29.7	55.0
	U	16/17	0.10	2.90	10.70	1.20	5.7	25.4
July	G	10/17	0.02	0.04	0.04	0.90	5.9	24.2
	U	12/16	0.10	0.80	1.90	5.70	26.7	412.0
Nov.	G	9/11	0.03	0.24	0.79	0.50	1.1	1.9
	U	5/14	0.05	0.52	1.56	1.30	65.5	155.0

<sup>1</sup>Number of experiments that conformed to saturation kinetics (X) over the number of experiments run (Y).

Table 36. Maximum uptake rates ( $V_{\max}$ , n moles liter<sup>-1</sup> hr<sup>-1</sup>) of glycolic acid (G) and urea (U) calculated from <sup>14</sup>C incorporated by heterotrophic microflora in experiments that conformed to saturation kinetics (includes samples from the surface and bottom layers).

Month	Substrate	X/Y <sup>1</sup>	Water column	
			Mean	Range
March	G	17/17	0.5	0.0 - 1.3
	U	6/7	1.2	0.3 - 7.7
May	G	17/17	10.7	0.1 - 62.7
	U	14/14	1.7	0.6 - 10.0
July	G	10/17	25.3	1.3 - 120.7
	U	9/15	7.6	0.1 - 16.4
Nov	G	9/11	6.7	0.3 - 27.1
	U	9/9	1.2	0.1 - 10.5

<sup>1</sup> Number of experiments that conformed to saturation kinetics (X) over the number of experiments run (Y).

Table 37. Turnover times ( $T_t$ , hours) and maximum uptake rates ( $V_{\max}$ , n moles g<sup>-1</sup> hr<sup>-1</sup>) of respired CO<sub>2</sub> from glycolic acid (G) and urea (U) for those experiments that conformed to saturation kinetics.

Month	Substrate	X/Y <sup>1</sup>	Benthic			
			$T_t$		$V_{\max}$	
			Mean	Range	Mean	Range
March	G	8/11	152.3	15.0-532.6	0.04	0.01 - 0.20
	U	10/11	122.4	4.7-485.7	0.33	0.01 - 1.65
May	G	6/7	0.6	0.1- 1.0	1.06	0.29 - 2.63
	U	5/7	87.4	12.2-253.2	0.18	0.03 - 0.36
July	G	5/7	6.6	0.0- 14.7	1.04	0.01 - 5.00
	U	4/7	59.8	46.6- 68.3	0.42	0.21 - 0.67
Nov	G	3/4	27.2	2.5- 64.4	0.07	0.01 - 0.19
	U	4/4	44.8	0.3-160.9	0.39	0.01 - 1.50

<sup>1</sup> Number of experiments that conformed to saturation kinetics (X) over the number of experiments run (Y).

uptake was highest on average during March, July, and November, and low during May (Table 37). Turnover times of both substrates were one to four orders of magnitude longer in the benthos than in the water column, but benthic turnover times exhibited a seasonal pattern of variation that was similar to that of the water column (Tables 35 and 37). This suggests that bacterial activity in benthic and water column environments were coupled.

Glycolytic and ureoclastic bacteria were abundant in the bottom layer and scarce in the surface layer during July when growth potential on both substrates was highest. When growth potential was low in March, abundance was high in the surface layer and low in the bottom layer. These observations and the seasonal grazing by copepods on non-phytoplankton particulates implicate grazing and associated fluxes of fecal material as probable factors controlling bacterial abundance. During March when macrozooplankton were scarce and grazing pressure was low, bacteria were abundant in the surface layer even though growth potential was low. During July when grazing pressure was high and non-phytoplankton particulate organic matter constituted 74 percent of the POC assimilated by copepods, bacteria were scarce in the surface layer and abundant in the bottom layer. High growth potential and low abundance in the surface layer could be due to high grazing rates; the abundance of bacteria in the bottom layer would then be a consequence of the downward flux of fecal material produced by grazers.

Potential rates of glycolate uptake and mineralization were high in May and July and low in November and March (Table 35). Glycolate concentrations were also high during May and July (Table 30) when increases in phytoplankton biomass and estuarine runoff were correlated with increases in DOC (section 3.05). High rates in the bottom layer relative to the surface layer in March coincided with high rates of DOC release by phytoplankton (Table 19) and high netplankton biomass in the bottom layer. These observations provide evidence for a coupling between glycolate supplied by phytoplankton and estuarine runoff and its metabolism by microorganisms in the water column.

In contrast to potential glycolate uptake, potential rates of urea uptake were high in July and November (Table 35). Urea concentrations showed little seasonal variability and were 1 to 2 orders of magnitude less concentrated than ammonia. The constancy of the urea levels in the water column cannot result from sewage sludge dumping since urea concentrations are negligible after secondary treatment processes. Direct raw sewage input does result in localized elevated urea levels which are rapidly depleted by the microorganisms present near the outfall. The source of urea must therefore be from within the apex environment and derived primarily from animal excretions. The lack of variability in urea concentration could be a consequence of seasonal variations in phytoplankton productivity and potential rates of urea utilization by ureoclastic bacteria being out of phase.

## 5.0 CONCLUSIONS AND IMPLICATIONS

### 5.01 Assimilation Capacity: Inorganic Nitrogen Inputs

The capacity of coastal ecosystems to assimilate inorganic and organic nitrogen inputs without exhibiting adverse effects in terms of water quality and fisheries is fundamental to the development of waste management strategies for the coastal zone. The problem of assimilation capacity is obviously complex in that it involves exchanges of carbon, nitrogen, and oxygen among living and nonliving pools which are largely governed by trophic interactions among a diverse group of organisms. With this report, we begin the difficult task of defining the assimilation capacity of one coastal ecosystem, the plume of the Hudson and Raritan Rivers.

Over 90 percent of the anthropogenic nitrogen produced in the New York metropolitan region reaches the coastal environment rapidly and with relatively little modification by organisms within the estuary (Garside et al. 1976; Malone 1982a). The plume typically occurs within the apex north of  $40^{\circ}10'N$  and west of  $73^{\circ}30'W$  and occupies an area of about  $1250 \text{ km}^2$ , based on the distribution of salinity (cf. Malone et al. in press b). It is the plume ecosystem that receives most of the anthropogenic nitrogen discharge, and it is in such a system that

relationships between allochthonous nutrient inputs (nutrients new to the system), nutrient uptake, production and consumption of organic matter, and nutrient exports ("leakage" of nutrients in organic and inorganic form) are best addressed, i.e., that the concept of assimilation capacity becomes meaningful.

The importance of phytoplankton as consumers of inorganic nutrients and producers of organic matter and oxygen is evidenced by low nutrient concentrations in the plume relative to estuarine and coastal water masses (Fig. 7; Garside et al. 1976; Malone 1976), by variations in percent saturation of oxygen in the surface layer and the relationship of these variations to inorganic nutrient concentrations (Tables 9 and 10), and by the effect of variations in phytoplankton biomass on suspended organic matter (section 3.05). Phytoplankton accounted for most of the variance in the field of suspended particles, both in terms of bulk composition (POC, PN) and in terms of the frequency distribution of particle size. This implies that inputs from estuarine and other external sources (e.g., ocean dumping and resuspension) provide a relatively stable background and is consistent with the conclusion, based on the comparison of phytoplankton productivity and anthropogenic inputs, that phytoplankton production is the major source of particulate organic matter in the plume. Nevertheless, phytoplankton generally account for less than 50 percent of suspended organic carbon (Table 18) and less than 25 percent of light attenuation in the euphotic zone (Fig. 20). The exception to this generalization occurs during late fall and early winter when phytoplankton productivity is low due to increased vertical mixing, resuspension of sediments, and low incident radiation. Particulates exported from the estuary and resuspended from the benthos have a greater effect on the field of suspended particles under these conditions.

The ability of phytoplankton in the plume to assimilate inputs of new nutrients is determined primarily by the availability of light energy and by temperature (Fig. 20; section 3.06). Anthropogenic inputs influence this ability through their effect on suspended particulate loads and, therefore, on the amount of light energy available to

phytoplankton. Thus, variations in the ratio of chlorophyll a concentration (Chl, phytoplankton biomass) to the concentration of particulate organic carbon (POC, consisting mainly of phytoplankton and organic detritus with contributions from bacteria and microzooplankton) accounted for 88 percent of the variance in the proportion of downwelling radiation absorbed by phytoplankton (%I<sub>Chl</sub>). The relationship between %I<sub>Chl</sub> and Chl/POC (mg/g) was best fitted by the power function

$$\%I_{Chl} = 0.966 ( Chl/POC )^{1.29} .$$

Such sensitivity to variations in Chl/POC indicates the potential impact of changes in suspended particulate loads due to vertical mixing, freshwater runoff, and waste treatment. A decrease in the suspended particulate load on a time scale of days to weeks is likely to result in an increase in primary productivity on a similar time scale. However, it is not clear how phytoplankton would respond on seasonal or annual time scales because of interactions involving nutrient cycling and grazing.

Light levels under current conditions appear to be high enough to restrict the influence of anthropogenic inputs of dissolved inorganic nitrogen (DIN) to a relatively small area of the New York Bight. For example, if anthropogenic inputs were the only source of nitrogen to the plume, the area required to assimilate these inputs would vary from 120 to 200 km<sup>2</sup> during March, May, and July to 1330 km<sup>2</sup> during November (based on estimates of phytoplankton productivity in Table 38, C/N in Table 17, and inputs in Table 1).

A more meaningful approach to nitrogen assimilation capacity at the phytoplankton level is to consider the relationship between allochthonous nitrogen inputs and recycling within the plume. Turnover rates of DIN ( $t_N$ ), the ratio of DIN uptake (estimated from phytoplankton productivity and ratios of N/C) to DIN concentration, varied from 0.02 d<sup>-1</sup> during November to 1.19 d<sup>-1</sup> during May (Table 38). Turnover rates of phytoplankton biomass ( $t_C$ ) followed a similar pattern of variation but were higher. These rates are consistent with the turnover rates

reported by Malone (1976) and by Malone and Chervin (1979). The ratio,  $t_N/t_C$ , gives an estimate of the proportion of DIN uptake that is based on DIN regeneration within the plume (Malone et al. in press a) and provides a means of distinguishing between new and recycled nitrogen in a system where ammonium can be supplied from external sources (e.g., sewage wastes) as well as by regeneration within the system.

Based on this argument, nitrogen regeneration was the major source of DIN utilized by primary producers during May and July in contrast with March and November when new nitrogen was the major source (Table 38). The proportion of phytoplankton production supported by nitrogen regenerated within the plume increased from 37 percent during March to 75 percent and 64 percent during May and July, respectively. This is similar to the seasonal pattern of regeneration deduced from variations in the concentration of ammonium (section 3.01). The low proportion during November reflects low phytoplankton productivity and low plankton respiration (Table 38) and is consistent with the quasi-conservative behavior of nutrients in the plume at this time (section 3.03). Malone et al. (in press a) reached the same conclusion based on long-term monthly means which indicated that nitrogen regeneration supported about 30 percent of phytoplankton production during February-April and about 60 percent during July-August.

These proportions and rates provide a means of evaluating the anthropogenic nitrogen input in terms of allochthonous inputs as a whole. Given  $t_N/t_C$  (Table 38), C/N (table 17) and monthly mean phytoplankton productivity (Fig. 4), anthropogenic nitrogen inputs (Table 1) potentially accounted for 24, 65, 26, and 113 percent of the allochthonous nitrogen input utilized by phytoplankton during March, May, July, and November, respectively. The relatively low proportion of new nitrogen supplied by anthropogenic inputs during March reflects high phytoplankton productivity and the cross-shelf transport of shelf water during winter (Riley 1967; Malone et al. in press a). Thus, the assimilation capacity of the apex for DIN of anthropogenic origin is high under conditions that favor high phytoplankton biomass (March) or high phytoplankton growth rate (May, July) and is low under conditions

Table 38. Mean primary productivity (PP), assimilation of phytoplankton-carbon ( $A_{Ph-C}$ ), microbial respiration ( $R_m$ ), copepod respiration ( $R_c$ ), ratio of total respiration ( $R = R_m + R_c$ ) to primary productivity, and turnover rates of dissolved inorganic nitrogen ( $t_N$ ) and phytoplankton biomass as carbon ( $t_C$ ) in the euphotic zone at reference stations (calculated from mean concentrations of chlorophyll a and copepods and relationships in Tables 20, 26, and 27).

Month	$g\ C\ m^{-2}\ d^{-1}$				R/PP	$d^{-1}$		
	PP	$A_{Ph-C}$	$R_m$	$R_c$		$t_N$	$t_C$	$t_N/t_C$
Mar	5.60	0.02	1.57	0.01	0.28	0.27	0.73	0.37
May	3.72	0.35	1.50	0.69	0.59	1.19	1.58	0.75
July	6.30	1.46	4.68	2.07	1.07	1.16	1.80	0.64
Nov	0.96	0.01	1.37	0.23	1.67	0.02	0.34	0.06

Table 39. Nitrogen production (new = production based on nitrogen from outside sources, regenerated = production based on nitrogen recycled within the plume) and regeneration rates in the euphotic zone of the plume calculated from rates of primary production and respiration (Table 38) and C/N (Table 17); production based on new and regenerated nitrogen was calculated from  $t_N/t_C$  (Table 38).

Month	$10^8\ g\ N\ d^{-1}$					
	N-Production			N-Regeneration		
	New	Regenerated	Total	$R_m$	$R_c$	Total
Mar	6.68	3.92	10.60	2.97	0.02	2.99
May	2.47	7.42	9.89	3.99	1.84	5.83
July	4.65	8.26	12.91	9.59	4.24	13.83
Nov	1.41	0.09	1.50	2.14	0.37	2.50

that favor low phytoplankton biomass and growth rate (November). Given the annual cycle of phytoplankton productivity (Fig. 4), export of anthropogenic DIN from the apex is significant only during November-January.

Variations in the importance of regenerated nitrogen ( $t_N/t_C$ ) were not paralleled by the ratio of total respiration to phytoplankton productivity (Table 38). This has two important implications:

(1) high rates of nitrogen regeneration ( $t_N/t_C$ ) during the period of thermal stratification (represented by May and July) are mainly a consequence of the heterotrophic metabolism of organic substrates produced by phytoplankton in the euphotic zone; and

(2) the importance of external sources of organic matter as substrates for heterotrophic metabolism increases through summer into fall, i.e., the system progresses from having a trophic structure with a predominantly phytoplankton-based food web during February-May to one with a predominantly detrital-based food web during fall.

Comparison of nitrogen regeneration rates (calculated from respiration and C/N) with primary productivity supported by regeneration (calculated from primary production,  $t_N/t_C$  and C/N) shows relatively good agreement between supply and demand (Table 39) given the uncertainties associated with such calculations. Agreement was best during March and May when nitrogen regeneration was 76 to 79 percent of the calculated demand. High rates of regeneration relative to demand during July (167 percent) and November (2780 percent) are consistent with the presence of residual ammonium but probably are also a consequence of overestimating  $R_m$  (section 3.10) and of an increase in the metabolism of external sources of organic substrates, the former being more important during July and the latter more important during November.

#### 5.02 Assimilation Capacity: Organic Inputs

In contrast with the assimilation capacity of phytoplankton for inorganic nitrogen, the ability of heterotrophs to assimilate organic inputs appears to be low during the diatom bloom period (February-April) and high during the period of thermal stratification.

Comparison of phytoplankton production and plankton respiration during March and July (Table 40) indicates a large excess of production over respiration during March in contrast to July when production and respiration appeared to be in approximate balance.

Low respiration rates and assimilation rates by copepods (Table 38) suggest that much of the excess production during March is exported from the plume, either to the benthos or seaward across the shelf. As argued by Eppley et al. (1981), biomass export must be balanced by inputs of new nutrients. The ratio,  $t_N/t_C$  (Table 38) should be inversely related to inputs of new nitrogen and, therefore, to exports of biomass (assuming that a balance between input and output is approached over the period of observation). The ratio of 0.37 during March would then indicate that 63 percent of the March production was exported. This export,  $4.4 \times 10^6 \text{ kg C d}^{-1}$ , agrees reasonably well with the estimate of  $5.7 \times 10^6 \text{ kg C d}^{-1}$  from carbon budget calculations (Table 40). Benthic respiration in the apex (area =  $1250 \text{ km}^2$ ) metabolized on the order of  $0.5 \times 10^6 \text{ kg C d}^{-1}$  (Garside and Malone 1978) or about 10 percent of the phytoplankton biomass exported from the plume. Thus, most of the biomass produced by phytoplankton in March either accumulates in benthic sediments or is exported seaward across the shelf. Malone et al. (in press b) presented evidence that very little biomass accumulates in the benthos and that most is exported across the shelf. Consequently, diatom production prior to the onset of thermal stratification during May is not likely to be a source of oxygen demand or nutrient regeneration in or beneath the plume during the stratified period.

The balance between phytoplankton production and respiration during July is probably not as close as indicated in Table 40 due to the overestimation of total plankton respiration (section 3.10). However,  $t_N/t_C$  also indicates that a much smaller fraction (36 percent since 64 percent was recycled) of phytoplankton production was exported from the plume (Table 38), i.e., most phytoplankton production was consumed and invested in heterotrophic growth or recycled within the plume.

Table 40. Carbon budget for the plume (area = 1250 km<sup>2</sup>). The plume is assumed to occupy the entire water column when the seasonal thermocline is weak or absent (November-April) and to occupy the surface layer when the thermocline is present (May-October).

	10 <sup>6</sup> kg C d <sup>-1</sup>		10 <sup>8</sup> kg C yr <sup>-1</sup>
	March	July	Annual
<b>A. Inputs</b>			
Primary production <sup>1</sup>	7.00	7.88	7.4
Estuarine runoff <sup>2</sup>	0.16	0.16	0.6
Ocean dumping <sup>3</sup>	0.49	-	0.9
Total	7.65	8.04	8.9
<b>B. Respiration<sup>4</sup></b>			
	1.97	8.44	7.6
<b>C. A - B</b>			
	5.68	-0.40	1.3

<sup>1</sup> Monthly estimates from Table 38; annual estimate from Malone et al. (in press a).

<sup>2</sup> Garside and Malone (1978).

<sup>3</sup> Thomas et al. (1976) and Garside and Malone (1978); assumes that input due to ocean dumping (sludge and dredge spoil) is metabolized below the plume when the seasonal thermocline is present.

<sup>4</sup> Monthly estimates from Table 38; annual estimate assumes that R/PP = 0.86 (Table 38).

Two likely mechanisms of export are sinking and grazing. Sinking losses were probably small in July since nanoplankton (which have low sinking rates) accounted for most chlorophyll a in the euphotic zone, and chlorophyll a varied over a wide range of concentrations in the plume but remained persistently low beneath the plume (cf. Malone and Chervin 1979). Assimilation of phytoplankton by copepods averaged  $1.46 \text{ g C m}^{-2} \text{ d}^{-1}$  during July (Table 38). Assuming an assimilation efficiency of 70 percent (Conover 1966), this translates into an ingestion rate of  $2.09 \text{ g C m}^{-2} \text{ d}^{-1}$  which is roughly equivalent to new production ( $6.30 \times 0.36 = 2.27 \text{ g C m}^{-2} \text{ d}^{-1}$ ; Table 38). Of this, about  $0.63 \text{ g C m}^{-2} \text{ d}^{-1}$  ( $2.09 - 1.46$ ) or  $0.78 \times 10^6 \text{ kg C d}^{-1}$  probably settled from the plume into bottom water in the form of fecal pellets. This exceeds the input due to ocean dumping of sludge and dredge spoils (Table 40), and together these two inputs to the bottom layer amount to  $1.4 \times 10^6 \text{ kg C d}^{-1}$ . Respiration in bottom water averaged  $0.47 \text{ g C m}^{-2} \text{ d}^{-1}$  (Table 25) or  $0.59 \times 10^6 \text{ kg C d}^{-1}$  compared to benthic respiration of  $1.53 \times 10^6 \text{ kg C d}^{-1}$  (Garside and Malone 1978). Thus, organic inputs associated with fecal pellet production by copepods and ocean dumping potentially account for 67 percent of the oxygen demand below the pycnocline (water column and benthos).

In summary, most phytoplankton production during the unstratified period (November–April) is exported into adjacent coastal environments. This is due to low grazing rates (Table 27) and the high frequency of storm events (Walsh et al. 1978) which not only uncouple primary and secondary production but result in a net transport of biomass from the apex. Under stratified conditions (May–October), most phytoplankton production appears to be metabolized within the plume, resulting in high rates of regeneration in the plume and reduced oxygen concentrations below the plume due to the fecal pellet input from above.

The importance of phytoplankton production and grazing by copepods during the summer period of thermal stratification cannot be overemphasized. Net copepod production was directly dependent on the assimilation of phytoplankton even though nonphytoplankton organic matter

accounted for more organic carbon assimilated on average. As a consequence, copepods play a major role in limiting accumulations of organic matter and in channeling phytoplankton production into metazoan food chains. The net effect is to limit accumulations of both phytoplankton and organic detritus and, therefore, to limit the vertical flux of organic particles from the plume to bottom water and the benthos. In the absence of grazing control by copepods, phytoplankton biomass alone could cause a three- to fourfold increase in BOD below the pycnocline due to increased microbial respiration.

Organic matter from external sources, most of which is anthropogenic and transported into the plume by estuarine runoff and ocean dumping, does not appear to undergo substantial metabolism in the plume. This is particularly true of dissolved organic carbon which generally decreased linearly with increasing salinity (Table 13) except during May when DOC increased in association with a diatom bloom (Fig. 17). The concentration of nonphytoplankton-carbon (NPh-C) also decreased with salinity in a quasi-conservative way except during July (Table 41) when copepod grazing was high and NPh-C accounted for an average of 74 percent of the carbon assimilated by copepods (Table 27). Chervin et al. (1981) concluded that copepod grazing limited phytoplankton and nonphytoplankton crops during July but not during March, May, or November. Thus, the capacity of heterotrophs to assimilate organic inputs from external sources is low, especially during the unstratified period (November-April) when water temperature in the plume is relatively low. Under these conditions, most organic inputs are probably exported from the apex. As a consequence, the areal influence of anthropogenic organic inputs to the coastal zone is much greater than that of anthropogenic inorganic nutrient inputs (cf. Ryther and Dunstan 1971).

Once the seasonal thermocline forms, most phytoplankton production is metabolized in the plume with 20 to 25 percent being transferred directly into food chains involving copepods. Under these conditions, about 10 percent of phytoplankton production is transported into bottom water in the form of copepod fecal pellets. This flux potentially

Table 41. Results of linear correlation and regression analyses of nonphytoplankton organic carbon (NPh-C, mg liter<sup>-1</sup>) on salinity in the surface layer at reference stations; NPh-C was calculated as the difference between the concentration of particulate organic carbon and phytoplankton-carbon (product of chlorophyll a concentration and C/Chl from Table 17).

Month	n	r <sup>2</sup>	a	b
Mar	12	0.73	6.49	-0.20
May	12	0.86	3.10	-0.09
July	12	0.52	8.35	-0.25
Nov	12	0.85	3.28	-0.09

accounts for about 37 percent of the oxygen demand below the pycnocline. Most of the remaining oxygen demand appears to be supported by organic inputs from estuarine runoff and ocean dumping (sludge and dredge spoil). This is reasonably good agreement and consistent with the results of Thomas et al. (1976) and Garside and Malone (1978) who showed that high rates of benthic oxygen consumption were associated with the sewage sludge and dredge spoil dump sites and with periods of high runoff.

The above findings have several implications in terms of the treatment of sewage wastes. In general, waste management strategies should be designed to reduce inputs of organic matter and to enhance the flux of carbon and nitrogen through phytoplankton-metazoan food chains. This can best be accomplished through a reduction in suspended organic loads by improved secondary treatment and land management practices (less soil erosion and associated losses of organic detritus from the water shed) which should have the following consequences:

(1) a reduction in turbidity and a small increase (about 15 percent) in response to a reduction in the proportion of light attenuated by nonphytoplankton materials in the euphotic zone and an increase in new nitrogen inputs;

(2) an increase in copepod production and nitrogen regeneration during the period of thermal stratification in response to the increase in phytoplankton production;

(3) a reduction in BOD of bottom water due to a decrease in particulate organic exports from the estuary; and

(4) a decrease in the area of the New York Bight that is influenced by organic inputs of anthropogenic origin.

## 6.0 ACKNOWLEDGMENTS

This research was performed as part of the Marine EcoSystems Analysis (MESA) New York Bight Project of NOAA. The Project would not have been possible without the shipboard and laboratory assistance of David Boardman, Monica Devanas, Hank Edenborn, Gretchen Hull, Susan Murray, Stuart Patterson, Craig Robertson, and Joe Zindulis. Jean

Garside and Patrick Neale were primarily responsible for computer programming and the efficiency with which data were made available to the principal investigators. Jay O'Reilly provided technical assistance and made significant contributions to the preparation of this report. Finally, we thank the officers and crew of the NOAA ship, GEORGE B. KELEZ for making it all possible.

## 7.0 REFERENCES

- Barsdate, R. J. and R. C. Dugdale, 1965. Rapid conversion of organic nitrogen to  $N_2$  for mass spectrometry: an automated Dumas procedure. Anal. Biochem., 13:1-5.
- Beardsley, R. C., W. B. Boicourt and D. V. Hansen, 1976. Physical oceanography of the Middle Atlantic Bight. In: M. G. Gross (ed.), MIDDLE ATLANTIC CONTINENTAL SHELF AND THE NEW YORK BIGHT, Limnol. and Oceanogr. Special Symp., 2:20-34.
- Bowman, M.J., 1978. Spreading and mixing of the Hudson River effluent into the New York Bight. In: Nihoul, J.C. (ed.), HYDRODYNAMICS OF ESTUARIES AND FJORDS, Elsevier, New York, 373-386.
- Bowman, M.J. and L.D. Wunderlich, 1976. Distribution of hydrographic properties in the New York Bight apex. In: Gross, M.G. (ed.), MIDDLE ATLANTIC CONTINENTAL SHELF AND THE NEW YORK BIGHT, Limnol. and Oceanogr. Special Symp., 2:58-68.
- Burris, J. E., 1980. Respiration and photorespiration in marine algae. In: Falkowski, P. G. (ed.), PRIMARY PRODUCTIVITY IN THE SEA, Plenum Press, New York, 411-432.
- Charnell, R. L. and D. V. Hansen, 1974. Summary and analyses of physical oceanographic data collected in the New York Bight apex during 1969 and 1970. MESA Rep. 74-3, NOAA-ERL. 44 pp.
- Checkley, D. M., 1980. The egg production of a marine planktonic copepod in relation to its food supply: laboratory studies. Limnol. Oceanogr., 25:430-446.
- Chervin, M., 1978. Assimilation of particulate organic carbon by estuarine and coastal copepods. Mar. Biol., 49(3):265-275.
- Chervin, M. B., T. C. Malone and P. J. Neale, 1981. Interactions between suspended organic matter and copepod grazing in the plume of the Hudson River. Estuar., Coast. and Mar. Sci., 13:169-184.
- Conover, R. J., 1966. Factors affecting the assimilation of organic matter by zooplankton and the question of superfluous feeding. Limnol. Oceanogr., 11:338-345.
- Davis, B. D., R. Dulbecco, H. N. Eisen, H. S. Ginsberg, W. B. Wood, Jr. and M. McCarthy, 1972. MICROBIOLOGY, 2nd ed., Hayer and Row Publishers, Inc., New York, 1562 pp.
- Duedall, I.W., H.B. O'Connors, R.E. Wilson and J.H. Parker, 1979. The Lower Bay complex. MESA New York Bight Atlas Monograph 29, New York Sea Grant Institute, 47 pp.
- Eppley, R. W., 1972. Temperature and phytoplankton growth in the sea. Fish. Bull., 70:1063-1085.

- Eppley, R. W., J. H. Sharp, E. J. Renger, M. J. Perry and W. G. Harrison, 1977. Nitrogen assimilation by phytoplankton and other microorganisms in the surface waters of the central north Pacific Ocean. Mar. Biol., 39:111-120.
- Eppley, R. W., S. G. Horrigan, J. A. Fuhrman, E. R. Brooks, C. C. Price and K. Sellner, 1981. Origins of dissolved organic matter in southern California coastal waters: experiments on the role of zooplankton. Mar. Ecol., 6:149-159.
- Ferguson, A.L. and P. Rublee, 1976. Contribution of bacteria to standing crop of coastal plankton. Limnol. Oceanogr., 21:141-145.
- Fogg, G. E. and W. D. Watt, 1965. The kinetics of release of extracellular products of photosynthesis by phytoplankton. Mem. Inst. Ital. Hydrobiol., 18(suppl):165-174.
- Fredericks, A. D. and W. M. Sackett, 1970. Organic carbon in the Gulf of Mexico. J. Geophys. Res., 75:2199-2206.
- Fuhrman, J.A. and F. Azam, 1980. Bacterioplankton secondary production estimates for coastal waters of British Columbia, Antarctica, and California. Appl. Environ. Microbiol., 39:1085-1095.
- Fuhrman, J.A., J.W. Ammerman and F. Azam, 1980. Bacterioplankton in the coastal euphotic zone: distribution, activity and possible relationships with phytoplankton. Mar. Biol., 60:201-207.
- Garside, C., 1981. Nitrate and ammonia uptake in the apex of the New York Bight. Limnol. and Oceanogr., 26:731-739.
- Garside, C. and T. C. Malone, 1978. Monthly oxygen and carbon budgets of the New York Bight apex. Estuar. Coast. Mar. Sci., 6:93-104.
- Garside, C., G. Hull and S. Murray, 1978. Determination of submicromolar concentrations of ammonia in natural waters by a standard addition method using a gas-sensing electrode. Limnol. Oceanogr., 23:1073-1076.
- Garside, C., T. C. Malone, O. A. Roels and B. A. Sharfstein, 1976. An evaluation of sewage-derived nutrients and their influences on the Hudson Estuary and the New York Bight. Estuar. Coast. Mar. Sci., 4:281-289.
- Haines, E. G. and W. M. Dunstan, 1975. The distribution and relation of particulate organic material and primary productivity in the Georgia Bight, 1973-1974. Estuar. Coast. Mar. Sci., 3:431-441.
- Hammond, D. E., 1975. Dissolved gases and kinetic processes in the Hudson River estuary. Ph.D. Dissertation, Columbia University, New York, 150 pp.

- Han, G. and T. Niedrauer, 1981. Hydrographic observations and mixing processes in the New York Bight, 1975-1977. Limnol. Oceanogr., 26:1126-1141.
- Heinle, D.B., D.A. Flemer, J.F. Ustach, R.A. Murtagh and R.P. Harris, 1974. The role of organic debris and associated microorganisms in pelagic estuarine food chains. Final Report Office of Water Resources, U.S. Department of the Interior, National Research Institute, 74-129.
- Heinle, D.R., R.P. Harris, J.F. Ustach, and D.A. Flemer, 1977. Detritus as food for estuarine copepods. Mar. Biol., 40:341-353.
- Hobbie, J. E. and C. C. Crawford, 1969. Respiration corrections for bacterial uptake of dissolved organic compounds in natural waters. Limnol. Oceanogr., 14:528-532.
- Hobbie, J. E., R. J. Daley and S. Jasper, 1977. Use of Nucleopore filters for counting bacteria by epifluorescence microscopy. Appl. Environ. Microbiol., 33:1225-1228.
- Hopkins, T. S. and D. Dieterle, 1982. An externally forced barotropic circulation model for the New York Bight. J. Geophys. Res. (in press).
- Judkins, D.C., C.D. Wirick and W.E. Esaias, 1980. Composition, abundance, and distribution of zooplankton in the New York Bight, September 1974 - September 1975. Fish. Bull., 77:669-683.
- Karl, D.M. and P.A. LaRock, 1975. ATP measurements in soil and marine sediments. J. Fish. Res. Bd. Canada, 32:599-607.
- Ketchum, G. H., A. C. Redfield and J. C. Ayers, 1951. The oceanography of the New York Bight. Pap. Phys. Oceanogr. Meteorol., 12(1):46.
- Kitchen, J. C., D. Menzies, H. Pak and J. R. V. Zaneveld, 1975. Particle size distributions in a region of coastal upwelling analyzed by characteristic vectors. Limnol. Oceanogr., 20:775-783.
- Kroner, R. C., J. E. Longbottom and R. Gorman, 1964. A comparison of various reagents proposed for use in the Winkler procedure for dissolved oxygen. PHS Water Pollut. Surveillance System Appl. Develop. Rep. 12. Public Health Serv., Department of Health, Education and Welfare, Washington, D.C., 18 pp.
- Litchfield, C. D., J. B. Rake, J. Zindulis, R. T. Watanabe and D. J. Stein. 1975. Optimization of procedures for the recovery of heterotrophic bacteria from marine sediments. Microbial Ecol., 1:219-233.
- Litchfield, C. D., J. P. Nakas and R. H. Vreeland, 1976. Bacterial flux in some New Jersey estuarine sediments. Am. Sco. Limnol. Oceanogr. Special Symp., 2:340-353.

- Malone, T. C., 1976. Phytoplankton productivity in the apex of the New York Bight: environmental regulation of productivity/chlorophyll a. In: M. G. Gross (ed.), MIDDLE ATLANTIC CONTINENTAL SHELF AND NEW YORK BIGHT, Limnol. and Oceanogr. Special Symp., 2:260-272.
- Malone, T. C., 1977. Light-saturated photosynthesis by phytoplankton size fractions in the New York Bight, USA. Mar. Biol., 42:281-292.
- Malone, T. C., 1982a. Factors influencing the fate of sewage-derived nutrients in the lower Hudson Estuary and New York Bight. In: G. F. Mayer (ed.), ECOLOGICAL STRESS IN THE NEW YORK BIGHT: SCIENCE AND MANAGEMENT, Estuarine Research Federation, Columbia, South Carolina, 389-400.
- Malone, T. C., 1982b. Phytoplankton photosynthesis and carbon-specific growth: light-saturated rates in a nutrient-rich environment. Limnol. and Oceanogr., 27:226-235.
- Malone, T. C. and M. Chervin, 1979. The production and fate of phytoplankton size fractions in the plume of the Hudson River, New York Bight. Limnol. Oceanogr., 24:683-696.
- Malone, T. C. and P. J. Neale, 1981. Parameters of light-dependent photosynthesis for phytoplankton size fractions in temperate estuarine and coastal environments. Mar. Biol., 61:289-297.
- Malone, T. C., M. Chervin and D. Boardman, 1979. Effects of 22  $\mu$ m screens on size frequency distributions of suspended particles and biomass estimates of phytoplankton size fractions. Limnol. Oceanogr., 24(4):956-959.
- Malone, T. C., T. S. Hopkins, P. G. Falkowski and T. E. Whitledge. In press a. Production and transport of phytoplankton biomass over the continental shelf of the New York Bight. Continental Shelf Research.
- Malone, T. C., P. G. Falkowski, T. S. Hopkins, G. T. Rowe and T. E. Whitledge. In press b. Mesoscale response of diatom populations to a wind event in the plume of the Hudson River. Deep-Sea Res.
- Martin, J. H., 1968. Phytoplankton-zooplankton relationships in Narraganset Bay. III. Seasonal changes in zooplankton excretion rates in relation to phytoplankton abundance. Limnol. Oceanogr., 13:63-71.
- McCarthy, J. J., W. R. Taylor and J. L. Taft, 1977. Nitrogenous nutrient availability and phytoplankton preferences. Limnol. Oceanogr., 22:996-1011.

- Menzel, D. W. and J. H. Ryther, 1970. Distribution and cycling of organic matter in the oceans. In: D.W. Hood (ed.), ORGANIC MATTER IN NATURAL WATERS, University of Alaska, Institute of Marine Science Occasional Publ. No. 1, 31-54.
- Milliman, J. D., 1981. Transfer of river-borne particulate material to the oceans. RIVER INPUTS TO OCEAN SYSTEMS, United Nations, New York, 5-12.
- Morel, A., 1978. Available, usable, and stored radiant energy in relation to marine photosynthesis. Deep-Sea Res., 25:673-688.
- Nakas, J. P. and C. D. Litchfield, 1976. Application of the diacetylmonoxime thiosemicarbazide method to the analysis of urea in estuarine sediments. Estuar. Coast. Mar. Sci., 5:143-150.
- O'Reilly, J. E., J. P. Thomas and C. Evans, 1976. Annual primary production (nanoplankton, netplankton, dissolved organic matter) in the lower New York Bay. (U.S. Dept. of Commerce, NOAA) Paper No. 19 In: W. J. McKeon and G. J. Lauer (eds.), FOURTH SYMPOSIUM ON HUDSON RIVER ECOLOGY, Hudson River Environmental Society, Inc., New York, 1-39.
- Pavlou, S. P., G. E. Friederick and J. J. MacIsaac, 1974. Quantitative determination of total organic nitrogen and isotope enrichment in marine phytoplankton. Anal. Biochem., 61:16-24.
- Remsen, C. C., C. J. Carpenter, and B. W. Schroeder, 1974. The role of urea in marine microbial processes. In: R. R. Colwell and R. Y. Morita (eds.), EFFECTS OF THE OCEAN ENVIRONMENT ON MICROBIAL ACTIVITIES, University Park Press, Baltimore, Md., 286-304.
- Riley, G. A., 1967. Mathematical model of nutrient conditions in coastal waters. Bull. Bingham Oceanogr. Coll., 19:72-80.
- Riley, G. A., 1970. Particulate organic matter in seawater. Adv. Mar. Biol., 8:1-118.
- Roman, M.R., 1977. Feeding of the copepod Acartia tonsa on the diatom Nitzschia bosterium and brown algae (Fucus vesiculosus) detritus. Mar. Biol., 42:149-155.
- Ryther, J. H., 1959. Potential productivity of the sea. Sci., 130:602-608
- Ryther, J. H. and W. M. Dunstan, 1971. Nitrogen, phosphorus and eutrophication in the coastal marine environment. Sci., 171:100-113.
- Schindler, D. W., G. J. Brunskill, S. Emerson, W. S. Broecker and T. H. Peng, 1972. Atmospheric carbon dioxide: its role in maintaining phytoplankton standing crops. Sci., 177:1192-1194.

- Segar, D. A. and G. A. Berberian, 1976. Oxygen depletion in the New York Bight apex: causes and consequences. In: M. G. Gross (ed.), MIDDLE ATLANTIC CONTINENTAL SHELF AND THE NEW YORK BIGHT, Limnol. Oceanogr. Special Symp., 2:220-239.
- Shah, N. M. and R. T. Wright, 1974. The occurrence of glycolic acid in coastal seawater. Mar. Biol., 24:121-124.
- Sieburth, J. McN., 1979. SEA MICROBES. Oxford University Press, Oxford, 491 pp.
- Simpson, H. J., S. C. Williams, C. R. Olsen and D. E. Hammond, 1977. Nutrient and particulate matter budgets in urban estuaries. ESTUARIES, GEOPHYSICS, AND THE ENVIRONMENT, National Academy of Sciences, Washington, D.C., 94-103.
- Stepien, J. C., T. C. Malone and M. B. Chervin, 1981. Copepod communities in the estuary and coastal plume of the Hudson River. Estuar., Coast. and Shelf Sci., 13:185-195.
- Stewart, H. B., 1958. Upstream bottom currents in New York Harbor. Sci., 127:1113-1115.
- Strickland, J. D. H. and T. R. Parsons, 1972. A Practical Handbook of Seawater Analysis. Fish. Res. Bd. Canada Bull., 169, 310 pp.
- Takahaski, M. and T. R. Parsons, 1972. Maximization of the standing stock and primary productivity of marine phytoplankton under natural conditions. Ind. J. Mar. Sci., 1:61-62.
- Thomas, J. P., W. C. Phoel, F. W. Steimle, J. E. O'Reilly and C. A. Evans, 1976. Seabed oxygen consumption-New York Bight Apex. In: M. G. Gross (ed.), THE MIDDLE ATLANTIC SHELF AND NEW YORK BIGHT, Limnol. Oceanogr. Spec. Publ. 2:354-369.
- Tranter, D. J., 1976. Herbivore production. In: Cushing, D. H. and J. J. Walsh (eds.), THE ECOLOGY OF THE SEAS, Blackwell, Oxford, 186-224.
- U.S. Environmental Protection Agency, 1974. Methods for chemical analysis of water and wastes. Methods Develop. Qual. Assurance Res. Lab., National Environmental Research Center, EPA-625/6-74/003, Cincinnati, Ohio, 196 pp.
- van Bennekom, A. J. and W. Salomons, 1981. Pathways of nutrients and organic matter from land to ocean through rivers. RIVER INPUTS TO OCEAN SYSTEMS, United Nations, New York, 33-51.
- Walsh, J. J., G. T. Rowe, R. L. Iverson and C. P. McRoy, 1981. Biological export of shelf carbon is a sink of the global CO<sub>2</sub> cycle. Nature, 291:196-201.

Walsh, J. J., T. E. Whitley, F. W. Barvenik, C. D. Wirick and S. O. Howe, 1978. Wind events and food-chain dynamics within the New York Bight. Limnol. Oceanogr., 23(4):659-683.

Wright, R. T. and J. E. Hobbie, 1966. Use of glucose and acetate by bacteria and algae in aquatic ecosystems. Ecol., 47:446-464.

Wright, R. T. and N. M. Shah, 1975. The trophic role of glycolic acid in coastal seawater. I. Heterotrophic metabolism in seawater and bacterial cultures. Mar. Biol., 33:175-183.